Spatio-temporal modelling of tree-grass dynamics in humid savannas: Interplay between nonlocal competition and nonlocal facilitation

S. R. Tega, Ivric Valaire Yatat Djeumen, Jean Jules Tewa, Pierre Couteron

Version of Record: https://www.sciencedirect.com/science/article/pii/S0307904X21005710
Manuscript_6e741e050ea09c0d2e82b4fc7272834e

Spatio-temporal modelling of tree-grass dynamics in humid savannas: interplay between nonlocal competition and nonlocal facilitation

S.R. Tega II[a,b], I. V. Yatat-Djeumen[b,c,*], J.J. Tewa[b,c], P. Couteron[d]

[a] *Faculty of Science,University of Yaoundé 1, Yaoundé, Cameroon*
[b] *UMI 209, IRD/UPMC UMMISCO, Bondy, France*
[c] *National Advanced School of Engineering of Yaoundé,University of Yaoundé 1, Yaoundé, Cameroon*
[d] *AMAP, University of Montpellier, CIRAD, CNRS, INRAE, IRD, Montpellier, France*

Abstract

For about twenty years, the question about the essential factors promoting the long-lasting coexistence of trees and grasses in humid savannas is at the center of several mathematical works, by the construction of deterministic and/or stochastic mathematical models. A closely related topic is coexistence of open savanna and forest patches at landscape scales, which raises the challenge of accounting for contrasted spatial patterns under similar climate conditions through fire mediated tree-grass interaction models. In this work, we propose and study a deterministic spatio-temporal fire-mediated tree-grass interactions model. The model is based on two nonlocal reaction-diffusion equations with kernels of intra and inter-specific interactions, corresponding to woody and grassy biomasses. A novelty in this paper is the consideration of a kernel-based nonlocal facilitation of trees by other trees to promote growth of seedlings/shrubs and, indirectly, limit fire propagation and its impact. We also take into account a kernel-based nonlocal competition of trees on grasses for light availability and nutrients. A qualitative analysis of the model is carried out and it reveals several ecological thresholds that shape the overall dynamics of the system. Depending on these thresholds, monostability of the forest, grassland or savanna space-homogeneous stationary state and multistabilities (i.e. involving more that one space-homogeneous stationary state) are proven possible. Thanks to the nonlocal biomasses interactions, our model accounts for the occurrence of space inhomogeneous solutions, including a possibly periodic spatial structuring sometimes observed in the humid savanna zone. Specifically, linear stability analyses, performed in the vicinity of space-homogeneous stationary states, provides conditions for the appearance of space inhomogeneous solutions including spatially periodic or aperiodic ones. Finally, numerical simulations are presented to illustrate our theoretical results. Notably, we verify that the computed spatial wavelengths were in good agreement with the predictions from the theoretical analysis.

Keywords: Tree, Grass, Nonlocal interaction, Facilitation, Competition, Reaction-diffusion equations, Vegetation patterns

1. Introduction

Savannas are complex ecosystems characterized by the co-occurrence of trees and grasses without one lifeforms excluding the other (Higgins and Bond [1]). They are also defined as a biome that corresponds to warm mean annual temperatures ($> 20°C$) and a broad range of intermediate mean annual rainfall (Yatat Djeumen et al. [2], Sarmiento [3]). Covering *ca.* 12% of the global land surface (February and Higgins [4]), savannas occupy in Africa, *ca.* 50% of the land area.

Within specific stretches of the rainfall gradient, vegetation may sometimes exhibit plausibly self-organized physiognomies also termed as patchy vegetation or vegetation mosaics. Indeed, as

*Corresponding author: yatat.valaire@gmail.com

pointed out by Yatat Djeumen et al. [5], there are several empirical evidences that highlight the existence of vegetation mosaics. Patches of vegetation display dense clusters of shrubs, grasses or trees and can be interpreted as regular spot structures or localized structures (Tlidi et al. [6]). These mosaics involve either bare soil ("desert") versus vegetation (herbaceous or woody) in arid, semi-arid regions (Lefever and Lejeune [7]; Lefever et al. [8]; Lefever and Turner [9]; Couteron and Lejeune [10]; Couteron et al. [11]; HilleRisLambers et al. [12]; Rietkerk et al. [13]; Gilad et al. [14]; Pueyo et al. [15, 16]; Deblauwe et al. [17]), or grasslands/savannas versus forests in temperate as well as humid tropical regions (Youta Happi [18]; Hirota et al. [19]; Jeffery et al. [20]; Xu et al. [21]; Stall et al. [22] and references therein; see also figure 1). Empirical evidences suggest that vegetation mosaics in humid regions barely feature periodic patterns. Most often, they are aperiodic but, with quite sharp boundaries like isolated groves or savanna patches encircled by forests.

Observation of these mosaics further motivated several researches that aimed to study and understand how these patterns may arise and the modalities of transitions between vegetation states that could substantiate or not the theory of abrupt shifts or catastrophic transitions in vegetation ecology (see for instance Scheffer et al. [23, 24]; Scheffer and Carpenter [25]; Staver et al. [26]; Favier et al. [27] for more details). It is well-known that at biome scale, vegetation cover displays complex interactions with climate. For instance, any shift from savanna to forest vegetation not only means increase in vegetation biomass and carbon sequestration but also may translate into changes in the regional patterns of rainfall (Oliveras and Malhi [28]). Therefore, being able to predict or understand the process that shapes savanna dynamics and possible transitions within vegetation patterns can help to figure out global distribution of savannas, orient their evolution in the face of recurring climatic changes in Africa (Dohn et al. [29]) and sustainably manage the natural resources provided by savanna ecosystems.

To understand such self-organized vegetation formations and associated dynamics along the rainfall gradient, theoretical approaches are required. Mathematical modelling is a useful tool to describe dynamics of complex systems and has been used since decades in various fields that include finance, biology, epidemiology, agronomy, ecology. Despite field observations that point out spatial patterns of vegetation or vegetation mosaics (see e.g. figure 1), how tree-grass interactions proceed in space and make vegetation propagate has insufficiently been taken into account in the study of savanna dynamics, in contrast to the insights provided by modelling regarding bare soil-vegetation mosaics in drylands. Indeed, tree-grass interactions in savanna ecosystems (fire-prone or not) have been very often modelled through frameworks that implicitly acknowledge space (see the review of Yatat Djeumen et al. [5]). According to Borgogno et al. [30], the modelling of spatial mechanisms of tree-grass interactions includes discrete kernel-based and partial differential equations (PDE) frameworks. Discrete kernel-based frameworks include cellular automaton (CA) models. CA models have been use in ecology, to explain formation of patterns in fire-prone savannas (Accatino et al. [31]), in arid and semi-arid savannas (Borgogno et al. [30], Feagin et al. [32]). Accatino et al. [31] developed a CA model to investigate how trees can invade the grass stratum in humid savannas despite repeated fires. Their results show that trees can invade the grass stratum and finally suppress fire spread because one of the following occurs: (a) trees may frequently resprout and form a population that persists despite repeated effective fires; (b) trees may be fire-resistant; (c) if trees are fire-vulnerable they may cluster and grow in density until grass growth is suppressed and fire prevented. One should note that, only (c) may require spatially-explicit modelling of tree-grass interactions. However, they also show that fire may be effective in preventing the initiation of the invasion process in the grass stratum. But once the invasion process has begun, fire alone is not able to reverse it because of the combinated strategies employed by trees i.e. resprouting, fire resistance or clumping (see also Yatat Djeumen et al. [5]).

However, since CA models are simulation-based and generally involve a fairly large number of parameters, it is not easy/possible to assess how model parameter variations may influence the model outcomes. In many cases, it is not easy to use mathematical analysis to thoroughly

understand the behavior and properties of CA models (Yatat Djeumen et al. [2]). Therefore, for the specific case of fire-prone savannas, it is desirable to provide insights into the dynamical properties of extensive savanna-forest areas for which data are scarce but that however need decisions in aspects such as fire management, grazing rules, or wood harvest. Spatially-explicit mathematical models that may allow mathematical tractability are thus desirable and rely on PDE frameworks.

Most of the works done using PDE, were carried out in the arid or semi-arid environmental context, using a reaction-diffusion-advection system (emphasizing the dynamics of vegetation and water) or using an integro-differential equation expressing kernel-based modelling of interactions between plants (see the review of Borgogno et al. [30]). The goal of that type of modelling is to understand the mechanisms that produce spatial patterns in arid and semi-arid savannas. In reaction-diffusion-advection systems, authors attribute pattern formation to positive feedback between vegetation (trees and grasses) and water availability (Klausmeier [33], Gilad et al. [14], Meron et al. [34], Sherratt [35]). Two main processes are identified as responsible for this positive feedback. The first one is the flow and infiltration of surface water into vegetated areas and the second feedback process is water up-take by the plant roots that is longer for larger plants (Meron et al. [34]). Such feedback is central to another framework to address vegetation patterns in arid and semi-arid savannas and that is entirely based on kernels that express nonlocal interactions between plants. Two types of non-local mechanisms received a particular attention: facilitative interactions between plants, that promote water infiltration and reduce evapotranspiration, and competitive interactions among them for water and nutrients. It is now acknowledged that pattern formation in arid systems can be explained by a combination of long distance competition and short distance facilitation (Lefever and Lejeune [7], Lejeune et al. [36], Lefever et al. [8], Lefever and Turner [9], Couteron et al. [11]). A common point of these two classes of studies is the view that the pattern formation phenomenon is a symmetry-breaking process that induces instability in an uniform vegetation state.

(a) Pattern of spots of forest vegetation within a grassland matrix as observable in Zambia at and around 13°46'40 S and 25°16'24E (image from 01/05/2014 accessed on Google Earth®).

(b) Pattern of spots of forest vegetation within a savanna matrix as observable in Cameroon (Mpem-Djim National Park) from an UAV-borne photograph taken on 16/12/2019, P. Couteron).

Figure 1: Some vegetation mosaics of trees and grasses in Zambia and in Cameroon.

Only a few mathematically tractable and space-explicit tree-grass interactions models have been designed for humid environments. For instance, Yatat Djeumen et al. [2] studied a PDE-based model where dynamics of a forest-grassland pattern were studied by the mean of a bistable travelling wave. Notably, they showed that depending on the fire frequency, forest could either invade grassland (i.e. forest encroachment) or recede. Goel et al. [37] examined, using a reaction-

diffusion model, the contribution of dispersal to determining savanna and forest distributions. Their reaction-diffusion model considered a one-variable (scalar) equation describing the dynamics of tree cover and took into account fire and mean annual rainfall. Their 2D reaction-diffusion model was able to reproduce the spatial aggregation of biomes with a stable savanna-forest boundary.

In the same vein, Wuyts et al. [38] proposed a reaction-diffusion model of Amazonian tree cover. Their model was able to reproduce some observations of spatial distribution of forest versus savanna. However, as pointed out in Yatat Djeumen et al. [2], modelling biomasses, instead of covers like in [37, 38], helps to take into account the fact that plant types are not mutually exclusive at a given point in space since field studies suggested that grass often develops under scattered tree crowns (see Yatat Djeumen et al. [2] and references therein). Moreover, [37, 38] emphasized the effect of precipitation on possible vegetation transitions while Yatat Djeumen et al. [39] suggested that, interplay between fire and water availability may give more realistic scenarios of vegetation distribution or transitions. Recently, Patterson et al. [40] proposed to bridge the gap between ecological models with macroscopic viewpoints (deterministic models) and microscopic descriptions of stochastic transitions (stochastic models). They studied a spatial extension of the tropical cover model of Staver and Levin [41], characterized by nonlocal interactions describing the evolution of the probability for a patch of landscape to be in a given state (to be understood as, small spatial areas of the typical size of a single tree, allowing growth of new trees). From an ecological stand point, the analysis of their model enabled a more thorough understanding of the determinant of forest-savanna boundary, particularly in the presence of precipitation, resources limitation and climate changes. Notwithstanding notable exceptions, like Patterson et al. [40], a common point of some of these models is that authors mainly relied on numerical simulations to render some spatial structures and relate them to processes. However, due to the absence of qualitative analyses, it is quite difficult to assess how model outcomes respond to model parameter variations.

In the context of humid savannas, patterns approaching regularity are fairly scarce, but not absent (see Figure 1 pannel (a) and also Lejeune et al. [36] or Tlidi et al. [6]). Another class of patterns is made of clearly aperiodic groves in the context of a mosaic that often corresponds to savannas transiting to forests (e.g. see Figure 1 pannel (b)).

Our objective in this paper is therefore to build a mathematically tractable space-explicit PDE-like model in order to study dynamics of spatial structuring of vegetation in wet savanna zones (Figure 1, pannel (b)). Tractability is an important property because it allows an efficient exploration of all parts of the parameter space ensuring that interesting situations, notably linked to multistability, are not missed as it might happen if only relying on computer simulations like in CA-based models (Yatat Djeumen et al. [39]). Another aim is to identify key mechanisms and bifurcation parameters that may shape possible transitions of vegetation physiognomy and trigger spatial pattern emergence in wet savannas. Therefore, based on a mathematical model, we aim to give new insights for the development of relevant management plans of forest-savanna mosaics. Our model is based on, and therefore extend, the recent ODE model of Yatat Djeumen et al. [39]. Indeed, based on a minimalistic (in terms of state variables and parameters) ODE model, Yatat Djeumen et al. [39] analysed fire-mediated tree-grass interactions and obtained a stability map within the fire vs. mean annual rainfall parameters space. They delineated regions of monostabilities (i.e. where desert, forest, grassland or savanna is stable), regions of multistabilities involving forest, grassland and savanna as well as multistabilities involving several savanna states. In addition, for all levels of rainfall, decreasing woody biomass with increasing fire frequency was verified contrary to almost all recent works of the same complexity or less (e.g. Accatino et al. [42]). Our model takes into account the fire resistance strategy of trees, and the main processes present in Yatat's model, such as the grass-fire feed-back and decreasing fire impact with woody biomass. In addition, we incorporate nonlocal interaction terms of intra and interspecific competition. In fact, intraspecific competition influences the growth of species (either trees or grasses) and ultimately changes the dynamics of the entire population (Kothari et al. [43]) and interspecific competition (i.e. asymmetric competition

of trees on grasses) leads to a reduction in grass cover and therefore a reduction in the spread and intensity of fires. Though this paper puts emphasis on the conditions for stable, spatially regular patterns, it opens prospects for studying transient and metastable patterns. The rest of the paper is organized as follows: section 2 presents the construction of the model, section 3 deals with the theoretical analyses of the model including the existence and uniqueness of solutions and linear stability analysis of homogeneous stationary solutions. Section 4 deals with numerical illustrations of theoretical results.

2. Model construction

Our model is based on Yatat Djeumen et al. [39] where authors considered two state variables, $G(t)$ and $T(t)$ that stand for the grassy biomass and the woody biomass at time t, respectively (G in $t.ha^{-1}$ and T in $t.ha^{-1}$). In Yatat Djeumen et al. [39], the following hypotheses are done:

- Trees and grasses biomasses have a logistic growth.
- Grass biomass mortality or suppression may result from natural mortality, external factors (grazing, termites, human actions, etc), interactions with tree biomass and fire.
- Tree biomass mortality may result from natural mortality, external factors (browsers, human actions, etc) or is fire-induced. In fact, fire momentum is an increasing nonlinear function of G, while its impact on woody vegetation is a decreasing nonlinear function of woody biomass T.

Starting from these assumptions, we incorporated a spatial component on state variables. Precisely, $G(x,t)$ and $T(x,t)$ denote the normalized densities (by grass and tree carrying capacities K_G and K_T, in $t.ha^{-1}$) of biomass of grass and tree, respectively, at a spatial point x and at a time t. Then, $0 \leq T(x,t) \leq 1$ and $0 \leq G(x,t) \leq 1$. We consider the following assumptions:

- Tree and grass biomasses, have a logistic growth but with an intraspecific competition which takes place in a nonlocal way, through the respective root systems of the two lifeforms. In fact, a tree (respectively grass) located at a point x, can consume resources (water, nutriment) at a point y where, another tree (respectively grass) is located or where its roots are present. Then,

$$\gamma_T T(x,t)\left(1-\int_{-\infty}^{+\infty}\phi_{M_2}(x-y)T(y,t)dy\right) \text{ and } \gamma_G G(x,t)\left(1-\int_{-\infty}^{+\infty}\phi_{M_1}(x-y)G(y,t)dy\right) \tag{1}$$

  describe the logistic growth with intraspecific competition where, for $i = 1, 2$, the kernel $\phi_{M_i}(x-y)$ represents, the level of consumption of resources in the area $[-M_i; M_i]$ of the space domain, γ_G (respectively, γ_T) denotes the intrinsic growth rate of grasses (respectively, trees).

- According to Craine and Dybzinski [44], trees facilitate the germination and the recruitment of new trees by improving the conditions under or around the canopy. In fact, sapling establishment for example depends on tree cover, not just because of seed production but also by local facilitation of seedlings and saplings by other trees via hydrological facilitation and shading (Li. et al. [45]). Then, we assume that there is a factor of cooperation Ω between trees that promotes regrowth and growth of young trees, helping them to reach a fire and/or browser non-vulnerability height. Hence the γ_T coefficient of exponential growth in equation (1) is substituted by $\gamma_T(1+\Omega T)$.

- Trees negatively impact the dynamics of grass biomass in a nonlocal way. Indeed, a tree located at a point y can, either by its root system or by the shade created by its crown, reduces the density of grasses located at a point x by reducing the resources (light availability, nutrients) in x. Then, the term

$$\gamma_{TG} G(x,t) \int_{-\infty}^{+\infty} \phi_{M_2}(x-y) T(y,t) dy \tag{2}$$

describes this nonlocal interspecific impact where $\gamma_{TG} = K_T \eta_{TG}$ and η_{TG} is the tree-grass interaction parameter in $ha.t^{-1}.yr^{-1}$. The consequence here is the reduction of the grass continuum on the ground, which will reduce the spread of fire. This term will depress grass biomass growth.

- The function describing the impact of fires, $\omega(G)$, on tree biomass depends on G. Indeed, in savanna ecology it is widely admitted that dried-up grass biomass is the main factor controlling both fire intensity and spreading capacity. For simplicity, we combined these two properties of fire in a single (fire momentum), increasing function of grass-biomass, expressing that when the average herbaceous biomass is in its highest range, fires simultaneously display the highest intensity and affect all the landscape. Conversely, low grass biomass due to aridity, grazing or tree competition, will make fires of low intensity and/or unable to reach all locations in a given year thereby decreasing the actual average frequency (see for instance Yatat Djeumen et al. [39]). Following Tchuinte et al. [46], Yatat Djeumen et al. [2, 39], we consider a Holling Type III function

$$\omega(G) = \frac{G^2}{G^2 + g_0^2}, \tag{3}$$

where $g_0 = \dfrac{\mu}{K_G}$ and μ is the grass biomass at which fires reach its half maximal momentum.

- We consider a function of fire-induced tree mortality that decreases with the cumulated woody biomass around any space point x. If trees are numerous and/or tall, then their mortality due to fire will be reduced. Indeed, tree parts above the flame zone are immune to topkills. This function is therefore, a decreasing function of tree biomass. In analogy with the work of Martinez-Garcia et al. [47], we consider a function of the form :

$$\mathcal{V}_T(x) = \exp\left(-p \int_{-\infty}^{+\infty} \phi_{M_2}(x-y) T(y,t) dy\right), \tag{4}$$

where $p = K_T \delta$ and δ is a parameter proportional to the inverse of biomass destroyed at intermediate level of mortality, in $t^{-1}.ha$, see also Yatat Djeumen et al. [39] for a nonspatial version of $\mathcal{V}_T$.

- We also assume, according to Yatat Djeumen et al. [2], that grass biomass and tree biomass, display local isotropic biomass diffusion in space with the coefficient D_G and D_T respectively, that are modelled with Laplace operators. Here, as a first approximation, we consider local diffusion of biomasses and neglect the long-range seed dispersal.

All this leads to the following model:

$$\begin{cases} \dfrac{\partial G}{\partial t} &= D_G \dfrac{\partial^2 G}{\partial x^2} + \gamma_G G \left(1 - \displaystyle\int_{-\infty}^{+\infty} \phi_{M_1}(x-y) G(y,t) dy\right) - \delta_G G \\ & \quad -\gamma_{TG} G \left(\displaystyle\int_{-\infty}^{+\infty} \phi_{M_2}(x-y) T(y,t) dy\right) - \lambda_{fG} f G, \\ \dfrac{\partial T}{\partial t} &= D_T \dfrac{\partial^2 T}{\partial x^2} + \gamma_T T(1+\Omega T) \left(1 - \displaystyle\int_{-\infty}^{+\infty} \phi_{M_2}(x-y) T(y,t) dy\right) - \delta_T T \\ & \quad -\lambda_{fT} f \omega(G) \exp\left(-p \displaystyle\int_{-\infty}^{+\infty} \phi_{M_2}(x-y) T(y,t) dy\right) T, \end{cases} \tag{5}$$

where $x \in K = (-l, l)$ and $t > 0$. Parameters are defined in table 1 bellow. The initial data are

$$0 \leq T(x,0) = T_0(x) \quad \text{and} \quad 0 \leq G(x,0) = G_0(x), \tag{6}$$

where $G_0(x)$ and $T_0(x)$ are bounded and sufficiently smooth functions. In addition, we also consider homogeneous Neumann boundary condition:

$$\frac{\partial T(x,t)}{\partial x} = \frac{\partial G(x,t)}{\partial x} = 0 \quad \text{at} \quad x = -l \quad \text{and} \quad x = l, \quad l > 0. \tag{7}$$

We assume that the kernels ϕ_{M_i}, $(i = 1, 2)$ are nonnegative even functions with compact support in the interval $[-M_i, M_i]$. Then, for $0 \leq M_i \leq l$, we consider the step function kernels:

$$\phi_{M_i}(x) = \begin{cases} \dfrac{1}{2M_i} & , \quad |x| \leq M_i, \\ 0 & , \quad |x| > M_i, \end{cases} \qquad i = 1, 2,$$

with ϕ_0 a Dirac function and $\displaystyle\int_{-\infty}^{+\infty} \phi_{M_i}(y) dy = 1$. For the chosen kernel function ϕ_{M_i}, the strength of nonlocal interaction is the same with the range $[x - M_i, x + M_i]$. However, other forms of kernels have been considered in the literature dedicated to pattern formation, notably Gaussian kernels and Laplace kernels (see for instance Lefever and Lejeune [7], Lefever et al. [8], Lefever and Turner [9]). The choice of the step function kernels in this work was mainly motivated by the type of nonlinearities in our model and model's mathematical analysis. Indeed, we found that Gaussian and Laplace kernels are not able to induce patterns with our model (see also Remark 4, page 15 or Remark 6, page 16). Following Yatat Djeumen et al. [39], the f (in yr^{-1}) parameter is taken as constant multiplier of $\omega(G)$ in system (5), and we interpret it as a man-induced 'targeted' fire frequency (as for instance in a fire management plan), which will not automatically translate everywhere into actual frequency of fires of notable intensity (because of $\omega(G)$). With this interpretation, the actual fire regime may substantially differ from the targeted one, as frequently observed in the field (see for instance Diouf et al. [48] in southern Niger). We therefore distinguish fire frequency from fire intensity because grass biomass controls fire spread (see e.g. Govender et al. [49], McNaughton [50], Yatat Djeumen et al. [2] and references therein).

Symbols	Description	Units
γ_G	Intrinsic growth of grasses	yr^{-1}
δ_G	Grass biomass loss due to human activities and herbivory	yr^{-1}
λ_{fG}	Portion of grass biomass loss due to fire	
γ_{TG}	Tree grass interaction parameter	yr^{-1}
γ_T	Intrinsic growth of trees	yr^{-1}
δ_T	Tree biomass loss due to human activities	yr^{-1}
λ_{fT}	Portion of tree biomass loss due to fire	
p	proportional to the inverse of biomass destroyed at intermediate level of mortality	
Ω	Cooperation factor	
f	fire frequency	yr^{-1}
D_G	Grass biomass diffusion rate	$ha^2.yr^{-1}$
D_T	Tree biomass diffusion rate	$ha^2.yr^{-1}$
M_1	Range of grass spatial nonlocal interaction	m
M_2	Range of tree spatial nonlocal interaction	m

Table 1: Definition of parameters used in the model.

3. Mathematical analysis

3.1. Existence and uniqueness of solutions of system (5)-(7)

Let $\overline{K} = [-l, l]$ be the closure of K, and for any $\tau > 0$, we set:

$$D_\tau = K \times (0, \tau], \quad \overline{D}_\tau = \overline{K} \times [0, \tau], \quad S_\tau = \partial K \times (0, \tau]. \tag{8}$$

Denote by $C^\alpha(D_\tau)$ the set of Hölder continuous functions in D_τ with the exponent $\alpha \in (0; 1)$, and $C(D_\tau)$, the set of continuous functions in D_τ. Denote also by $C^{2,1}(D_\tau)$ the set of functions that are twice continuously differentiable in x and once continuously differentiable in t. For simplicity, throughout this paper, we denote:

$$\begin{array}{rcl} f_1(G,T) & = & \gamma_G G\left(1-\phi_{M_1} * G\right) - \delta_G G - \gamma_{TG} G\left(\phi_{M_2} * T\right) - \lambda_{fG} f G, \\ f_2(G,T) & = & \gamma_T T(1+\Omega T)\left(1-\phi_{M_2} * T\right) - \delta_T T - \lambda_{fT} f \omega(G) \exp\left(-p\phi_{M_2} * T\right) T, \end{array} \tag{9}$$

with

$$\left(\phi_{M_1} * G\right)(x) = \int_{-\infty}^{+\infty} \phi_{M_1}(x-y) G(y,t) dy \quad \text{and} \quad \left(\phi_{M_2} * T\right)(x) = \int_{-\infty}^{+\infty} \phi_{M_2}(x-y) T(y,t) dy \tag{10}$$

where ϕ_{M_i} is a spatial kernel function satisfying:

$$\int_{-\infty}^{+\infty} \phi_{M_i}(y) dy = 1, \quad i = 1, 2. \tag{11}$$

Definition 1. *(Tian et al. [51])*
A pair of nonnegative functions $\tilde{\mathbf{U}} = (\tilde{G}, \tilde{T})'$ *and* $\hat{\mathbf{U}} = (\hat{G}, \hat{T})' \in \mathcal{C}(\overline{D}_\tau) \cap \mathcal{C}^{2,1}(D_\tau)$ *is called upper*

and lower solutions of (5) *if* $\tilde{\mathbf{U}} \geq \hat{\mathbf{U}}$ *and if*

$$\begin{aligned}
&\frac{\partial \tilde{G}}{\partial t} - D_G \Delta \tilde{G} \geq \gamma_G \tilde{G}\left(1 - \phi_{M_1} * \tilde{G}\right) - \delta_G \tilde{G} - \gamma_{TG} \tilde{G}\left(\phi_{M_2} * \hat{T}\right) - \lambda_{fG} f \tilde{G}, && in \quad D_\tau \\
&\frac{\partial \tilde{T}}{\partial t} - D_T \Delta \tilde{T} \geq \gamma_T \tilde{T}(1 + \Omega \tilde{T})\left(1 - \phi_{M_2} * \tilde{T}\right) - \delta_T \tilde{T} - \lambda_{fT} f \omega(\hat{G}) \exp\left(-p \phi_{M_2} * \tilde{T}\right) \tilde{T}, && in \quad D_\tau \\
&\frac{\partial \hat{G}}{\partial t} - D_G \Delta \hat{G} \leq \gamma_G \hat{G}\left(1 - \phi_{M_1} * \hat{G}\right) - \delta_G \hat{G} - \gamma_{TG} \hat{G}\left(\phi_{M_2} * \tilde{T}\right) - \lambda_{fG} f \hat{G}, && in \quad D_\tau \\
&\frac{\partial \hat{T}}{\partial t} - D_T \Delta \hat{T} \leq \gamma_T \hat{T}(1 + \Omega \hat{T})\left(1 - \phi_{M_2} * \hat{T}\right) - \delta_T \hat{T} - \lambda_{fT} f \omega(\tilde{G}) \exp\left(-p \phi_{M_2} * \hat{T}\right) \hat{T}, && in \quad D_\tau
\end{aligned} \tag{12}$$

$$\frac{\partial \hat{G}}{\partial t}, \frac{\partial \hat{T}}{\partial t} \leq 0, \frac{\partial \tilde{G}}{\partial t}, \frac{\partial \tilde{T}}{\partial t} \geq 0 \quad on \quad S_\tau.$$

$$\tilde{G}(x,0) \geq G(x,0), \quad \tilde{T}(x,0) \geq T(x,0), \quad \hat{G}(x,0) \leq G(x,0) \quad \hat{T}(x,0) \leq T(x,0) \quad x \in K.$$

The ordering relation $\tilde{\mathbf{U}} \geq \hat{\mathbf{U}}$ means that $\tilde{G} \geq \hat{G}$ and $\tilde{T} \geq \hat{T}$ for $(x,t) \in D_\tau$.
For a given pair of ordered upper and lower solutions $\tilde{\mathbf{U}}$ and $\hat{\mathbf{U}}$, we set:

$$\langle \hat{\mathbf{U}}, \tilde{\mathbf{U}} \rangle = \left\{ \mathbf{U} = (G,T)' \in \mathcal{C}(\overline{D}_\tau) : \hat{\mathbf{U}} \leq \mathbf{U} \leq \tilde{\mathbf{U}} \right\}. \tag{13}$$

Let us consider the following thresholds:

$$\begin{cases} \mathcal{R}_G = \dfrac{\gamma_G}{\delta_G + f\lambda_{fG}}, \\ \mathcal{R}_{G,0} = \dfrac{\gamma_G}{\delta_G}, \\ \mathcal{R}_{T,0} = \dfrac{\gamma_T}{\delta_T}. \end{cases} \tag{14}$$

Our model is designed for humid savannas where we assume that rainfall is sufficient to ensure that

$$\mathcal{R}_{G,0} > 1, \quad \text{and} \quad \mathcal{R}_{T,0} > 1. \tag{15}$$

Hence, in the rest of the paper, we assume that (15) holds true.

Theorem 1 (Existence and uniqueness of global solution)**.** *Assume that the following three conditions are valid.*

- $\mathcal{R}_G > 1$,
- *the initial functions* $G(x,0)$ *and* $T(x,0) \in C^\alpha(D_\tau) \cap C(\overline{D}_\tau)$ *and*
- $0 \leq (G_0(x), T_0(x))' \leq 1$.

Then, the nonlocal reaction-diffusion system (5)-(7) admits a unique global solution $\mathbf{U}^*(x,t) = (G^*(x,t), T^*(x,t))'$ *for* $(x,t)' \in K \times (0,+\infty)$ *and*

$$0 \leq G^*(x,t) \leq W_1, \qquad 0 \leq T^*(x,t) \leq W_2, \tag{16}$$

where

$$
\begin{aligned}
W_1 &= \max\left\{\sup_K G(0,x), 1-\frac{1}{\mathcal{R}_G}\right\},\\
W_2 &= \max\left\{\sup_K T(0,x), 1-\frac{1}{\mathcal{R}_{T,0}}\right\}, \quad \textit{if} \;\; \Omega = 0,\\
W_2 &= \max\left\{\sup_K T(0,x), \frac{\sqrt{(1-\Omega)^2+4\Omega\left(1-\frac{1}{\mathcal{R}_{T,0}}\right)}-(1-\Omega)}{2\Omega}\right\}, \quad \textit{if} \;\; \Omega > 0.
\end{aligned}
$$

Proof. See Appendix A, page 35. □

3.2. Space homogeneous steady states and linear stability analysis

Our aim in this section is to derive a condition on spatial convolution such that an equilibrium or space homogeneous steady state is locally stable in the case $M_1 = M_2 = 0$ but unstable for some $M_i > 0$, $i = 1, 2$.

3.2.1. The local case: $M_1 = M_2 = 0$

Due to the fact that the local spatio-temporal model (LSTM) associated to the system (5) is quasi-monotone decreasing (Smith [52]), we have the two following consequences. First, the LSTM can not lead to pattern formation (see e.g Kishimoto and Weinberger [53], Banerjee and Volpert [54], [55]) and second, the linear stability analysis of homogeneous steady states associated to LSTM is the same as for the space-implicit model i.e., the ODE model associated to system (5). The space-implicit ODE model corresponding to system (5) is:

$$
\left\{
\begin{array}{rcl}
\dfrac{dG}{dt} &=& \gamma_G G(1-G) - \delta_G G - \gamma_{TG} TG - \lambda_{fG} fG,\\
\dfrac{dT}{dt} &=& \gamma_T T\left(1+\Omega T\right)(1-T) - \delta_T T - \lambda_{fT} f\omega(G)\exp(-pT)T,
\end{array}
\right. \tag{17}
$$

with non negative initial data.

In this part, we are interested in the behavior of steady states of system (17), notably in the characterization of their stability properties. Recall that steady states of system (17) are also space homogeneous steady states of system (5). Steady states of (17) are solutions of system (18):

$$
\left\{
\begin{array}{rcl}
\gamma_G G(1-G) - \delta_G G - \gamma_{TG} TG - \lambda_{fG} fG &=& 0,\\
\gamma_T T(1+\Omega T)(1-T) - \delta_T T - \lambda_{fT} f\omega(G)\exp(-pT)T &=& 0.
\end{array}
\right. \tag{18}
$$

Recall that we assumed that (15) is valid meaning that, the desert (the state with absence of vegetation) can not be stable. The following result is valid.

Proposition 1. ***(Steady states of system (17))***
The system (5) admits three homogeneous steady states.

a) a desert steady state $E_0 = (0,0)'$.

b) a forest steady state such that:

- *When $\Omega = 0$, then $E_{T_1} = \left(0, 1-\dfrac{1}{\mathcal{R}_{T,0}}\right)'$ is the forest steady state. This is the case of no tree-tree facilitation.*

$*$ *When* $\Omega > 0$, *then* $E_{T_2} = (0, T_2)' = \left(0, \dfrac{\sqrt{(1-\Omega)^2 + 4\Omega\left(1 - \dfrac{1}{\mathcal{R}_{T,0}}\right)} - (1-\Omega)}{2\Omega} \right)'$ *is the forest steady state. This is the case of tree-tree facilitation.*

c) a grassland steady state:

$$E_{G_e} = (G_e, 0)' = \left(1 - \frac{1}{\mathcal{R}_G}, 0\right)'.$$

Remark 1. *It is straightforward to observe that* E_{T_2} *is an increasing function of* Ω.

We are now interested in the coexistence steady state (savanna steady state); set:

$$\begin{aligned}
a &= -\frac{\lambda_{fG} f + \delta_G}{\gamma_{TG}}, \\
b &= \frac{\gamma_G}{\gamma_{TG}}, \\
\theta &= 2(a+b)b\Omega\gamma_T + \gamma_T(1-\Omega)b, \\
\alpha &= \Omega\gamma_T b^2, \\
q &= (\gamma_T - \delta_T) + \gamma_T(\Omega - 1)(a+b) - \Omega\gamma_T(a+b)^2, \\
m &= \lambda_{fT} f \exp\left(-p(a+b)\right), \\
\theta^* &= \frac{24\alpha + mpb\left((pb)^2 + 6(pb) + 6\right)\exp(pb)}{6},
\end{aligned}$$

and

$$\mathcal{R}_T = \frac{\gamma_T}{\delta_T + \lambda_{fT} f \omega(G_e)}, \quad \mathcal{R}_{F,f} = \frac{\gamma_G}{\delta_G + \lambda_{fG} f + \gamma_{TG} T_i}, \quad \mathcal{R}^1_\Omega = \frac{\gamma_T(1-\Omega)}{p\lambda_{fT} f \omega(G_e)}. \tag{19}$$

Proposition 2. ***(Savanna steady state)***

- ***case I****:* $f = 0$.
  If $\mathcal{R}_{F,f=0} > 1$, *then we have a unique savanna steady state* $E_s = (G^*, T^*)'$ *such that*

$$G^* = 1 - \frac{1}{\mathcal{R}_{F,f=0}} \quad \textit{and} \quad T^* = T_i, i = 1, 2. \tag{20}$$

- ***case II****:* $f > 0$ *and* $\gamma_{TG} = 0$.
  The savanna steady state $E^* = (G^*, T^*)'$ *verifies:*

$$\begin{cases} G^* = G_e \\ \Omega\gamma_T(T^* - T_2)(T^* - T_{2-}) + \lambda_{fT} f \omega(G_e)\exp(-pT^*) &= 0 \end{cases} \tag{21}$$

  where $T_{2-} = -\dfrac{(1-\Omega) + \sqrt{(1-\Omega)^2 + 4\Omega(1 - \frac{\delta_T}{\gamma_T})}}{2\Omega}$. *Hence:*
  - $*$ *if* $\mathcal{R}^1_\Omega > 1$, *then there may exist* 0 *or* 1 *savanna steady state.*
  - $*$ *if* $\mathcal{R}^1_\Omega < 1$, *then there may exist* 0, 1 *or* 2 *savanna steady states.*

- ***case III****:* $f > 0$ *and* $\gamma_{TG} \neq 0$.
  The savanna steady state $E_s = (G^*, T^*)'$ *must satisfy these two relations:*

$$-\alpha(G^*)^4 + \theta(G^*)^3 - m\exp(pbG^*)(G^*)^2 + (q - \alpha g_0^2)(G^*)^2 + \theta g_0^2 G^* + q g_0^2 = 0, \tag{22}$$

  and

$$T^* = (a+b) - bG^*. \tag{23}$$

Moreover G^* must satisfy the inequality

$$\max\left\{G_e - \frac{\gamma_{TG}}{\gamma_G}; 0\right\} < G^* < G_e. \tag{24}$$

We can therefore summarize the maximum number of savanna steady states according to the following cases:

- ***Case 1**: $\theta < mpb$*

Condition	$q < m + \alpha g_0^2$	$q > m + \alpha g_0^2$
Maximal number of savanna steady states	2	3

Table 2: Maximal number of savanna steady states of system (17) with $\theta < mpb$

- ***Case 2**: $\theta > mpb$,*

Condition	$\theta < \theta^*$	$\theta > \theta^*$
Maximal number on savanna steady states	4	3

Table 3: Maximal number of savanna steady states of system (17) with $\theta > mpb$

Proof. See Appendix B, page (38). □

Remark 2. *Let us set*

$$\mathcal{R}_G^0 = \frac{2\gamma_G}{2\lambda_{fG}f + 2\delta_G + \gamma_{TG}}, \quad \mathcal{R}_{TG} = \frac{2\gamma_{TG}}{2\lambda_{fG}f + 2\delta_G + \gamma_{TG}} \quad \textit{and} \quad \mathcal{R}^* = \frac{\gamma_T\left(1 + \Omega\frac{\mathcal{R}_G^0}{\mathcal{R}_{TG}}\right)}{p\lambda_{fT}f\exp\left(-p(a+b)\right)}.$$

- *If $\mathcal{R}^* < 1$, then $\theta < mpb$ and if $\mathcal{R}^* > 1$, then $\theta > mpb$.*
- *$\mathcal{R}^*$ is the primary production of tree including a portion of tree production due to tree-tree cooperation and asymmetric tree-grass competition relative to fire induced tree and grass loss.*

Now, we want to characterize local stability property of previous steady states. System (17) is a planar, competitive and dissipative system. Hence, based on Smith [52, Theorem 2.2, page 35], we deduce that solutions of system (17) will always converge toward an equilibrium point. That is, no stable limit cycles may exist for system (17).

Proposition 3. ***(Stability properties of trivial and semi trivial steady states).*** *The following results are valid for system (17).*

(a) *The desert steady state $E_0 = (0, 0)'$ is always unstable.*

(b) *If $\mathcal{R}_F < 1$ then the forest steady state E_{T_i} is locally asymptotically stable (LAS).*

(c) *If $\mathcal{R}_T < 1$ then the grassland steady state $E_{G_e} = (G_e; 0)'$ is LAS.*

Now we deal with conditions of stability of a savanna steady state when its exists. Set:

$$\begin{aligned} \mathcal{R}_1^* &= \frac{\gamma_T\left[(1-\Omega) + 2\Omega T^*\right]}{p\lambda_{fT}f\omega(G^*)\exp(-pT^*)}, \\ \mathcal{R}_2^* &= \frac{\gamma_{TG}\omega'(G^*)}{p\gamma_G\omega(G^*)}. \end{aligned} \tag{25}$$

Proposition 4. ***(Stability condition of a savanna steady state).*** *The stability conditions of a coexistence steady state, of system (17), when it exists are given by the following cases:*

- ***case 1****:Assume $f = 0$, then $(G^*, T^*)'$ is LAS.*
- ***case 2****: Assume $f > 0$. If:*

$$\mathcal{R}_1^* - \mathcal{R}_2^* > 1, \tag{26}$$

then $(G^*, T^*)'$ is LAS.

Proof. See Appendix C, page 56. □

Remark 3. *(i) $\mathcal{R}_{T,0} = \dfrac{\gamma_T}{\delta_T}$ denotes the primary production of tree biomass relative to tree biomass loss due to human activities and herbivory.*

(ii) $\mathcal{R}_{G,0} = \dfrac{\gamma_G}{\delta_G}$ is the primary production of grass biomass relative to grass biomass loss due to human activities and herbivory.

(iii) $\mathcal{R}_G = \dfrac{\gamma_G}{\delta_G + f\lambda_{fG}}$ denotes the primary production of grass biomass relative to grass biomass loss due to grazing or human action and additional fire induced biomass loss.

(iv) $\mathcal{R}_T = \dfrac{\gamma_T}{\delta_G + \lambda_{fT} f\omega(G_e)}$ is the primary production of tree biomass relative to fire-induced biomass loss at the grassland equilibrium and the additional loss due to herbivory (grazing) or human action.

(v) $\mathcal{R}_{F,f} = \dfrac{\gamma_G}{\delta_G + f\lambda_{fG} + \gamma_{TG} T_i}$ represents the primary production of grass biomass, relative to grass biomass loss induced by fire, herbivory (grazing) or human action and additional grass suppression due to tree competition, at the closed forest equilibrium.

3.2.2. The nonlocal case (M_1 or $M_2 > 0$)

Our aim now is to derive a condition on spatial convolution such that a steady state $(G_s, T_s)' \in \{(G_e, 0)'; (0, T_2)'; (G^*, T^*)'\}$ is locally asymptotically stable in the case $M_1 = M_2 = 0$, but unstable for some $M_i > 0, \quad i = 1, 2$.
In fact, the spatial patterns appearing in the nonlocal savanna model (5) can be studied by performing a linear stability analysis of the stationary homogeneous solution of (5) given by the system (18). Linearizing the integro-differential system (5) around $(G_s; T_s)'$, leads to the following results:

Proposition 5. ***(linearized system)***
Set: $g(x,t) = G(x,t) - G_s$ and $h(x,t) = T(x,t) - T_s$ two perturbations around a non trivial homogeneous steady state. The system obtained after linearization is:

$$\begin{cases} \dfrac{\partial g}{\partial t} &= D_G \dfrac{\partial^2 g}{\partial x^2} + \left[\gamma_G(1 - G_s) - \delta_G - \gamma_{TG} T_s - \lambda_{fG} f\right] g - \gamma_G G_s \displaystyle\int_{-\infty}^{+\infty} \phi_{M_1}(x-y) g(y,t)dy \\ & \quad -\gamma_{TG} G_s \displaystyle\int_{-\infty}^{+\infty} \phi_{M_2}(x-y) h(y,t)dy, \\ \dfrac{\partial h}{\partial t} &= D_T \dfrac{\partial^2 h}{\partial x^2} + \left[(\gamma_T(1 + \Omega T_s)(1 - T_s) - \delta_T - \lambda_{fT} f\omega(G_s)\exp(-pT_s)) + \gamma_T \Omega T_s(1 - T_s)\right] h \\ & \quad + \left(p\lambda_{fT} f\omega(G_s)\exp(-pT_s)T_s - \gamma_T T_s(1 + \Omega T_s)\right) \displaystyle\int_{-\infty}^{+\infty} \phi_{M_2}(x-y) h(y,t)dy \\ & \quad -\lambda_{fT} f\omega'(G_s)\exp(-pT_s)T_s g. \end{cases} \tag{27}$$

Proof. See Appendix D, page 57. □

Now we are in position to study linear stability around all non trivial homogeneous steady state.

Linear stability analysis around the grassland homogeneous steady state $E_G = (G_e, 0)'$.
Set :

$$\begin{array}{rcl} b_{11} & = & \gamma_G G_e, \\ b_{12} & = & \gamma_{TG} G_e, \\ b_{22} & = & \gamma_T - \delta_T - \lambda_{fT} f \omega(G_e). \end{array} \tag{28}$$

The following results hold:

Proposition 6. ***(Linearized system around the grassland homogeneous steady state)*** *Let* $g(x,t) = G(x,t) - G_e$ *and* $h(x,t) = T(x,t)$ *be two perturbations around the grassland homogeneous steady state. The system obtained after linearization is:*

$$\left\{ \begin{array}{rcl} \dfrac{\partial g}{\partial t} & = & D_G \dfrac{\partial^2 g}{\partial x^2} - b_{11} \displaystyle\int_{-\infty}^{+\infty} \phi_{M_1}(x-y) g(y,t) dy - b_{12} \int_{-\infty}^{+\infty} \phi_{M_2}(x-y) h(y,t) dy, \\ \dfrac{\partial h}{\partial t} & = & D_T \dfrac{\partial^2 h}{\partial x^2} + b_{22} h. \end{array} \right. \tag{29}$$

By considering the eigenvalue problem of the system (29) where λ is the eigenvalue and taking the Fourier transform of this eigenvalue problem, we obtain the following system:

$$\left\{ \begin{array}{rcl} \lambda \overline{g}(k) & = & -D_G k^2 \overline{g}(k) - b_{11} \overline{\phi_{M_1}}(k) \overline{g}(k) - b_{12} \overline{\phi_{M_2}}(k) \overline{h}(k), \\ \lambda \overline{h}(k) & = & -D_T k^2 \overline{h}(k) + b_{22} \overline{h}(k), \end{array} \right. \tag{30}$$

where k is the wavenumber ($k \in \mathbb{R}$) with $\overline{\phi_{M_i}}(k) = \dfrac{\sin kM_i}{kM_i}$, where, $\overline{g}(k)$, $\overline{h}(k)$ *and* $\overline{\phi_{M_i}}(k)$ are the Fourier transforms of the functions $g(x,t)$, $p(x,t)$ and $\phi_{M_i}(x)$, respectively.
Therefore, the system in (30) can be written in the matrix form:

$$\lambda \begin{pmatrix} \overline{g}(k) \\ \\ \overline{h}(k) \end{pmatrix} = \begin{bmatrix} -D_G k^2 - b_{11} \overline{\phi_{M_1}}(k) & -b_{12} \overline{\phi_{M_2}}(k) \\ \\ 0 & -D_T k^2 + b_{22} \end{bmatrix} \begin{pmatrix} \overline{g}(k) \\ \\ \overline{h}(k) \end{pmatrix}. \tag{31}$$

Let us consider:

$$M = \begin{bmatrix} -D_G k^2 - b_{11} \overline{\phi_{M_1}}(k) & -b_{12} \overline{\phi_{M_2}}(k) \\ \\ 0 & -D_T k^2 + b_{22} \end{bmatrix}, \tag{32}$$

$$Tr(M) = -\left(D_G + D_T\right) k^2 - b_{11} \overline{\phi_{M_1}}(k) + b_{22}, \tag{33}$$

and

$$Det(M) = D_G D_T k^4 + \left[b_{11} D_T \overline{\phi_{M_1}}(k) - b_{22} D_G \right] k^2 - b_{11} b_{22} \overline{\phi_{M_1}}(k). \tag{34}$$

Therefore, the grassland homogeneous steady state is locally asymptotic stable if:

$$Tr(M) < 0, \tag{35}$$

and

$$Det(M) > 0. \tag{36}$$

If (36) is not satisfied then we have an inhomogeneous solution call pattern (deriving from a Turing bifurcation).
We are now in position to find Turing bifurcation threshold around the grassland homogeneous steady state. Because of the form of $\overline{\phi_{M_1}}(k)$, we set $z = kM_1$ and denote, for simplicity, $\overline{\phi_{M_1}}(k)$ by $\overline{\phi_1}(z)$.

Theorem 2. ***(Stability of the Grassland homogeneous steady state)***

If $\mathcal{R}_T < 1$ and $\overline{\phi_1}(z) > 0$ for all z, then the grassland homogeneous steady state is locally asymptotically stable for system (5).

Proof. Assume that $\mathcal{R}_T < 1$. Then, $b_{22} < 0$ thanks to the stability conditions of the grassland steady state in the space-implicit model (see for instance proposition 3, page 12). Therefore, if $\overline{\phi_1}(z) > 0$, then $Tr(M) < 0$ and $Det(M) > 0$. □

Remark 4. *The previous theorem ensures that for this model, the choice of Gaussian kernels can not lead to pattern formation around the grassland homogeneous steady state. More generally, due to the type of nonlinearities involved in our model, the class of kernel-functions called "positive-definite functions" and characterized by a positive Fourier transform (see also Bochner [56] and Tzanakis [57]) are such that the empirically evidenced vegetation patterns are not reachable with the model. Then, $\overline{\phi_1}(z) < 0$ is a necessary condition for spatial Turing instability around the grassland homogeneous steady state and this could happen if ϕ_1 has discontinuities.*

Theorem 3. ***(Grassland homogeneous steady state instability)***
Assume that $\mathcal{R}_T < 1$ and we have a range of positive values of z such that:

$$\overline{\phi_1}(z) < 0 \tag{37}$$

holds ; If there exists a critical point M_1^T such that :

$$M_1 > M_1^T \Rightarrow \frac{1}{(M_1)^2} \leq S_1(z_1), \tag{38}$$

where

$$S_1(z) = \frac{-\overline{\phi}_1(z)}{z^2}\left(\frac{b_{11}}{D_G}\right), \tag{39}$$

and z_1 is the value of z such that $S_1(z)$ takes it global maximum, then the homogeneous grassland steady state is unstable. Furthermore, system (5) undergoes Turing bifurcation at $M_1 = M_1^T$.

Proof. See Appendix E page 58. □

Remark 5. *The space period σ_G of the spatial structure is given by: $\sigma_G = \dfrac{2\pi M_1}{z_1}$ (see also Genieys et al. [58, page 71]) where z_1 is given in the previous theorem.*

Linear stability analysis around the forest homogeneous steady state $E_T = (0, T_i)'$**,**$i = 1, 2..$ Set:

$$\begin{array}{rcl} m_{11} & = & -\gamma_G + (\delta_G + \lambda_{fG} f) + \gamma_{TG} T_i, \\ m_{22}^* & = & \gamma_T \Omega T_i (1 - T_i), \\ m_{22}^{**} & = & \gamma_T T_i (1 + \Omega T_i). \end{array}$$

Proposition 7. ***(linearized system around the forest homogeneous steady state)***
Set: $g(x,t) = G(x,t)$ and $h(x,t) = T(x,t) - T_i$ two perturbations around the forest homogeneous steady state. The system obtained after linearization is:

$$\left\{ \begin{array}{rcl} \dfrac{\partial g}{\partial t} & = & D_G \dfrac{\partial^2 g}{\partial x^2} - m_{11} g, \\ \dfrac{\partial h}{\partial t} & = & D_T \dfrac{\partial^2 h}{\partial x^2} + m_{22}^* h - m_{22}^{**} \displaystyle\int_{-\infty}^{+\infty} \phi_{M_2}(x - y) h(y,t) dy. \end{array} \right. \tag{40}$$

By considering the eigenvalue problem of the system (40) and in the same way like in proposition 6, we obtain the following theorem:

Theorem 4. ***(Forest homogeneous steady state stability)***
If $\mathcal{R}_F < 1$ *and* $\overline{\phi_2}(z) > \dfrac{m_{22}^*}{m_{22}^{**}}$ *for all* z*, then the forest homogeneous steady state is locally asymptotically stable for system* (5)*, where* $\overline{\phi_2}(z)$ *denotes the Fourier transform of* ϕ_{M_2}*.*

Proof. The proof is done like for theorem 2, page 14. Hence, we omitted it. □

Remark 6. *In the case of no tree-tree facilitation, by the previous theorem, the use of Gaussian kernels can not lead to inhomogeneous patterned solution in the vicinity of forest homogeneous steady state because with* $\Omega = 0$*,* $m_{22}^* = 0$ *and then, the condition (with Gaussian kernels) of local stability of the forest homogeneous steady state is always verified.*

Theorem 5. ***(Forest homogeneous steady state instability)***
Assume that $\mathcal{R}_{F,f} < 1$ *and we have a range of positive values of* z *such that:*

$$\overline{\phi_2}(z) < \frac{m_{22}^*}{m_{22}^{**}} \tag{41}$$

holds. If there exist a critical value $M_2^T > 0$ *such that:*

$$M_2 > M_2^T \Rightarrow \frac{1}{(M_2)^2} \leq S_2(z_2), \tag{42}$$

where

$$S_2(z) = -\frac{\overline{\phi}_2(z)}{z^2}\left(\frac{m_{22}^{**}}{D_T}\right) + \frac{1}{z^2}\left(\frac{m_{22}^*}{D_T}\right), \tag{43}$$

and z_2 *is the value of* z *such that* $S_2(z)$ *takes a global maximum. Then, the forest homogeneous steady state is unstable and system* (5) *undergoes a Turing bifurcation at* $M_2 = M_2^T$*.*

Proof. The proof is similar to the proof of the theorem 3 in *Appendix E*, page 58. Therefore, it is omitted. □

Remark 7. *The space period of the spatial structures* σ_T *observed in this case is given by* $\sigma_T = \dfrac{2\pi M_2}{z_2}$ *(see also Genieys et al. [58]), where* z_2 *is given in the previous theorem.*

Linear stability analysis around the savanna homogeneous steady state $E^* = (G^*, T^*)$.
Set:

$$\begin{aligned}
a_{11} &= -\gamma_G G^*,\\
a_{12} &= -\gamma_{TG} G^*,\\
a_{21} &= -\lambda_{fT} f\omega'(G^*)\exp(-pT^*)T^*,\\
a_{22} &= -\gamma_T\left[(1-\Omega)T^* + 2\Omega(T^*)^2\right] + p\lambda_{fT} f\omega(G^*)\exp(-pT^*)T^*,\\
c &= \gamma_T \Omega T^*(1-T^*).
\end{aligned}$$

Proposition 8. ***(Linearized system around the savanna coexistence state)***
Let $g(x,t) = G(x,t) - G^*$ *and* $h(x,t) = T(x,t) - T^*$ *be two perturbations around the savanna homogeneous steady state. The system obtained after linearization is:*

$$\begin{cases}
\dfrac{\partial g}{\partial t} &= D_G \dfrac{\partial^2 g}{\partial x^2} + a_{11}\displaystyle\int_{-\infty}^{+\infty} \phi_{M_1}(x-y)g(y,t)dy + a_{12}\int_{-\infty}^{+\infty} \phi_{M_2}(x-y)h(y,t)dy,\\
\dfrac{\partial h}{\partial t} &= D_T \dfrac{\partial^2 h}{\partial x^2} + (a_{22}-c)\displaystyle\int_{-\infty}^{+\infty} \phi_{M_2}(x-y)h(y,t)dy + ch + a_{21}g.
\end{cases} \tag{44}$$

Then, by considering the eigenvalue problem of the system (44) where λ is the eigenvalue and taking the Fourier transform of this eigenvalue problem, we obtain the following system:

$$\begin{cases} \lambda\overline{g}(k) &= -D_G k^2\overline{g}(k) + a_{11}\overline{\phi_{M_1}}(k)\overline{g}(k) + a_{12}\overline{\phi_{M_2}}(k)\overline{h}(k), \\ \lambda\overline{h}(k) &= -D_T k^2\overline{h}(k) + c\overline{h}(k) + (a_{22}-c)\overline{\phi_{M_2}}(k)\overline{h}(k) + a_{21}\overline{g}(k), \end{cases} \tag{45}$$

where k is the wavenumber ($k \in \mathbb{R}$) with $\overline{\phi_{M_i}}(k) = \dfrac{\sin kM_i}{kM_i}$, $i = 1, 2$ where, $\overline{g}(k)$, $\overline{h}(k)$ *and* $\overline{\phi_{M_i}}(k)$ are the Fourier transforms of the functions $g(x,t)$, $p(x,t)$ and $\phi_{M_i}(x)$.

Proposition 9. ***(Characteristic equation)***
The Characteristic equation of system (45) is:

$$\lambda^2 - Tr(k, M_1, M_2)\lambda + Det(k, M_1, M_2) = 0, \tag{46}$$

where:

$$Tr(k, M_1, M_2) = -(D_G + D_T)k^2 + a_{11}\overline{\phi_{M_1}}(k) + a_{22}\overline{\phi_{M_2}}(k) + (1 - \overline{\phi_{M_2}}(k))c, \tag{47}$$

and

$$\begin{aligned} Det(k, M_1, M_2) &= D_G D_T k^4 - \left[a_{22}D_G\overline{\phi_{M_2}}(k) + a_{11}D_T\overline{\phi_{M_1}}(k) + cD_G(1 - \overline{\phi_{M_2}}(k))\right]k^2 + \\ & a_{11}(a_{22}-c)\overline{\phi_{M_1}}(k)\overline{\phi_{M_2}}(k) + ca_{11}\overline{\phi_{M_1}}(k) - a_{12}a_{21}\overline{\phi_{M_2}}(k). \end{aligned} \tag{48}$$

From the characteristic equation (46), we can write the stability conditions of the savanna homogeneous steady state (G^*, T^*) as follows:

$$Tr(k, M_1, M_2) < 0, \tag{49}$$

and

$$Det(k, M_1, M_2) > 0. \tag{50}$$

To determine the stability boundary, we need to determine the thresholds for k, M_1, and M_2 such that only one of the eigenvalue of the characteristic equation (46) crosses the origin from the left to the right and other eigenvalues have negative real parts. If (49) holds and (50) is not satisfied, then there is a real eigenvalue crossing the origin. Initially ($k = M_1 = M_2 = 0$), (49) and (50) hold. So we find the thresholds k^T, M_1^T and M_2^T so that (50) is not satisfied (it is call Turing Bifurcation). Therefore, we find the value of parameters for which $Det(k, M_1, M_2)$ is non-negative for all values of k, M_1 and M_2 and equals to zero at the points of its minima. Then, these thresholds correspond to the minima of the stability boundary region and satisfy:

$$Det(k, M_1, M_2) = 0, \quad \frac{\partial Det(k, M_1, M_2)}{\partial M_1} = 0, \quad \frac{\partial Det(k, M_1, M_2)}{\partial M_2} = 0, \quad \frac{\partial Det(k, M_1, M_2)}{\partial k} = 0. \tag{51}$$

With the given conditions in (51) we deduce the following result:

Theorem 6. ***(Stationary pattern condition around the savanna homogeneous steady state)***
Consider z_1 and z_2 two positive solutions of the equation $\tan(z) = z$ ($z_1 < z_2$) such that: $\mu_j = \dfrac{\sin z_j}{z_j} < 0$, $j = 1, 2$. Then, suppose that:

$$\mathcal{R}_1^* - \mathcal{R}_2^* > 1 \quad \textit{and} \quad \frac{a_{11}(c - a_{22})\mu_1\mu_2}{ca_{11}\mu_1 - a_{12}a_{21}\mu_2} < 1. \tag{52}$$

Assume also that:

$$M_j > M_j^T := z_j \left(\frac{D_G D_T}{(a_{11}a_{22} - ca_{11})\,\mu_1\mu_2 + ca_{11}\mu_1 - a_{12}a_{21}\mu_2} \right)^{1/4}, \quad j = 1, 2, \tag{53}$$

and

$$k > k^T := \left(\frac{(a_{11}a_{22} - ca_{11})\,\mu_1\mu_2 + ca_{11}\mu_1 - a_{12}a_{21}\mu_2}{D_G D_T} \right)^{1/4}. \tag{54}$$

Then we have the appearance of periodic solutions in space in the neighborhood of savanna homogeneous steady state.

Proof. See Appendix F, page 58. □

Because of the difficulty of interpretation of the second condition in (52), we find a sufficient condition to the previous one. Set:

$$\mathcal{R}_3^* = \frac{\gamma_T(1 + \Omega T^*)}{p\lambda_{fT} f\omega(G^*)\exp(-pT^*)}.$$

It is straightforward to observe that $\mathcal{R}_1 - \mathcal{R}_2 < \mathcal{R}_3$ and that $\mathcal{R}_3 > 1$ implies that the second condition of (52) is valid. Therefore, the following result holds true:

Theorem 7. ***(Sufficient condition)***
If $\mathcal{R}_1^* - \mathcal{R}_2^* > 1$, then the conclusion of Theorem 6 is valid.

Remark 8.
1. *$\mathcal{R}_3^*$ is the primary production of tree biomass and additional production of tree biomass due to tree-tree facilitation relative to fire induced tree biomass loss.*
2. *Condition (53) gives the range beyond which the nonlocal interactions are sufficient for the coexistence of both tree and grass inhomogeneous solutions in the same space domain.*
3. *Due to the implicit nature of the equation (48), it is difficult to provide explicit expression of Turing bifurcation threshold analytically and hence we have describe one way in previous theorem to determine a triplet (k^T, M_1^T, M_2^T) as a suitable choice of M_1 and M_2 to obtain stationary Turing Pattern (see also Banerjee and Volpert [59]). However the space period of spatial structure is $\sigma = \dfrac{2\pi}{k_{max}}$ where k_{max} is the most unstable mode, that could be computed numerically.*

4. Numerical illustration

Our model is designed for humid savannas. Then, carrying capacities considered, before the normalization of biomasses are $K_G = 17t.ha^{-1}$ and $K_T = 340t.ha^{-1}$. These values were obtained from Yatat Djeumen et al. [39] considering that the mean annual rainfall $\mathbf{W}$ is equal to 1500 $mm.yr^{-1}$. We also assume that $D_G = 0.1$ and $D_T = 1$ (see e.g. Yatat Djeumen et al. [2]). The finite difference method was used to discretize the spatial part and on the other hand, the non standard finite difference method (Anguelov et al. [60]) was used to discretize the temporal part of the problem given by the system (5) (see for instance Appendix G). Our numerical illustrations in this paper are suitable for a 9 hectare (ha) savanna square domain (for instance, Martinez-Garcia et al. [47] considered for example a square patch of savanna of 1 ha). Due to the fact that we have restricted the mathematical analysis to a domain of dimension 1, numerical illustrations are carried out in the space interval $[0; 300]$. The unit of space considered is meter (m) and unit of time is year (yr).

Parameters	D_G	D_T	γ_G	δ_G	γ_T	δ_T	λ_{fG}	λ_{fT}	p	g_0	Ω
Values	0.1	1	2.7	0.1	1	0.3	0.7	0.8	3.4	0.14	5

Table 4: Parameter values for simulation.

Parameter values (see Table 4, page 18) used for model (5) are based on (Yatat Djeumen et al. [5, 39], Accatino et al. [42]). Only Ω, D_G and D_T are assumed.
We first illustrate a bifurcation diagram, for the space-implicit model related to system (5), with respect to variations of the fire frequency f and γ_{TG}, the parameter that shapes the competition of tree on grass.

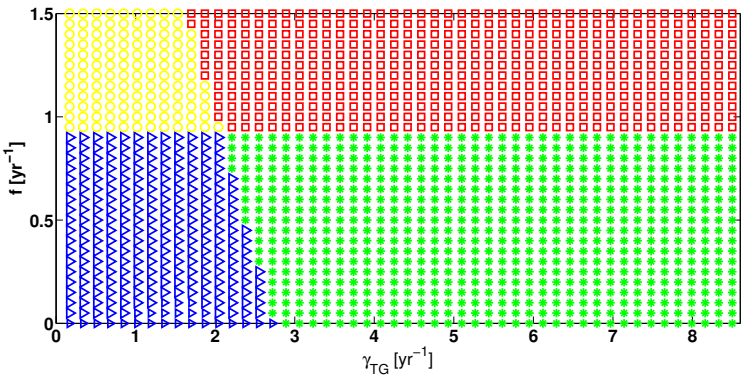

Figure 2: Bifurcation diagram according to variations of γ_{TG} and f. The blue triangle corresponds to the savanna monostability, the red square stands for the forest-grassland bistability, the green star denotes the forest monostability and the yellow circle represents the grassland-savanna bistability.

From figure 2, one deduces that, at least for parameters considered in table 4, stable forest state is easily found, but, for low values of tree-grass competition, savannas are present. We also notice that when we approach the annual fire regime and proceed beyond we manage to recover the grassland state as part of a bistability situation. Then, the increase of the tree-grass competition parameter γ_{TG}, leads to the transition from savanna to forest or grassland-savanna to forest-grassland. In fact, in humid zone, the vegetation is intrinsically dominated by trees, that exert competition pressure on grass biomass, such that grass may be easily suppressed.
The increase of fire frequency leads to the reduction of tree biomass but thanks to tree-tree cooperation, trees can perpetuate. Therefore depending on the tree-grass competition parameter, the system switches are either savanna to grassland-savanna or forest to forest-grassland.
Now we want to illustrate the spatial structuring of trees and grasses in the various cases displayed on the previous bifurcation diagram (see figure 2 in page 19).

4.1. Case of forest monostability ($f = 0.9$ *and* $\gamma_{TG} = 5.1$)

With the choice of parameters in table 4, the homogeneous forest steady state $E_{T_2} = (0, 0.9477)'$ is locally asymptotic stable in absence of nonlocal interactions. Based on theorem 5, figure 3

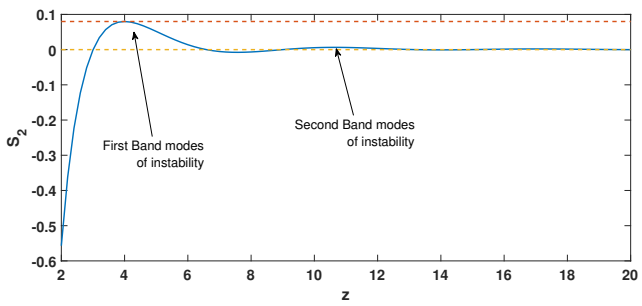

Figure 3: Graph of S_2 as a function of z. The parameter values are given in table 4. The red dashed line stands for $\frac{1}{(M_2)^2}$.

depicts that the forest homogeneous steady state is unstable for those M_2 such that the curve of $S_2(z)$ intersects with the line $\frac{1}{(M_2)^2}$. For those values, we see that the minimum M_2 required for the emergence of the Turing instability verified approximately $\frac{1}{(M_2^T)^2} = 0.0798$ (see the red dashed line in figure 3), then $M_2^T = 3.54m$. Therefore, we choose $M_1 = 0.5m$ and $M_2 = 20m$ and we consider the initial data as a random perturbation of the forest homogeneous steady state $(0, T_2)'$:

$$G(x,0) = 0 + \epsilon_1, \quad T(x,0) = T_2 + \epsilon_2 \quad \text{with} \quad 0 \leq \epsilon_i \leq 10^{-3}$$

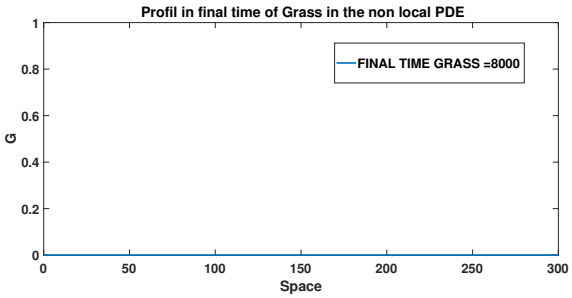

(a) Grass distribution in space at $t = 8000$.

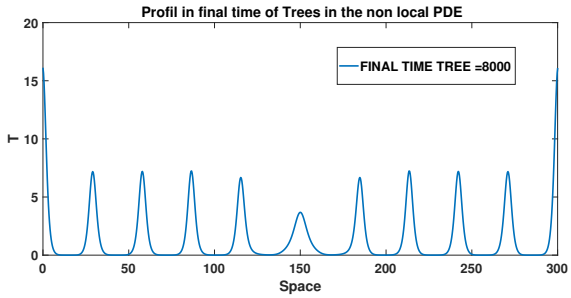

(b) Tree distribution in space at $t = 8000$.

Figure 4: Illustration of Grass and Tree profiles in space.

We observe from Figure 4 that the solution of system (5) converges toward a space inhomogeneous forest solution, thanks to a Turing bifurcation.

The key thresholds in that situation are $\mathcal{R}_F$ (the primary production of grass biomass, relative to grass biomass loss induced by fire, herbivory (grazing) or human action and additional grass suppression due to tree competition, at the closed forest equilibrium) and M_2 the range of nonlocal competition of trees on grasses. Using a periodogram, we can numerically determine the number of patches in our inhomogeneous solution and we can therefore compute the associated spatial wavelength.

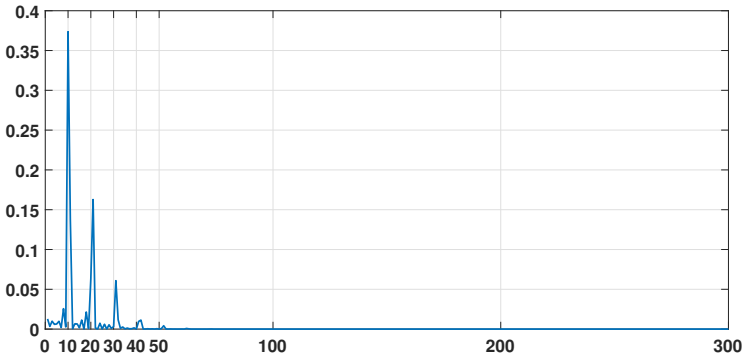

Figure 5: Graph of a periodogram of forest inhomogeneous solution

From figure 5, we have 10 patches in the spatial profile of forest distribution (see also panel (d) in figure 4). Therefore, the numerical wavelength is $\sigma_T = \frac{300}{10} = 30m$. However, from the linear stability analysis and the parameter values considered in this case, the theoretical wavelength is $\sigma_T = 31.4m$ which is quite close of the numerical space period. We also found that for increasing values of M_2, the space period (wavelength) σ_T increases.

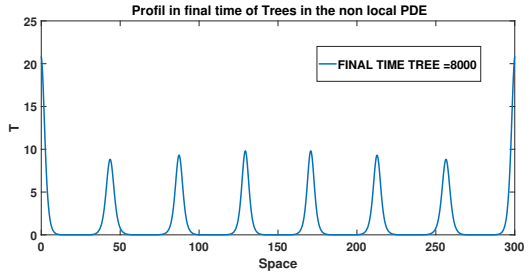

(a) Trees distribution at $t = 8000$ with $M_2 = 30m$.

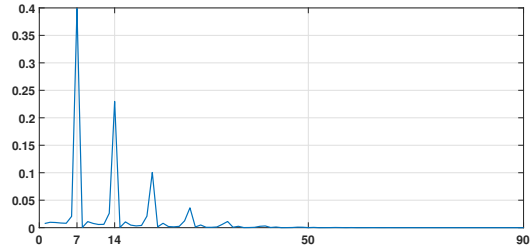

(b) Periodogram of trees distribution with $M_2 = 30m$

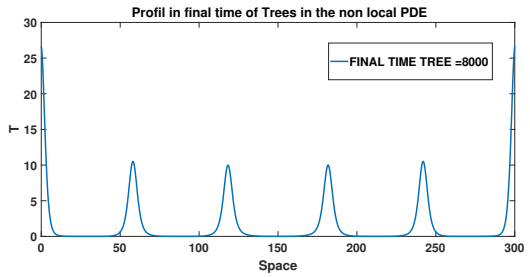

(c) Trees distribution at $t = 8000$ with $M_2 = 40m$.

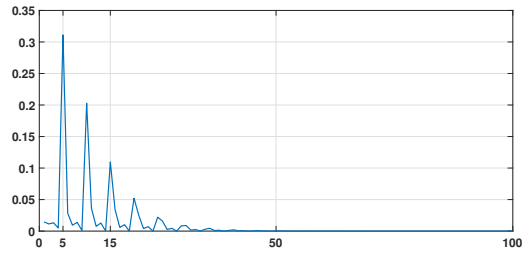

(d) Periodogram of trees distribution with $M_2 = 40m$

Figure 6: Illustration of Trees distribution profiles in final time and the corresponding periodogram.

Figure 6 shows that the numerical wavelength of tree distribution is $\sigma_T = \frac{300}{7} = 42.8m$ with $M_2 = 30m$ and $\sigma_T = \frac{300}{5} = 60m$ with $M_2 = 40m$. By linear stability analysis, the space period is $\sigma_T = 47.1m$ for $M_2 = 30m$, $\sigma_T = 62.8m$ for $M_2 = 40m$

4.2. Case of savanna monostability ($f = 0.9$ *and* $\gamma_{TG} = 1.7$)

We find that the savanna steady state $E^* = (0.1345, 0.9453)'$ is locally asymptotically stable in the absence of nonlocal interactions. Moreover, the minimal positive solution of the equation $\tan(z) = z$ is $z_1 = 4.49$. We take $z_2 = 10.9$ which is also solution of $\tan(z) = z$.
From these two values, we find $\mu_1 = -0.22$, $\mu_2 = -0.09$ and we get the Turing bifurcation condition: $M_1 > 5.07m$ and $M_2 > 12.32m$. For illustration we choose $M_1 = 5.5m$, $M_2 = 15m$ and we consider the initial data as a random perturbation of the savanna equilibrium (G^*, T^*).

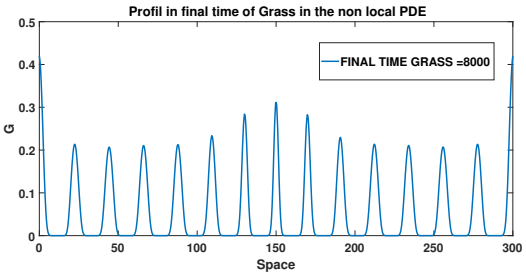

(a) grass distribution at $t = 8000$.

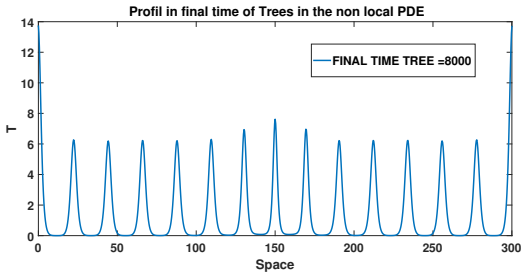

(b) Tree distribution at $t = 8000$.

Figure 7: Illustration of Grass and Tree profiles in space at final times.

We observe from figure 7 that, solutions of system (5) converge toward a space inhomogeneous tree-grass coexistence solution thanks, to a Turing bifurcation. In the same way as before, we are interested in the wavelength resulting from this inhomogeneous solution.

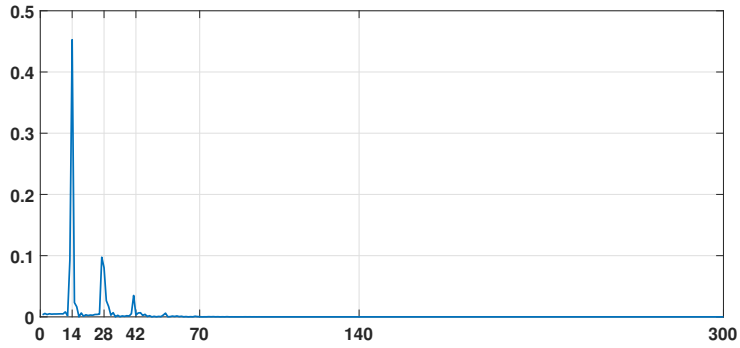

Figure 8: Periodogram of savana inhomogeneous solution

Figure 8 depicts that the savanna inhomogenous solution illustrated in figure 7 has 14 cells. Then, the numerical wavelength in this case is $\sigma = \frac{300}{14} = 21.43m$. Theoretically, it is necessary to determine the most growing mode k_{max} for wich $Det(k_{max}, M_1, M_2) < 0$ and the wavelength will be $\sigma = \dfrac{2\pi}{k_{max}}$.

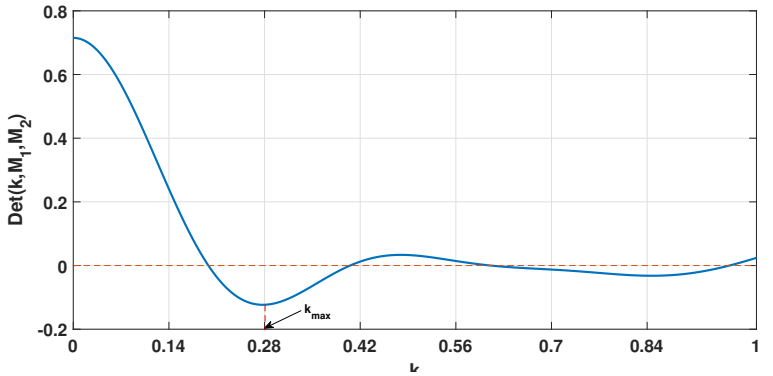

Figure 9: Graph of $Det(k, M_1, M_2)$ with $M_1 = 5.5m$ and $M_2 = 15m$

From figure 9, $k_{max} = 0.28$ and then $\sigma = 22.43m$.

The value of M_1 used previously could be questioned and seen too large. However, note that the Turing condition that we obtained is only a sufficient condition. Therefore, it may be possible that outside of these values, we can have a change of sign of $Det(k, M_1, M_2)$ which leads to a Turing bifurcation. To illustrate that point, we consider $M_1 = 0.5m$ and $M_2 = 25m$ and we draw $Det(k, M_1, M_2)$.

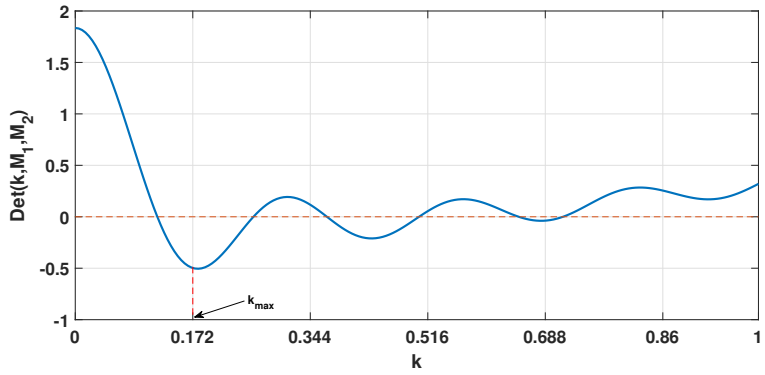

Figure 10: Graph of $Det(k, M_1; M_2)$ with $M_1 = 0.5m$ and $M_2 = 25m$.

From figure 10, we observe that it is possible to have a Turing bifurcation with $M_1 = 0.5m$ and $M_2 = 25m$ due to the change of sign of $Det(k, M_1, M_2)$. For these values of M_1 and M_2 we can thus illustrate the inhomogeneous solution obtained (see figure 11).

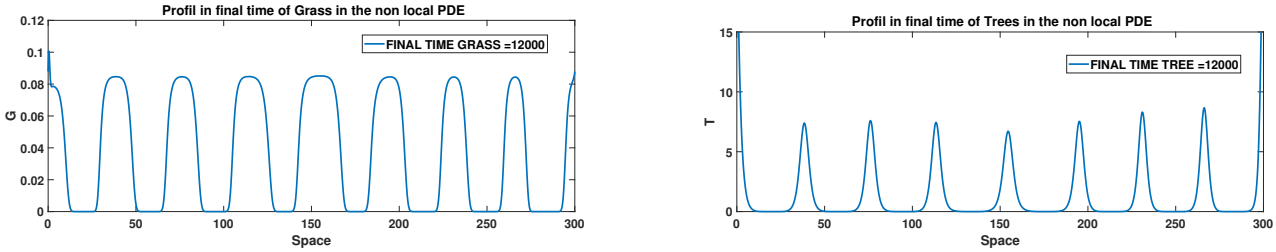

(a) Grass distribution at $t = 12000$.

(b) Tree distribution at $t = 12000$.

Figure 11: Illustration of Grass and Tree profiles in space at final times.

The graph of periodogram is illustrated in figure 12.

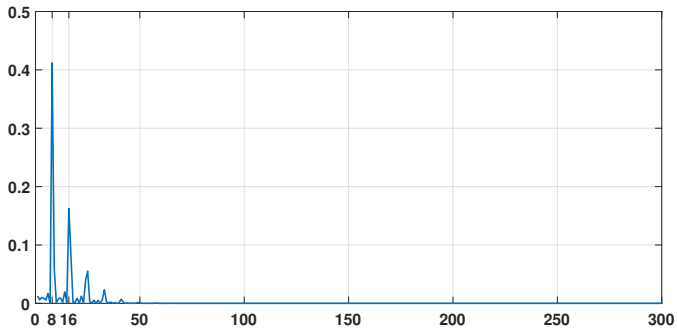

Figure 12: Periodogram of savana inhomogeneous solution

From figure 12, the numerical space period is $\sigma_T = 37.5m$ and the theoretical wavelength is $\sigma_T = \dfrac{2\pi}{0.172} = 36.5m$.

4.3. Case of bistability forest-grassland ($f = 0.98$ *and* $\gamma_{TG} = 5.1$)

In this case, in absence of nonlocal interactions we have a bistability situation with two homogeneous steady states: a grassland steady state E_G and a forest steady state E_{T_2}. We may

observe the spatial structuring of the two state variables in two cases: first around the grassland homogeneous steady state and second around the forest homogeneous steady state.

4.3.1. Around the grassland homogeneous steady state

In this section we will consider $D_G = 0.01$ and, for an easy display of figures, we reduce the size of the domain to $100m$, with $E_G = (0.7089; 0)'$.

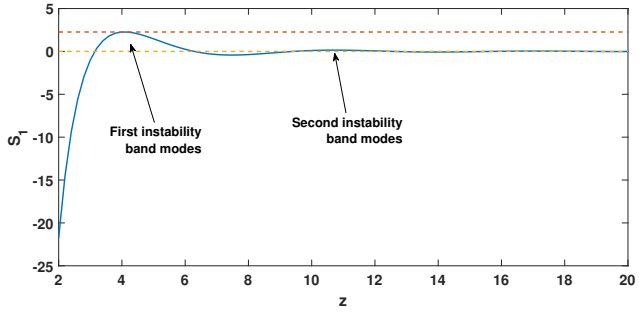

Figure 13: Graph of S_1 as a function of z with the parameter values given in table 4. The red dashed line stands for $\frac{1}{(M_1)^2}$.

Based on theorem 3, figure 13 illustrates that grassland homogeneous steady state is unstable for values of M_1 such that the curve of $S_1(z)$ intersects with the line $\frac{1}{(M_1)^2}$. The minimal value of M_1 such that the grassland equilibrium is unstable verified $\frac{1}{(M_1^T)^2} = 2.26$ (then $M_1^T = 0.6647m$) and we choose for illustration around the grassland equilibrium $M_1 = 1.5m$ and $M_2 = 20m$.

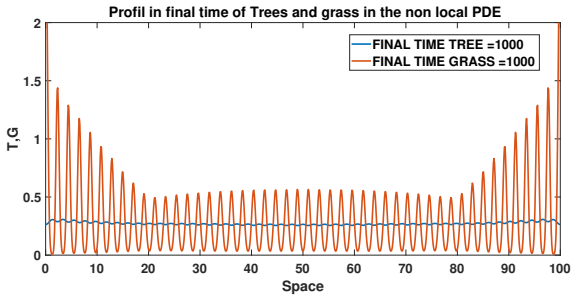

(a) Tree-grass distribution at $t = 1000$.

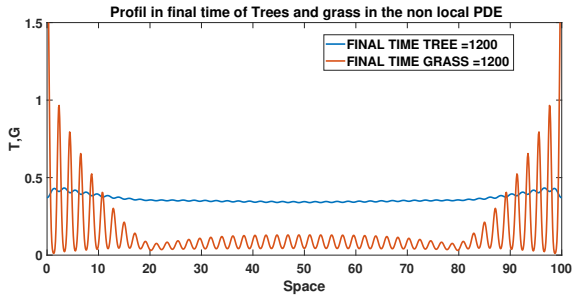

(b) Tree-grass distribution at $t = 1200$.

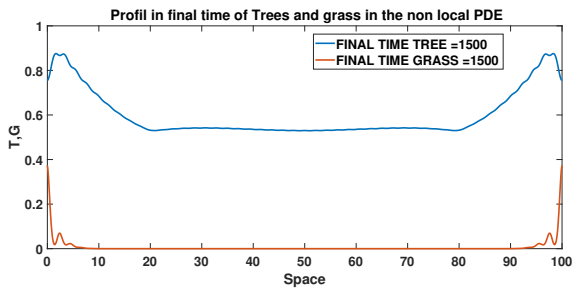

(c) Tree-grass distribution at $t = 1500$.

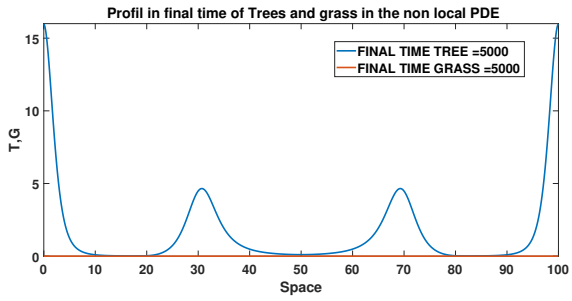

(d) Tree-grass distribution at $t = 5000$.

Figure 14: Illustration of Grass and Tree distributions.

Figure 14 suggests the existence of a metastable tree-grass pattern. In fact, from panel (a) one

could believe that we have an inhomogeneous solution of coexistence of the two species; but when we increase the simulation time, we observe that we are moving rather towards the inhomogeneous forest solution. So in this case we have the coexistence of unstable grassland inhomogenous solution and stable tree inhomogeneous solution. This type of solution is called a metastable state (see also Eigentler and Sheratt [61]). However, if we stop at a final time equal to 1000, we observe that the grassy biomass benefits from the space freed by the trees. We can further illustrate it with figure 15 for $M_1 = 3m$ and $M_2 = 20m$.

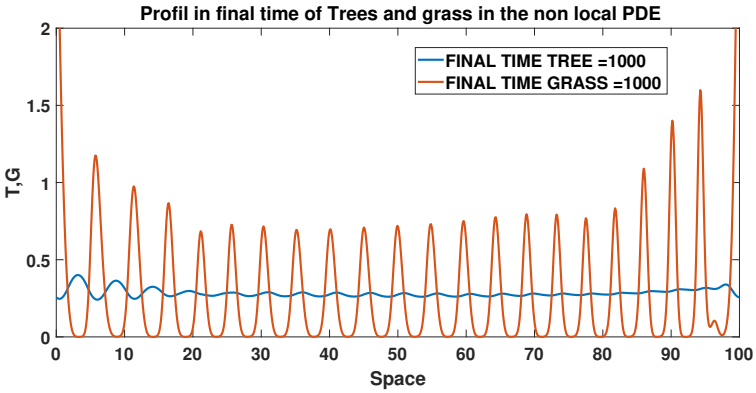

Figure 15: Tree-grass distribution at $t = 1000$

4.3.2. Around the forest homogeneous steady state

The forest homogeneous steady state is $E_{T_2} = (0, 0.9477)'$. As previously, to find the Turing bifurcation threshold M_2^T, we need to draw the curve of $S_2(z)$.

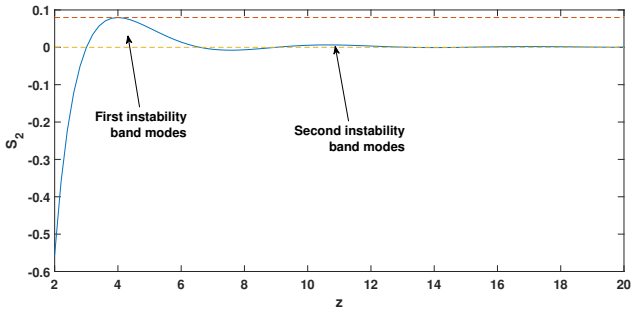

Figure 16: Graph of S_2 as a function of z with the parameter values given in table (4)

Figure 16 shows that the minimal value of M_2 such that the forest homogeneous steady state is unstable verified $\frac{1}{(M_2^T)^2} = 0.0798$ (then $M_2^T = 3.54m$). Hence, for illustration, we choose $M_1 = 0.5m$ and $M_2 = 20m$.

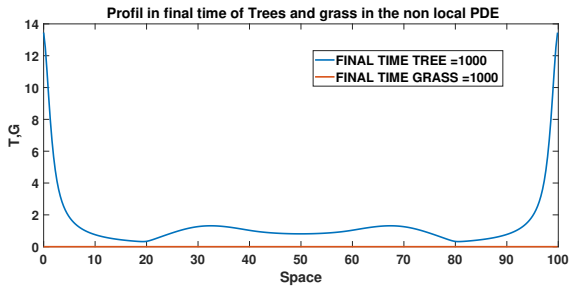

(a) Tree-grass distribution at $t = 1000$.

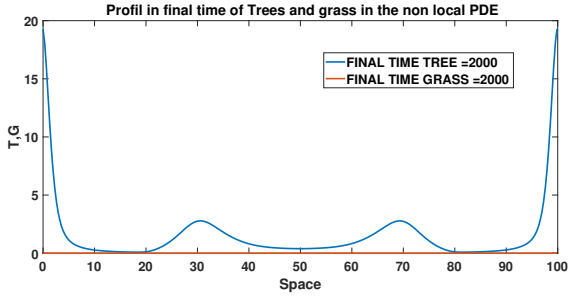

(b) Tree-grass distribution at $t = 2000$.

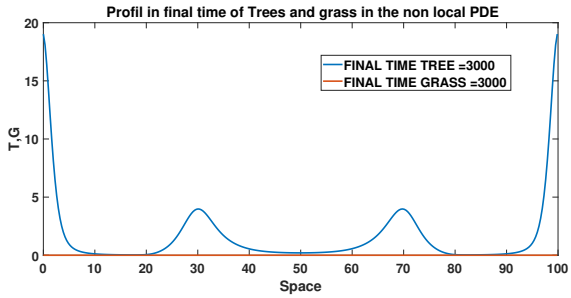

(c) Tree-grass distribution at $t = 3000$.

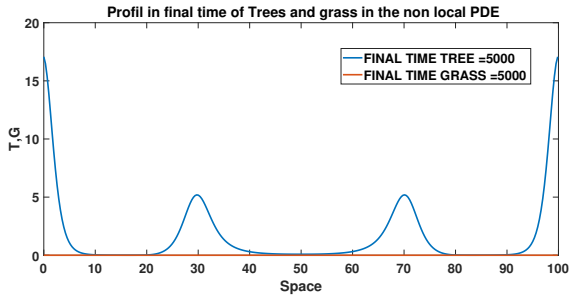

(d) Tree-grass distribution at $t = 5000$.

Figure 17: Illustration of Grass and Tree distributions.

Then by figure 17 the nonlocal system (5) converges toward a forest inhomogeneous stable solution, and numerical space period is $\sigma_T = 33.33m$ while theoretically, the space period is $\sigma_T = 31.42m$.

4.4. Case of bistability savanna-grassland ($f = 0.98$ and $\gamma_{TG} = 1.7$)

Considering parameter values in table 4, the savanna homogeneous steady state E^* and the grassland homogeneous steady state E_G are both locally asymptotically stable for the space implicit model related to system (5). In this section, the space domain is $[0, 100]$ and $D_G = 0.01$

4.4.1. Around the savanna homogeneous steady state

Around the savanna homogeneous steady state $E^* = (0.1136, 0.9455)'$ the Turing bifurcation condition are $M_1 > 2.97m$ and $M_2 > 7.21m$. To illustrate the appearance of inhomogeneous solution, we choose $M_1 = 3m$ and $M_2 = 20m$. Therefore, we have figure 18.

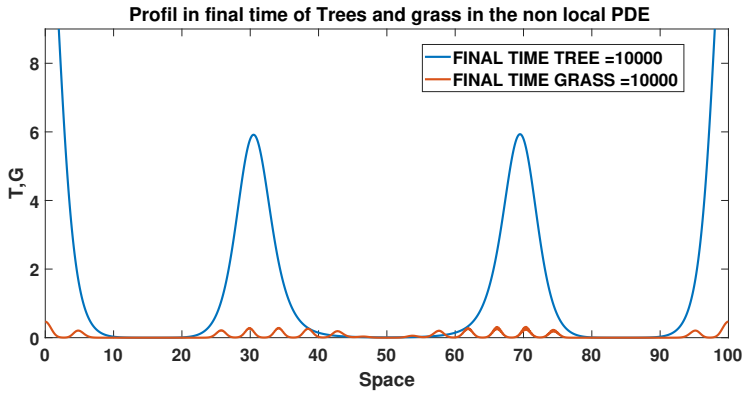

Figure 18: Tree-grass distribution at $t = 10000$.

The system converges toward a space inhomogeneous tree-grass coexistence solution (savanna) thanks, to a Turing bifurcation. We also observe that in figure 18, we have grass localized solution in space and regular tree spots.

4.4.2. Around the grassland homogeneous steady state

The grassland homogeneous steady state is $E_G = (0.7089, 0)'$ and is the same as before (see section 4.3.1). The Turing bifurcation threshold is the same as before. We choose $M_1 = 1.5m$, $M_2 = 20m$ for illustration. Figure 19 illustrates the spatial distribution of the inhomogeneous tree-grass (i.e. savanna) solution.

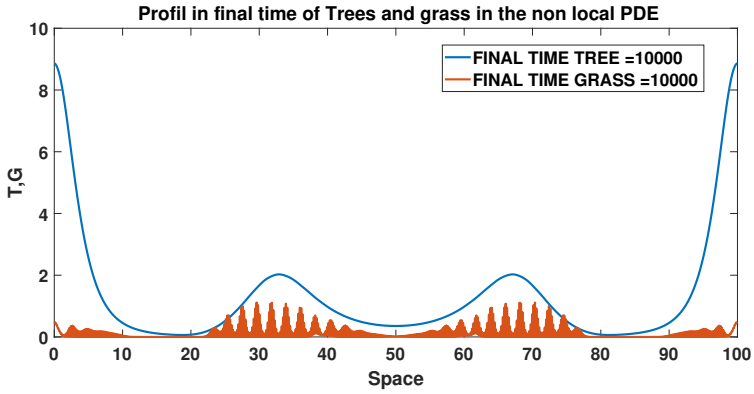

Figure 19: Tree-grass distributions at $t = 10000$.

Figure 19 shows a high density under the trees which is due to the range of interactions between the grasses which is quite low. However, if we push this range to $M_1 = 3m$, we obtain the following figure 20 which is similar to the structure obtained around the savanna homogeneous steady state.

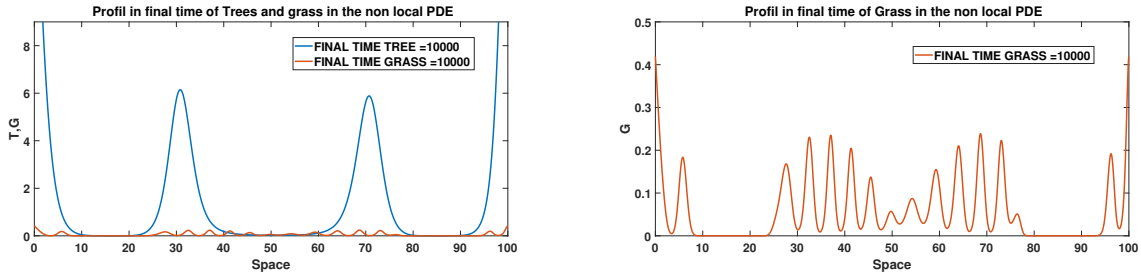

(a) Tree-grass distribution at $t = 10000$.

(b) zooming of grass distribution at $t = 10000$.

Figure 20: Illustration of Grass and Tree profiles in space at final times.

5. Discussion

We analyzed an integro-differential reaction-diffusion fire-mediated tree-grass interactions model, allowing to reach spatial patterns (namely, regular spotted pattern) sometimes observed in humid savannas. Starting from the parsimonious 2-dimensional ODE-based model of grassy and woody biomasses fire-mediated interactions studied in Yatat Djeumen et al. [39], we introduced local biomass propagation through Laplace operators, like in Yatat Djeumen et al. [2], as well as nonlocal interaction terms. Hence, our model improves and extends previous ODE models (e.g. Yatat Djeumen et al. [2, 39]) by explicitly taking into account spatial components and nonlocal terms of tree-grass interactions. We showed that the combination of the nonlocal tree-tree facilitation and the nonlocal tree-tree, grass-grass and tree-grass competition, may induce spatial patterns.

In fact, nonlocal interactions break up the homogeneous distribution of tree and grass biomass resulting in the emergence of a regular spotted pattern (see for instance Tian et al. [51]). Then, novelties in this paper include the consideration of nonlocal interaction terms (both facilitation and competition) on both trees and grasses dynamics. Indeed, in the absence of nonlocal terms, our model is unable to produce spatial patterns since the associated reaction-diffusion model is monotone decreasing (see also Yatat Djeumen et al. [2]). A key technical point is the requirement on kernels that must be constant functions with compact supports. Indeed, we show that Gaussian or Laplace-like kernels are not able to produce patterns in our model. According to Martinez-Garcia et al. [47], kernels whose Fourier transforms take negative values for some wavenumber values, will lead to clustering in some specific models with short range facilitation.

On the other hand, it is now acknowledged that fire is one of the key factors that shape the physiognomy of savanna vegetation, in general, and particularly, in humid savannas where rainfall is sufficient to promote very high grass biomass production which in turn constitutes the principal fuel for fires. However, as a response to the negative impact of fires, trees have developed 'defence' or resilience mechanisms in order to limit or to reduce the fire-induced tree mortality. Indeed, tree-tree facilitation or cooperation promotes germination of tree's seeds, the recruitment of new trees by improving the conditions under canopy (shading, litter and nutriments, enhanced water infiltration). We modelled this effect thanks to the Ω parameter that was added to the reference ODE model of Yatat Djeumen et al. [39] to make the unsaturated logistic growth a non linear function of trees biomass (T). By enhancing woody biomass growth, tree-tree facilitation indirectly reduces the grass layer or favours an heterogeneous spatial distribution of the grass layer which reduces fire intensity along with the potential of fire to spread all over the landscape.

Based on parameter values used for the bifurcation diagram (see figure 2, page 19), we explore and illustrate in the different regions of the bifurcation diagram, the spatial structuring of trees and grasses resulting from nonlocal interaction terms. We obtained broadly four types of inhomogeneous solutions: first, what we call forest inhomogeneous solution (obtained around the monostable forest space-homogeneous equilibrium) which are characterized by an absence of grass biomass and regular tree spots in the space domain. Second, the savanna inhomogeneous solutions which featured both tree and grass spots. Third, the coexistence of "localized" grass pattern and regular tree spots and, finally, the presence of metastable patterns obtained in the conditions of the forest-grassland bistable state. In each of these cases we were able to characterize a minimal range of nonlocal interactions for the appearance of spatial structures. In the case of the forest inhomogeneous state, we note that the grass biomass does not take advantage of the space between the ligneous plants, where it is absent. This may result from the fact that grassland space-homogeneous equilibrium is unstable and also from the strong pressure (competition) led by trees on grasses. We also observe the presence of extinction zones were none of the two life forms establish (see for example figure 4, page 20). In the case of the savanna inhomogeneous solution, we consider an initial distribution of the vegetation around the monostable savanna equilibrium. We find that the ligneous plants are in phase with the grass biomass. Likewise in this case, grasses do not take advantage of the space between the trees and exclusion zones are also created (see figure 7, page 21). On the other hand, we notice that the savanna inhomogeneous state is favored by the high level of woody biomass due to the fact that $\mathcal{R}_1^* - \mathcal{R}_2^*$ is an increasing function of T^*. In fact, one of the necessary conditions for the existence of savanna inhomogeneous solution is $\mathcal{R}_1^* - \mathcal{R}_2^* > 1$. We also notice the appearance of metastable structures when the initial setting is the forest-grassland bistability. Precisely, we considered vegetation initial distribution around the stable grassland homogeneous steady state while parameter values ensured that the forest homogeneous state is also stable. Therefore, for a substantial time of simulation up to an order of 10^3 years, we can see that the grass biomass takes advantage of the space between the trees (see figure 15, page 25).

Here, nonlocal competition between the grass tuft is responsible for this configuration. However, when the final simulation time is high ($> 10^3$ years), the previous tree and grass spots configuration

is no longer observed. Instead, we find a regular structure of tree spots (see panel (d) figure 14, page 24). In this case, coexistence of tree and grass spots appears as a long transient phase to a tree spots pattern, which seems qualitatively compatible with the type of pattern illustrated in Fig.1-a). According to Eigentler and Sheratt [61], metatastable pattern is an unstable pattern whose instability is caused by a very small unstable eigenvalue. In case of savanna-grassland bistability, we numerically observe another type of structure that we assimilate to a coexistence of localized grass inhomogeneous solution and regular tree spots (see figure 20, page 27). In fact, Vanag and Epstein [62] suggested that if the system is in the spatial bistability domain, then we must apply a perturbation of appropriate shape and sufficient amplitude in order to cause a transition to possibly localized inhomogeneous patterns. The necessary and sufficient condition for localized patches is the coexistence of homogeneous cover and periodic pattern (Tlidi et al. [6], Koga and Kuramoto [63]). In this case, localized inhomogeneous solutions can be interpreted as a nonlinear front between spatially periodic tree distribution and aperiodic grass distribution.

Another line of discussion relies on the size of tree patches observed numerically (i.e. σ_T) and its comparison with the size (width) of the tree nonlocal interaction kernel (M_2) and the value of the cooperation factor Ω. Our illustration around, the forest and savanna homogeneous steady states showed that $\sigma_T \approx 1.5M_2$. Note that, M_2 is to be related to the lateral extend of tree roots or tree canopy. In all cases, where we obtained regular spots, we find that the size of vegetation patches goes above $20m$. In Lejeune et al. [36] for example, the size of vegetation patches in Marahoué National Park in Ivory Coast, ranges from $10m$ to $20m$. The value of Ω used in our work was chosen for illustrative purposes. Nevertheless, within the framework of this paper, we noticed that Ω plays a role on the kinetics of our structures. In fact, for low values of Ω ($\Omega < 1$), the structures take longer time to set up, while the reverse occurs with Ω at large values. Lefever et al. [8] gave a range of value for Ω in the case of arid vegetation. Finally in this paper, first, we choose to work in first approximation with local operator for spatial propagation (Laplace operators). This choice allows us, from a mathematical point of view, to find a good characterization of the ranges of nonlocal interactions enabling the appearance of structures. Without these local operators it would become difficult to find a mathematical characterization of spatial ranges of nonlocal interactions that can be easily manipulated numerically. Secondly and as a perspective of this work, it is necessary to improve our numerical schemes, where for which during the simulations the densities sometimes exceed the carrying capacities. This ambiguity has also been observed in other models with similar structures of equations, notably in Banerjee and Volpert [59] and Genieys et al. [58]. It is also necessary to emphasize on the mathematical conditions allowing this model to exhibit localized structures and metastable patterns, that we observed numerically, and that may be of substantial relevance to account for field observations.

6. Conclusion

In this work, we developed and studied a spatio-temporal tree-grass fire-mediated interactions model allowing to illustrate the spatial structuring of vegetation in the wet savanna zone, where regular spotted patterns (tree groves) have been casually reported in presence of high grass production and frequent fires. To achieve this aim, we extended previous temporal models studied in Yatat Djeumen et al. [2, 39] into integro-differential reaction-diffusion systems. We explore in this model, the combination of nonlocal facilitation and nonlocal competition for the emergence of inhomogeneous solutions. In this context, we integrated kernel functions describing the area of influence of tree and grass roots and the extent of tree canopy-induced shadow effect. Both are modeled like in Martinez-Garcia et al. [47], Banerjee and Volpert [54, 59], Banerjee and Zhang [64] by a constant function of finite range. Accordingly, one of the major key in this paper is the simultaneous presence of nonlocal tree-tree facilitation along with nonlocal tree-tree, tree-grass and grass-grass competition. In fact, the associated model that results from the present contribution,

takes into account the tree-tree cooperation mechanisms modelled by the parameter Ω which is not considered in most of the works dedicated to tree-grass interactions in fire-prone savannas, specifically in Yatat Djeumen et al. [2, 39]. Thanks to the stability analysis, we found conditions of existence of patterned inhomogeneous solutions around space-homogeneous steady states of our system. From a mathematical point of view, our work summarizes all the methods generally used to capture inhomogeneous solutions in nonlocal reaction-diffusion systems, and it appeared necessary to include nonlocal terms as to induce the symmetry breaking instability leading to the patterns. The sequences of patterns observed in this paper consist of regular spot vegetation (tree and grass spots noticed around the forest and grassland homogeneous steady state), "localized" grass structures and metastable pattern. In all cases where we obtained regular spotted patterns, wavelength is an increasing function of the range of tree competitive or tree canopy influence, M_2. As a first approximation, we assumed that both grass and tree biomasses have local propagation through Laplace operators which is in line with rendering clonal propagation. But in reality, wind or even animals may also favor plant propagation through propagule dipersion. Thus Pueyo et al. [15] suggested that it is more reasonable to use nonlocal terms to describe plant dispersal, than diffusion terms. Hence, a line of improvement of the current work could rely on the consideration of nonlocal dispersion terms. Another important objective is to consider the same problem in a two-dimensional spatial domain as to reach more realistic prospects on the patterning processes addressed in the present paper. In so doing, we may expect to obtain very interesting multi-scale vegetation patterns.

Acknowledgements

We thank all the four anonymous reviewers and the associated editor for their insightful comments that helped us to improve the presentation of previous drafts of the manuscript.

References

[1] S. Higgins and W. Bond. Fire, resprouting and variability: a recipe for grass-tree coexistence in savanna. *J. Ecol.*, 88:213–229, (2000). URL https://doi.org/10.1046/j.1365-2745.2000.00435.x.

[2] I. V. Yatat Djeumen, P. Couteron, and Y. Dumont. Spatially explicit modelling of tree-grass interactions in fire prone savannas: a partial differential equations framework. *Ecol. Complex.*, 36:290–313, (2018). URL https://doi.org/10.1016/j.ecocom.2017.06.004.

[3] G. Sarmiento. *The Ecology of Neotropical Savannas*, volume 4. Harvard University Press, Cambridge, MA, 1984.

[4] E. C. February and I. Higgins, S. The distribution of tree and grass roots in savannas in relation to soil nitrogen and water. *S. Afr. J. Bot.*, 76:517–523, (2010). URL https://doi.org/10.1016/j.sajb.2010.04.001.

[5] I. V. Yatat Djeumen, A. Tchuinte Tamen, Y. Dumont, and P. Couteron. A tribute to the use of minimalistic spatially-implicit models of savanna vegetation dynamics to address a broad spatial scales in spite of scarce data. *Biomath.*, 7:1–29, (2018). URL https://doi.org/10.11145/j.biomath.2018.12.167.

[6] M. Tlidi, I. Bordeu, M. Clerc, and D. Escaff. Extended patchy ecosystems may increase their total biomass through self-replication. *Ecol. Indic.*, 94:534–543, (2018). URL https://doi.org/10.1016/j.ecolind.2018.02.009.

[7] R. Lefever and O. Lejeune. On the origin of tiger bush. *Bul.Math.Biol.*, 29:263–294, (1997). URL https://doi.org/10.1016/S0092-8240(96)00072-9.

[8] R. Lefever, P. Barbier, N. Couteron, and O. Lejeune. Deeply gapped vegetations patterns: on crown-roots allometry, critically and desertifiation. *J.Theo.Ecol.*, 261:194–209, (2009). URL https://doi.org/10.1016/j.jtbi.2009.07.030.

[9] R. Lefever and J.W. Turner. A quantitative theory of vegetation patterns based on plant structure and the non-local F-KPP equation. *C. R. Mecanique*, 340:818–828, (2012). URL https://doi.org/10.1016/j.crme.2012.10.030.

[10] P. Couteron and O. Lejeune. Periodic spot patterns in semi-arid vegetation explained by a propagation-inhibition model. *J.Ecol.*, 89:616–628, (2001). URL https://doi.org/10.1046/j.0022-0477.2001.00588.x.

[11] P. Couteron, F. Anthelme, M. Clerc, D. Escaff, C. Fernandez-Oto, and M. Tlidi. Plant clonat morphologies and spatial patterns as self-organized responses to ressource-limited environments. *Phil.Trans.Soc.A*, 132:211–227, (2014). URL https://doi.org/10.1098/rsta.2014.0102.

[12] R. HilleRisLambers, M. Rietkerk, F. Van den Bosch, H.H.T. Prins, and H. de Kroon. Vegetation pattern formation in semi-arid grazing systems. *Ecolgy*, 82:50–61, (2001). URL https://doi.org/10.2307/2680085.

[13] M. Rietkerk, M.C. Boerlijst, F. Van Langevelde, R. HillerisLambers, J. Van de Koppel, L. Kumar, H.H.T. Prins, and A.M. De Roos. Self organization of vegetation in arid vegetation. *Am. Nat.*, 160:524–530, (2002). URL https://doi.org/10.1086/342078.

[14] E. Gilad, J. Von Hardenberg, A. Provenzale, M. Schakak, and E. Meron. A mathematical model of plants as ecosystem engineers. *J. Theor. Biol.*, 244:680–691, (2007). URL https://doi.org/10.1016/j.jtbi.2006.08.006.

[15] Y. Pueyo, S. Kefi, C.L. Alados, and M. Rietkerk. Dispersal strategies and spatial organization of vegetation in arid ecosystems. *Oikos*, 117:1522–1532, (2008). URL https://doi.org/10.1111/j.0030-1299.2008.16735.x.

[16] Y. Pueyo, S. Kefi, R. Diaz-Sierra, C.L. Alados, and M. Rietkerk. The role of reproduction plant traits and biotic interactions in the dynamics of semi-arid plant communities. *Theor. Popul. Biol.*, 78:289–297, (2010). URL https://doi.org/10.1016/j.tpb.2010.09.001.

[17] V. Deblauwe, P. Couteron, O. Lejeune, , J. Bogaert, and N. Barbier. Environnemental modulation of self-organized periodic vegetation in sudan. *Ecography*, 34(6):990–1001, (2011). URL https://doi.org/10.1111/j.1600-0587.2010.06694.x.

[18] J. Youta Happi. *Arbres contre graminées: la lente invasion de la savane par la forêt au Centre-Cameroun*. PhD thesis, Université de Paris IV, 1998.

[19] M. Hirota, M. Holmgren, Van Nes EH., and M. Scheffer. Global resilience of tropical forest and savanna to critical transitions. *Science*, 334:232–235, (2011). URL https://doi.org/10.1126/science.1210657.

[20] K.J. Jeffery, L. Korte, F. Palla, G. Walters, L.J.T. White, and K.A. Abernethy. Fire management in a changing landscape: a case study from lope national park, gabon. *Parks*, 20:39–52, (2014). URL https://doi.org/10.2305/IUCN.CH.2014.PARKS-20-1.KJJ.en.

[21] C. Xu, R. Vergnon, J.H.C. Cornelissen, S. Hantson, M. Holmgren, E.H. Van Nes, and M. Scheffer. Temperate forest and open landscapes are distinct alternative states as reflected in canopy height and tree cover. *Trends. Ecol. Evol.*, 30 (9):501–502, (2015). URL https://doi.org/10.1016/j.tree.2015.07.002.

[22] A. Stall, S.C. Dekler, C. Xu, and E.H. Van Nes. Bistability, spatial interaction and distribution of tropical forest and savannas. *Ecosystems*, 19 No.16.:1080–1091, (2016). URL https://doi.org/10.1146/annurev-ecolsys-112414-054242.

[23] M. Scheffer, S.R. Carpenter, J.A. Foley, C. Folke, and B. Walker. Catastrophic regime shifts in ecosystems. *Nature*, 413:591–596, (2001). URL https://doi.org/10.1038/35098000.

[24] M. Scheffer, S.R. Carpenter, V. Dakos, and E; Van Nes. Generic indicators of ecological resilience inferring the chance of a critical transition. *Ann. Rev. Ecol. Sys.*, 46:145–167, (2015). URL https://doi.org/10.1146/annurev-ecolsys-112414-054242.

[25] M. Scheffer and S.R. Carpenter. Catastrophic regime shifts in ecosystems: linking theory to observation. *Trends. Ecol. Evol.*, 18:648–656, (2003). URL https://doi.org/10.1016/j.tree.2003.09.002.

[26] AC. Staver, S. Archibald, and SA. Kevin. Tree cover in sub-saharan africa: rainfall and fire constrain forest and savanna as alternative stable state. *Ecology*, 92(5):1063–1072, (2011). URL https://doi.org/10.2307/41151234.

[27] C. Favier, J. Aleman, L. Bremond, M.A. Dubois, V. Freycon, and J.-M. Yangakola. Abrupt shifts in african savanna tree cover along a climatic gradient. *Global Ecol. Biogeogr.*, 21(8): 787–797, (2012). URL https://doi.org/10.1111/j.1466-8238.2011.00725.x.

[28] I. Oliveras and Y. Malhi. Many shades of green: the dynamic tropical forest-savannah transition zones. *Phil. Trans. R. Soc.*, 371:1–15, (2016). URL http://dx.doi.org/10.1098/rstb.2015.0308.

[29] J. Dohn, J. Augustine, D, P. Hanan, N, J. Ratnam, and M. Sankaran. Spatial vegetation patterns and neighborhood competition among woody plants in a east african savanna. *Ecology*, 98:478–488, (2017). URL https://doi.org/10.1002/ecy.1659.

[30] F. Borgogno, P. D'odorico, L. Laio, and L. Ridolfi. Mathematical models of vegetation pattern formation in ecohydrology. *Rev.Geophys*, 47, (2009). URL https://doi.org/10.1029/2007RG000256.

[31] F. Accatino, K. Wiegand, D. Ward, and C. De Michele. Tree, grass and fire in humid savannas-the importance of life historical traits and spatial process. *Ecol. Model.*, 320:135–144, (2016). URL https://doi.org/10.1016/j.ecolmodel.2015.09.014.

[32] R.A. Feagin, X.B Wu, F.E. Smeins, and W. E. Whisenant, S. G.and Grant. Individual versus community level process and pattern formation on a model of stand dune plant succesion. *Ecol. Model.*, 183 (4):435–449, (2005). URL https://doi.org/10.1016/j.ecolmodel.2004.09.002.

[33] CA. Klausmeier. Regular and irregular patterns in semiarid vegetation. *Science*, 284:1826–1828, (1999). URL https://doi.org/10.1126/science.284.5421.1826.

[34] E. Meron, E. Gilad, J.V. Hardenberg, and M. Shachak. Vegetation patterns along a rainfall gradient. *Chaos Solit. Fractals*, 19:367–376, (2004). URL https://doi.org/10.1016/S0960-0779(03)00049-3.

[35] J.A Sherratt. When does colonisation of a semi-arid hillslope generate vegetation patterns? *Math. Biol.*, 73:199–226, (2016). URL https://doi.org/10.1007/s00285-015-0942-8.

[36] O. Lejeune, M. Tlidi, and P. Couteron. Localized vegetation patches: A self-organized responses to resource scarcity. *Phys.Rev.E.Stat. Nonlin. Soft. Matter. Phys.*, 66:010901–010904, (2002). URL https://doi.org/10.1103/PhysRevE.66.010901.

[37] N. Goel, V. Guttal, S. Levin, and A. Staver. Dispersal increases the resilience of tropical savanna and forest distributions. *Am. Nat.*, 195, 2020. URL https://doi.org/10.1086/708270.

[38] B. Wuyts, A. Champneys, N. Verschueren, and J. House. Tropical tree cover in a heterogeneous environment: A reaction-diffusion model. *PLoS ONE*, 14:1–16, (2019). URL https://doi.org/10.1371/journal.pone.0218151.

[39] I. V. Yatat Djeumen, Y. Dumont, A. Doizy, and P. Couteron. A minimalistic model of vegetation physiognomies in the savanna biome. *Ecol. Model.*, 440:109381, (2021). URL https://doi.org/10.1016/j.ecolmodel.2020.109381.

[40] D. Patterson, S. Levin, C. Staver, and J. Touboul. Probabilistic foundations of spatial mean-field models in ecology and applications. *SIAM J. Appl. Dyn. Syst.*, 19:2682–2719, (2020). URL https://doi.org/10.1137/19M1298329.

[41] A.C. Staver and S. Levin. Integrating theoretical climate and fire effects on savanna and forest systems. *Am. Nat.*, 180:211–24, (2012). URL https://doi.org/10.1086/666648.

[42] F. Accatino, C. De Michele, Renata Vezzoli., Davide Donzelli., and R. Scholes. Tree and grass co-existence in savanna:interactions of rain and fire. *J. Theor. Biol.*, 267:235–342, (2010). URL https://doi.org/10.1016/j.jtbi.2010.08.012.

[43] A. Kothari, N. Pandey, H, and C. Misra, K. Intraspecific competition in grassland species. *Agric. Ecosyst. Environ.*, 1:237–247, (1974). URL https://doi.org/10.1016/0304-3746(74)90030-4.

[44] M. Craine, J and R. Dybzinski. Mechanisms of plant competition for nutriments, water and ligth. *Funct. Ecol.*, 27:833–840, (2013). URL https://doi.org/10.1111/1365-2435.12081.

[45] Qianxio Li., A. Staver, E. Weinan, and S. Levin. Spatial feedbacks and the dynamics of savanna and forest. *Theoretical Ecology*, 12:237–262, (2019). URL https://doi.org/10.1007/s12080-019-0428-1.

[46] A. Tchuinte, Y. Dumont, JJ. Tewa, P. Couteron, and S. Bowong. A minimalistic model of tree-grass interactions using impulsive differential equations and non-linear feedback functions of grass biomass onto fire-induced tree mortality. *Math. Comput. Simul.*, 133:265–297, (2017). URL https://doi.org/10.1016/j.matcom.2016.03.008.

[47] R. Martinez-Garcia, J. Calabrese, and Cristobal Lopez. Spatial patterns in mesic savannas: The local facilitation limit and the role of demographic stochasticity. *J. Theor. Biol.*, 333: 156–165, (2013). URL https://doi.org/10.1016/j.jtbi.2013.05.024.

[48] A. Diouf, N. Barbier, A.M. Lykke, P. Couteron, V. Deblauwe, A. Mahamane, M. Saadou, and J. Bogaert. Relationships between fire history, edaphic factor and woody vegetation structure and composition in a semi-arid savanna landscape (Niger, West Africa). *Appl. Veg. Sci.*, 15: 488–500, (2012). URL www.jstor.org/stable/23253233.

[49] N. Govender, W. S. W. Trollope, and B. W. Van Wilgen. The effect of fire season, fire frequency, rainfall and management on fire intensity in savanna vegetation in South Africa. *J. Appl. Ecol.*, 43(4):748–758, (2006). URL https://doi.org/10.1111/j.1365-2664.2006.01184.x.

[50] S. J. McNaughton. The propagation of disturbance in savannas through food webs. *J. Veg. Sci.*, 3(3):301–314, (1992). URL https://doi.org/10.2307/3235755.

[51] C. Tian, Z. Ling, and L. Zhang. Nonlocal interactions driven pattern formation in a prey-predator model. *Appl. Math. Comput.*, 308:73–83, (2017). URL https://doi.org/10.1016/j.amc.2017.03.017.

[52] H. Smith. *Monotone dynamical systems: An introduction to the theory of competitive and cooperative systems*, volume 4. American Mathematical Society, 2008.

[53] K. Kishimoto and H.F Weinberger. The spatial homogeneity of stable equilibria of some reaction-diffusion systems on convex domain. *J. Differ. Equ.*, 51:15–21, (1985). URL https://doi.org/10.1016/0022-0396(85)90020-8.

[54] M. Banerjee and V. Volpert. Spatio-temporal pattern formation in rosenzweig-macarthur model : Effect of nonlocal interactions. *Ecol. Complex.*, 216, (2016). URL https://doi.org/10.1016/j.ecocom.2016.12.002.

[55] M. Banerjee, N. Mukherjee, and V. Volpert. Prey-predator model with a nonlocal bistable dynamics of prey. *Mathematics*, pages 6–41, (2018). URL https://doi.org/10.3390/math6030041.

[56] S. Bochner. Quasi-analytic functions, laplace operator, positive kernels. *Ann. Math.*, 51:68–91, (1950). URL https://doi.org/10.2307/1969498.

[57] C. Tzanakis. A note on the fourier transform of a positive-definite function. *Nuov. Cim. B.*, 108:339–342, (1993). URL https://doi.org/10.1007/BF02887493.

[58] S. Genieys, V. Volpert, and P. Auger. Pattern and waves for a model in population dynamics with nonlocal consumption of resources. *Math. Model. Nat. Phenom.*, 1(1):65–82, (2006). URL https://doi.org/10.1051/mmnp:2006004.

[59] M. Banerjee and V. Volpert. Prey-predator model with a nonlocal consumption of prey. *Chaos*, 26, (2016). URL https://doi.org/10.1063/1.4961248.

[60] R. Anguelov, Y. Dumont, and J.M. Lubuma. On nonstandard finite difference schemes in biosciences. *AIP Conf. Proc.*, 1487:212–223, (2012). URL https://doi.org/10.1063/1.4758961.

[61] L. Eigentler and J. Sheratt. Metastability as a coexistence mechanisms in a model for dryland vegetation pattern. *Bull. Math.Biol.*, (2019). URL https://doi.org/10.1007/s11538-019-00606-z.

[62] V. Vanag and I. Epstein. Localized patterns in reaction-diffusion systems. *Chaos*, 17,037110, (2007). URL https://doi.org/10.1063/1.2752494.

[63] S. Koga and Y. Kuramoto. Localized patterns in reaction-diffusion systems. *Prog. Theor. Phys.*, 63:106–121, (1980). URL https://doi.org/10.1143/PTP.63.106.

[64] M. Banerjee and L. Zhang. Stabilizing role of nonlocal interaction on spatio-temporal pattern formation. *Math. Model. Nat. Phenom.*, 11(5):103–118, (2016). URL https://doi.org/10.1051/mmnp/201611507.

Appendix A. Proof of Theorem 1.

Before we give the proof of Theorem 1, we first recall some results:

Definition 2. *A function f_i is called Lipschitz continuous with respect to $\langle \hat{\mathbf{U}}, \tilde{\mathbf{U}} \rangle$ if there exist a constant $k_i > 0$ for any $\mathbf{U} = (G_1, T_1)'$ $\mathbf{V} = (G_2, T_2)' \in \langle \hat{\mathbf{U}}, \tilde{\mathbf{U}} \rangle$ such that:*

$$\begin{aligned} |f_i(G_1, T_1, \phi_{M_1} * G_1, \phi_{M_2} * T_1) - f_i(G_2, T_2, \phi_{M_1} * G_2, \phi_{M_2} * T_2)| \quad \leq \quad & k_i \Big(|G_1 - G_2| + |T_1 - T_2| \\ & + \phi_{M_1} * |G_1 - G_2| + \phi_{M_2} * |T_1 - T_2| \Big). \end{aligned} \tag{A.1}$$

Furthermore, if f_1 and f_2 are Lipschitz continuous with respect to $\langle \hat{\mathbf{U}}, \tilde{\mathbf{U}} \rangle$, then we call $\mathbf{f} = (f_1; f_2)'$ is Lipschitz continuous with respect to $\langle \hat{\mathbf{U}}, \tilde{\mathbf{U}} \rangle$.

Proposition 10. ***(Lipschitz condition)***
If $\hat{\mathbf{U}}$ and $\tilde{\mathbf{U}}$ are bounded, direct calculations show that there exists constants k_1 and k_2 such that:

$$\begin{aligned} k_1 &= (\gamma_G + \delta_G + \lambda_{fG} f) + (\gamma_G + \gamma_{TG}) \|G_1\|_0 + \gamma_G \|G_2\|_0 + \gamma_{TG} \|T_2\|_0, \\ k_2 &= (\gamma_T + \delta_T) + \gamma_T (1 + \Omega)(\|T_1\|_0 + \|T_2\|_0) + \Omega \gamma_T \left[\|T_1\|_0^2 + \|T_2\|_0^2 (\|T_1\|_0 + \|T_2\|_0) \right] \\ &\quad + \lambda_{fT} \left(1 + (\theta_1 + \theta_2) \|T_2\|_0 \right) \end{aligned}$$

where θ_1 and θ_2 are respectively the Lipschitz constants of the function $\omega(G)$ and $\exp(-pT)$ and $\|G_1\|_0 = \sup_{\overline{D}_\tau} |G_1|$, $\|T_1\|_0 = \sup_{\overline{D}_\tau} |T_1|$ then, $\mathbf{f} = (f_1; f_2)$ defined in (9) is Lipschitz continuous with respect to $\langle \hat{\mathbf{U}}, \tilde{\mathbf{U}} \rangle$.

In addition, we define the following operators:

$$\begin{aligned} L_1 G &= \frac{\partial G}{\partial t} - D_G \Delta G + k_1 G, \\ L_2 T &= \frac{\partial T}{\partial t} - D_T \Delta G + k_2 T, \\ F_1(G, T) &= k_1 G + f_1(G, T), \\ F_2(G, T) &= k_2 T + f_2(G, T). \end{aligned} \tag{A.2}$$

Then the system (5) can be reformulated as follows:

$$\begin{cases} L_1 G = F_1(G, T) & \text{in} \quad D_\tau, \\ L_2 G = F_2(G, T) & \text{in} \quad D_\tau, \\ \dfrac{\partial G}{\partial x} = \dfrac{\partial T}{\partial x} = 0 & \text{on} \quad S_\tau, \\ G(x, 0) = G_{10}(x), \quad T(x, 0) = T_{20}(x) & \text{in} \quad K. \end{cases} \tag{A.3}$$

Now we are in position to show that the system (A.3) has a unique global solution. To this aim,

we construct a sequence $\left\{\mathbf{U}^{(m)}\right\} \equiv \left\{G^{(m)}, T^{(m)}\right\}$ according to the following iteration process:

$$\begin{cases} L_1 G^{(m)} = F_1(G^{(m-1)}, T^{(m-1)}) & \text{in} \quad D_\tau, \\ L_2 T^{(m)} = F_2(G^{(m-1)}, T^{(m-1)}) & \text{in} \quad D_\tau, \\ \dfrac{\partial G^{(m)}}{\partial x} = \dfrac{\partial T^{(m)}}{\partial x} = 0 & \text{on} \quad S_\tau, \\ G^{(m)}(x,0) = G_{10}(x), \quad T^{(m)}(x,0) = T_{20}(x) & \text{in} \quad K \end{cases} \tag{A.4}$$

with $\mathbf{U}^{(0)} \in \mathcal{C}^\alpha(D_\tau) \cap \mathcal{C}(\overline{D}_\tau)$.

To show the convergence of the sequence $\left\{\mathbf{U}^{(m)}\right\}$, set:

$$\begin{cases} w_1 &= e^{-\gamma t} G, \\ w_2 &= e^{-\gamma t} T, \end{cases} \tag{A.5}$$

where γ is a positive constant. The system (A.3) is equivalent to the following system:

$$\begin{cases} L_i w_i + \gamma w_i = H_i(w_1, w_2) \quad \text{for} \quad i = 1, 2 & \text{in} \quad D_\tau, \\ \dfrac{\partial w_1}{\partial x} = \dfrac{\partial w_2}{\partial x} = 0 & \text{on} \quad S_\tau \\ w_1(x,0) = w_{10}(x), \quad w_2(x,0) = w_{20}(x) & \text{in} \quad K \end{cases} \tag{A.6}$$

where,

$$\begin{aligned} w_{10}(x) &= e^{-\gamma t} G_{10}(x), \quad w_{20}(x) = e^{-\gamma t} T_{20}(x), \\ H_1(w_1, w_2) &= k_1 w_1 + \gamma_G w_1 (1 - e^{\gamma t} \phi_{M_1} * w_1) - \delta_G w_1 - \gamma_{TG} w_1 e^{\gamma t} \phi_{M_2} * w_2 - \lambda_{fG} f w_1, \\ H_2(w_1, w_2) &= k_2 w_2 + \gamma_T w_2 (1 + \Omega e^{\gamma t} w_2)(1 - e^{\gamma t} \phi_{M_2} * w_2) - \delta_T w_2 - \lambda_{fT} f \omega(w_1) \exp(-p e^{\gamma t} \phi_{M_2} * w_2) w_2 \end{aligned} \tag{A.7}$$

with $\omega(w_1) = \dfrac{w_1^2}{w_1^2 + (g_0 e^{-\gamma t})^2}$.

According to (A.6), we can construct sequences $\mathbf{w}^{(m)}$ via the following iteration process:

$$\begin{cases} L_i w_i^{(m)} + \gamma w_i^{(m)} = H_i(w_1^{(m-1)}, w_2^{(m-1)}) \quad \text{for} \quad i = 1, 2 & \text{in} \quad D_\tau, \\ \dfrac{\partial w_1^{(m)}}{\partial x} = \dfrac{\partial w_2^{(m)}}{\partial x} = 0 & \text{on} \quad S_\tau, \\ w_1^{(m)}(x,0) = w_{10}(x), \quad w_2^{(m)}(x,0) = w_{20}(x) & \text{in} \quad K. \end{cases} \tag{A.8}$$

In term of the integral representation theory for linear parabolic boundary-value problems, the sequence $\mathbf{w}^{(m)}$ can be expressed as:

$$\begin{aligned} w_i^{(m)}(x,t) &= \int_0^t d\tau \int_K \Gamma_i(x,t,\xi,\tau)(H_i(\mathbf{w}^{(m-1)}))(\xi,\tau) d\xi \\ &\quad + \int_0^t d\tau \int_{\partial K} \Gamma_i(x,t,\xi,\tau)(\psi_i(\mathbf{w}^{(m-1)}))(\xi,\tau) d\xi + \int_K \Gamma_i(x,t,\xi,\tau) w_{i0}(\xi) d\xi \end{aligned} \tag{A.9}$$

where Γ_i is the fundamental solution of the Linear parabolic operator $L_i + \gamma_i$ and ψ_i is the single-layer potential.
We now show that the sequence $\{\mathbf{w}^{(m)}\}$ converges in $\mathcal{C}(\overline{D}_\tau)$ to a unique solution of the associated integral in (A.9). Set $\mathcal{X} = X_1 \times X_2$, where :

$$X_i = \left\{ w_i \in C^\alpha(D_\tau) \cap C(\overline{D}_\tau) : w_i(0,x) = w_{i0}(x) \in K \right\} \quad \text{for} \quad i = 1, 2. \tag{A.10}$$

Lemma 1. *If* $\mathbf{w}$ *and* $\mathbf{w}' \in \mathcal{X}$, *then* $H_i(\mathbf{w}) \in \mathcal{C}^\alpha(D_\tau) \cap \mathcal{C}(\overline{D}_\tau)$ *and:*

$$|H_i(\mathbf{w}) - H_i(\mathbf{w}')| \leq 3k_i \Big(|w_1 - w_1'| + |w_2 - w_2'| + \phi_{M_1} * |w_1 - w_1'| + \phi_{M_2} * |w_2 - w_2'| \Big). \tag{A.11}$$

Proof. First $H_i(\mathbf{w}) \in \mathcal{C}^\alpha(D_\tau) \cap \mathcal{C}(\overline{D}_\tau)$, because the plus, multiplication, spatial convolution and composition do not change the Hölder continuous property of the functions.
Secondly,

$$\begin{aligned}
|H_i(\mathbf{w}) - H_i(\mathbf{w}')| &= \Big| k_i(w_i - w_i') + e^{-\gamma t} \Big(f_i(e^{\gamma t} w_1, e^{\gamma t} w_2, e^{\gamma t} \phi_{M_1} * w_1, e^{\gamma t} \phi_{M_2} * w_2) \\
&\quad - f_i(e^{\gamma t} w_1, e^{\gamma t} w_2, e^{\gamma t} \phi_{M_1} * w_1, e^{\gamma t} \phi_{M_2} * w_2) \Big) \Big|, \\
&\leq k_i |w_i - w' i| + k_i \Big[|w_1 - w_1'| + |w_2 - w_2'| \Big] + k_i \Big[\phi_{M_1} * |w_1 - w_1'| + \phi_{M_2} * |w_2 - w_2'| \Big], \\
&\leq 3k_i \Big(|w_1 - w_1'| + |w_2 - w_2'| + \phi_{M_1} * |w_1 - w_1'| + \phi_{M_2} * |w_2 - w_2'| \Big).
\end{aligned}$$

□

Theorem 8. *Let* $(\tilde{\mathbf{U}}, \hat{\mathbf{U}})$ *be a pair of coupled upper and lower solutions of system* (5). *Then the system* (5) *has a unique solution* $\mathbf{U}^*(x,t)$ *and* $\mathbf{U}^* \in \langle \tilde{\mathbf{U}}, \hat{\mathbf{U}} \rangle$. *Moreover, for any* $\mathbf{U}^{(0)} \in \mathcal{C}^\alpha(D_\tau) \cap \mathcal{C}(\overline{D}_\tau)$ *with* $\mathbf{U}^{(0)} = (G_{10}(x), T_{20}(x))$ *in* K, *the sequence obtained from* (A.4) *converges to* $\mathbf{U}^*$ *as* $m \to \infty$.

Proof. The proof is based on the contraction mapping theorem in the Banach space $\mathcal{C}(\overline{D}_\tau)$. For each $i = 1, 2$, we define the operators $A_i : D(A_i) \to R(A_i)$ and $H_i : \mathcal{X} \to C^\alpha(D_\tau) \cap C(\overline{D}_\tau)$ by:

$$\begin{array}{lcl} A_i w_i & = & L_i w_i + \gamma w_i \quad (w_i \in D(A_i)), \\ H_i(\mathbf{w}) & = & H_i(w_1, w_2) \quad (\mathbf{w} \in \mathcal{X}) \end{array} \tag{A.12}$$

where $D(A_i)$ is the domain of A_i given by:

$$D(A_i) = \left\{ w_i \in C^{2,1}(D_\tau) \cap C(\overline{D}_\tau) : \quad \frac{\partial w_i}{\partial x} = 0 \quad \text{on} \quad S_\tau, \quad w_i(0,x) = w_{i0}(x) \quad \text{in} \quad K \right\}. \tag{A.13}$$

$R(A_i)$ is the range of A_i, and $H_i(w_1, w_2)$ is given by (A.7). In terms of the operators A_i and H_i, the iteration process in (A.8) can be written as:

$$A_i w_i^{(m)} = H_i(w_1^{(m-1)}, w_2^{(m-1)}) \quad (w_i^{(m-1)} \in D(A_i)) \quad \text{for} \quad i = 1, 2, \tag{A.14}$$

and in vector form it becomes:

$$\mathcal{A}\mathbf{w}^{(m)} = \mathcal{H}(\mathbf{w}^{(m-1)}) \quad (\mathbf{w}^{(m)} \in D(\mathcal{A})). \tag{A.15}$$

From the standard parabolic theorem the inverse operator $\mathcal{A}^{-1}$ exists and possesses the property:

$$\|\mathcal{A}^{-1}\mathbf{w} - \mathcal{A}^{-1}\mathbf{w}'\|_0 \leq (\gamma + k_3)^{-1} \|\mathbf{w} - \mathbf{w}'\|_0, \quad \text{for} \quad \mathbf{w}, \mathbf{w}' \in \mathcal{C}^\alpha(D_\tau) \cap \mathcal{C}(\overline{D}_\tau) \tag{A.16}$$

where $k_3 = \min\{k_1, k_2\}$. This implies that (A.15) is equivalent to:

$$\mathbf{w}^{(m)} = \mathcal{A}^{-1}\mathcal{H}(\mathbf{w}^{(m-1)}), \quad (\mathbf{w}^{(m-1)} \in D(\mathcal{A})), \tag{A.17}$$

which can be considered as a compact form for the integral representation (A.9) in the space $\mathcal{C}^{\alpha}(D_\tau) \cap \mathcal{C}(\overline{D}_\tau)$. In term of lemma (1), there exists a constant k, independent of γ, such that:

$$\|\mathcal{H}(\mathbf{w}) - \mathcal{H}(\mathbf{w}')\|_0 \leq k\|\mathbf{w} - \mathbf{w}'\|_0, \quad \text{for} \quad \mathbf{w}, \mathbf{w}' \in \mathcal{X}. \tag{A.18}$$

Combining (A.16) and (A.18), we have:

$$\|\mathcal{A}^{-1}\mathcal{H}(\mathbf{w}) - \mathcal{A}^{-1}\mathcal{H}(\mathbf{w}')\|_0 \leq k(\gamma + k_3)^{-1}\|\mathbf{w} - \mathbf{w}'\|_0, \quad \text{for} \quad \mathbf{w}, \mathbf{w}' \in \mathcal{X}. \tag{A.19}$$

By choosing $\gamma > k$, we have $\|\mathcal{A}^{-1}\mathcal{H}(\mathbf{w}) - \mathcal{A}^{-1}\mathcal{H}(\mathbf{w}')\|_0 \leq k(\gamma + k_3)^{-1}\|\mathbf{w} - \mathbf{w}'\|_0$ for $\mathbf{w}, \mathbf{w}' \in \mathcal{X}$. Thus, the operator $\mathcal{A}^{-1}\mathcal{H}$ possesses a contraction property in $\mathcal{X}$. This ensures that the sequence $\left\{\mathbf{w}^{(m)}\right\}$ converges in $\mathcal{C}(\overline{D}_\tau)$. By the equivalence between (A.17) and (A.9) the sequence $\left\{w_i^{(m)}\right\}$ given by (A.9) converges in $C(\overline{D}_\tau)$ to w_i^* for $i = 1, 2$.
To show that $\mathbf{w}^*$ is the unique solution of (A.4). Since $\mathbf{U}^{(m)} = e^{\gamma t}\mathbf{w}^{(m)}$, the sequence $\mathbf{U}^{(m)}$ governed by (A.4) converges to a unique solution $\mathbf{U}^* = e^{\gamma t}\mathbf{w}^*$ to the equation (A.3). By the equivalence between (A.3) and (5), $\mathbf{U}^*$ is the unique solution of the system (5). □

In theorem (8) we prove that to show the existence and the uniqueness of the solution to the system (5), we only need to find a pair of coupled upper and lower solution $\tilde{\mathbf{U}}$ and $\hat{\mathbf{U}}$ which satisfy the Lipschitz condition. If we choose $\tilde{\mathbf{U}}$ and $\hat{\mathbf{U}}$ to be constant vectors $\tilde{\mathbf{c}}$ and $\hat{\mathbf{c}}$, these constant need to satisfy:

$$\begin{array}{rcl} 0 & \geq & \gamma_G\tilde{c}_1(1-\tilde{c}_1) - \delta_G\tilde{c}_1 - \gamma_{TG}\tilde{c}_1\hat{c}_2 - \lambda_{fG}f\tilde{c}_1, \\ 0 & \geq & \gamma_T\tilde{c}_2(1+\Omega\tilde{c}_2)(1-\tilde{c}_2) - \delta_T\tilde{c}_2 - \lambda_{fT}f\omega(\tilde{c}_1)\exp(-p\hat{c}_2)\tilde{c}_2, \\ 0 & \leq & \gamma_G\hat{c}_1(1-\hat{c}_1) - \delta_G\hat{c}_1 - \gamma_{TG}\hat{c}_1\tilde{c}_2 - \lambda_{fG}f\hat{c}_1, \\ 0 & \leq & \gamma_T\hat{c}_2(1+\Omega\hat{c}_2)(1-\hat{c}_2) - \delta_T\hat{c}_2 - \lambda_{fT}f\omega(\tilde{c}_1)\exp(-p\hat{c}_2)\hat{c}_2 \end{array} \tag{A.20}$$

and

$$\begin{array}{rl} \tilde{c}_1 & \geq \sup_K G(x,0), \\ \tilde{c}_2 & \geq \sup_K T(x,0), \\ \hat{c}_1 & \leq \inf_K G(x,0), \\ \hat{c}_2 & \leq \inf_K T(x,0). \end{array} \tag{A.21}$$

We choose $\hat{c}_1 = \hat{c}_2 = 0$. Then $\tilde{c}_1 = \max\left\{\sup_K G(0,x), 1 - \dfrac{\delta_G + \lambda_{fG}f}{\gamma_G}\right\}$ and

$$\begin{array}{rcl} \tilde{c}_2 & = & \max\left\{\sup_K T(0,x), \dfrac{\gamma_T - \delta_T}{\gamma_T}\right\}, \quad \text{if} \quad \Omega = 0, \\ \tilde{c}_2 & = & \max\left\{\sup_K T(0,x), \dfrac{\sqrt{(1-\Omega)^2 + 4\Omega\left(1 - \frac{\delta_T}{\gamma_T}\right)} - (1-\Omega)}{2\Omega}\right\}, \quad \text{if} \quad \Omega > 0. \end{array}$$

Appendix B. Proof of Proposition 2

If $f = 0$, savanna steady state $(G^*, T^*)'$ is a solution of

$$\left\{\begin{array}{rcl} \gamma_G(1-G) - \delta_G - \gamma_{TG}T & = & 0, \\ \gamma_T(1+\Omega T)(1-T) - \delta_T & = & 0. \end{array}\right. \tag{B.1}$$

The second equation of system (B.1) give :

$$T^* = T_i, i = 1, 2 \quad \text{(depending on the values of } \Omega).$$

The first system of (B.1) leads to

$$\begin{aligned} G^* &= 1 - \frac{\delta_G + \gamma_{TG} T_i}{\gamma_G}, \\ &= 1 - \frac{1}{\mathcal{R}_{F,f=0}}. \end{aligned}$$

If $f > 0$ and $\gamma_{TG} = 0$, then the savanna equilibrium $(G^*; T^*)'$, satisfies:

$$\left\{ \begin{array}{l} G^* = G_e, \\ \Omega\gamma_T(T^* - T_2)(T^* - T_{2-}) + \lambda_{fT} f\omega(G_e)\exp(-pT^*) = 0. \end{array} \right. \tag{B.2}$$

Let us set $J(T) = \Omega\gamma_T(T - T_2)(T - T_{2-}) + \lambda_{fT} f\omega(G_e)\exp(-pT)$, then:

$$\lim_{T\to 0} J(T) = \delta_T + \lambda_{fT} f\omega(G_e)(1 - \mathcal{R}_T). \tag{B.3}$$

We have also the first derivative of J:

$$\begin{array}{lcl} J'(T) & = & \Omega\gamma_T\left[2T - T_2 - T_{2-}\right] - p\lambda_{fT} f\omega(G_e)\exp(-pT), \\ \lim_{T\to 0} J'(T) & = & p\lambda_{fT} f\omega(G_e)[\mathcal{R}^1_\Omega - 1], \\ \lim_{T\to 1} J'(T) & = & p\lambda_{fT} f\omega(G_e)\exp(-p)[\mathcal{R}^2_\Omega - 1], \end{array} \tag{B.4}$$

where $\mathcal{R}^2_\Omega = \dfrac{\gamma_T(1+\Omega)}{p\lambda_{fT} f\omega(G_e)\exp(-p)}$.
The second derivative:

$$J"(T) = 2\Omega\gamma_T + p^2\lambda_{fT} f\omega(G_e)\exp(-pT) > 0. \tag{B.5}$$

Therefore, J' is increasing on $[0; 1]$.

(I) if $\mathcal{R}^1_\Omega > 1$, then $J'(T) > 0$ on $[0; 1]$, and J is increasing on $[0; 1]$;

- (a) if $\mathcal{R}_T < 1$, then $J(T) > 0$ on $[0; 1]$.
- (b) if $\mathcal{R}_T > 1$, then there exists at most one savanna steady state.

(II) if $\mathcal{R}^1_\Omega < 1$, then $\lim_{T\to 0} J'(T) < 0$ and due to J' increasing, we have:

- (a) if $\mathcal{R}^2_\Omega < 1$, then $J'(T) < 0$ on $[0; 1]$ and J is decreasing on that interval. Then
  - (a_1) if $\mathcal{R}_T > 1$, then $J(T) < 0$ on $[0; 1]$.
  - (a_2) if $\mathcal{R}_T < 1$, we have at most one savanna steady state.
- (b) if $\mathcal{R}^2_\Omega > 1$, then by the intermediate value theorem, there exist $T_0 \in [0; 1]$ such that $J'(T_0) = 0$. Then:
  - (b_1) if $J(T_0) > 0$, then $J(T) > 0$ on $[0; 1]$.
  - (b_2) if $J(T_0) < 0$, we have at most two savanna steady states $(G_e, T^*_i)'$,$i = 1, 2$ where $T^*_1 \in [0; T_0]$ and $T^*_2 \in [T_0; 1]$

If $f > 0$ and $\gamma_{TG} \neq 0$, savanna equilibrium is a solution of the system:

$$\left\{ \begin{array}{lcl} \gamma_G(1 - G) - \delta_G - \gamma_{TG} T - \lambda_{fG} f & = & 0, \\ \gamma_T(1 + \Omega T)(1 - T) - \delta_T - \lambda_{fT} f\omega(G)\exp(-pT) & = & 0, \end{array} \right. \tag{B.6}$$

the first equation of system (B.6) gives:

$$T = -\frac{\delta_G + \lambda_{fG} f}{\gamma_{TG}} + \frac{\gamma_G}{\gamma_{TG}}(1 - G)$$

set:

$$a = -\frac{\delta_G + \lambda_{fG} f}{\gamma_{TG}} \quad \text{and} \quad b = \frac{\gamma_G}{\gamma_{TG}}$$

then

$$T = (a + b) - bG. \tag{B.7}$$

Using the fact that $G, T \in]0; 1]$, (B.7) gives that:

$$\frac{a-1}{b} + 1 < G < \frac{a}{b} + 1.$$

Note that $\frac{a-1}{b} + 1 = (1 - \frac{1}{\mathcal{R}_G}) - \frac{\gamma_{TG}}{\gamma_G}$ and $\frac{a}{b} + 1 = 1 - \frac{1}{\mathcal{R}_G}$. Therefore, because $\mathcal{R}_G > 1$ then

$$G_e - \frac{\gamma_{TG}}{\gamma_G} < G < G_e. \tag{B.8}$$

The second equation of system (B.6) gives :

$$\lambda_{fT} f \omega(G) \exp(-pT) = (\gamma_T - \delta_T) + \gamma_T(\Omega - 1)T - \gamma_T \Omega T^2. \tag{B.9}$$

Substituting (B.7) in (B.9) we obtain first:

$$\begin{aligned}(\gamma_T - \delta_T) + \gamma_T(\Omega - 1)T - \gamma_T \Omega T^2 \quad &= \quad (\gamma_T - \delta_T) + \gamma_T(\Omega - 1)(a + b) - \gamma_T \Omega (a + b)^2 + \\ &\quad (2(a + b)b\gamma_T \Omega - b\gamma_T(\Omega - 1))\, G - \gamma_T \Omega b^2 G^2\end{aligned}$$

then,

$$\begin{aligned}\lambda_{fT} f \omega(G) \exp(-pT) \quad &= \quad (\gamma_T - \delta_T) + \gamma_T(\Omega - 1)(a + b) - \gamma_T \Omega (a + b)^2 + \\ &\quad (2(a + b)b\gamma_T \Omega - b\gamma_T(\Omega - 1))\, G - \gamma_T \Omega b^2 G^2.\end{aligned} \tag{B.10}$$

Set:

$$\begin{aligned} q &= (\gamma_T - \delta_T) + \gamma_T(\Omega - 1)(a + b) - \gamma_T \Omega (a + b)^2, \\ \theta &= 2(a + b)b\gamma_T \Omega - b\gamma_T(\Omega - 1), \\ \alpha &= \gamma_T \Omega b^2. \end{aligned}$$

Then, we obtain in (B.10)

$$\lambda_{fT} f \omega(G) \exp(-pT) = q + \theta G - \alpha G^2. \tag{B.11}$$

Substituting (B.7) in (B.11), we obtain:

$$\lambda_{fT} f \exp\left(-p(a + b)\right) \exp(pbG) G^2 = q g_0^2 + \theta g_0^2 G + (q - \alpha g_0^2) G^2 + \theta G^3 - \alpha G^4. \tag{B.12}$$

Set

$$m = \lambda_{fT} f \exp\left(-p(a + b)\right).$$

Hence,

$$-\alpha G^4 + \theta G^3 - m \exp(pbG) G^2 + (q - \alpha g_0^2) G^2 + \theta g_0^2 G + q g_0^2 = 0. \tag{B.13}$$

Define the function f by:

$$f(G) = -\alpha G^4 + \theta G^3 - m\exp(pbG)G^2 + (q - \alpha g_0^2)G^2 + \theta g_0^2 G + q g_0^2 \tag{B.14}$$

and fine the roots of f in the interval $[0;1]$.

$$\begin{cases} \lim_{G\to 0} f(G) &= q g_0^2, \\ \lim_{G\to +\infty} f(G) &= -\infty, \\ \lim_{G\to 1} f(G) &= (\theta - \alpha + q)(g_0^2+1) - m\exp(pb). \end{cases} \tag{B.15}$$

The first derivative of f is :

$$f'(G) = -4\alpha G^3 + 3\theta G^2 - mpb\exp(pbG)G^2 - 2m\exp(pbG)G + 2(q - \alpha g_0^2)G + \theta g_0^2 \tag{B.16}$$

and

$$\begin{cases} \lim_{G\to 0} f'(G) &= \theta g_0^2, \\ \lim_{G\to +\infty} f'(G) &= -\infty, \\ \lim_{G\to 1} f'(G) &= -4\alpha + 3\theta + 2(q - \alpha g_0^2) + \theta g_0^2 - m\exp(pb)[pb+2]. \end{cases} \tag{B.17}$$

The second derivative of f is given by:

$$f''(G) = -12\alpha G^2 + 6\theta G - m(pb)^2\exp(pbG)G^2 - 4mpb\exp(pbG)G - 2m\exp(pbG) + 2(q - \alpha g_0^2) \tag{B.18}$$

and:

$$\begin{cases} \lim_{G\to 0} f''(G) &= 2\left[q - (m + \alpha g_0^2)\right], \\ \lim_{G\to +\infty} f''(G) &= -\infty, \\ \lim_{G\to 1} f''(G) &= 6\theta + 2(q - \alpha g_0^2) - 12\alpha - m\exp(pb)\left[(pb)^2 + 4pb + 2\right]. \end{cases} \tag{B.19}$$

The third derivative of f is given by:

$$f'''(G) = -24\alpha G + 6\theta - m(pb)^3\exp(pbG)G^2 - 6m(pb)^2\exp(pbG)G - 6m(pb)\exp(pbG) \tag{B.20}$$

and:

$$\begin{cases} \lim_{G\to 0} f'''(G) &= 6(\theta - mpb), \\ \lim_{G\to +\infty} f'''(G) &= -\infty, \\ \lim_{G\to 1} f'''(G) &= 6\theta - \left[mpb\left((pb)^2 + 6pb + 6\right)\exp(pb) + 24\alpha\right]. \end{cases} \tag{B.21}$$

The fourth derivative of f is given by:

$$f''''(G) = -m(pb)^4\exp(pbG)G^2 - 8m(pb)^3\exp(pbG)G - 6m(pb)^2\exp(pbG) - 24\alpha. \tag{B.22}$$

$f''''(G) < 0$ on $[0, +\infty[$, therefore on $[0;1]$. Then f''' decreases on $[0;1]$.

- (I) if $\theta < mpb$, then $f'''(G) < 0$ in $[0;+\infty[$ and then f'' strictly decreases on $[0;+\infty[$. According to (B.19) we have:
  - $(I.1)$ if $q < m + \alpha g_0^2$ then $f''(G) < 0$ on $[0;+\infty[$. Therefore f' strictly decreases on $[0;+\infty[$. According to (B.17) we have:
    - $(I.1.1)$ if $\theta < 0$ then $f'(G) < 0$ on $[0;+\infty[$ and then f strictly decreases on $[0;+\infty[$. According to (B.15)
      - $(I.1.1.1)$ If $q < 0$ then $f(G) < 0$ on $[0;+\infty[$.
      - $(I.1.1.2)$ If $q > 0$ then,
        - A. if $q > \dfrac{m\exp(pb)}{g_0^2+1} + \alpha - \theta$, then $f(G) > 0$ on $[0;1]$.

B. if $q < \dfrac{m\exp(pb)}{g_0^2+1} + \alpha - \theta$, then $\exists G_1^* \in [0;1]$ such that $f(G_1^*) = 0$.

$(I.1.2)$ If $\theta > 0$ then $f'(G)$ has a positive root on $[0;+\infty[$.

$(I.1.2.1)$ If $q > \dfrac{1}{2}\left[4\alpha - 3\theta + (2\alpha-\theta)g_0^2 + m\exp(pb)\,[pb+2]\right]$, then $f'(G) > 0$ on $[0;1]$ and f strictly increases on $[0;1]$.

$(I.1.2.1.1)$ If $q > 0$, then $f(G) > 0$ on $[0;1]$.

$(I.1.2.1.2)$ If $q < 0$, then:

(a) if $q < \dfrac{m\exp(pb)}{g_0^2+1} + \alpha - \theta$, then $f(G) < 0$ on $[0;1]$.

(b) If $q > \dfrac{m\exp(pb)}{g_0^2+1} + \alpha - \theta$, then $\exists G_2^* \in [0;1]$ such that $f(G_2^*) = 0$.

$(I.1.2.2)$ If $q < \dfrac{1}{2}\left[4\alpha - 3\theta + (2\alpha-\theta)g_0^2 + m\exp(pb)\,[pb+2]\right]$, then $\exists G^{(0)} \in [0;1]$ such that $f'(G^{(0)}) = 0$ on and $f'(G) > 0$ on $[0;G^{(0)}]$ and $f'(G) < 0$ on $[G^{(0)};1]$.

$(I.1.2.2.1)$ If $f(G^{(0)}) < 0$, then $f(G) < 0$ on $[0;1]$.

$(I.1.2.2.2)$ If $f(G^{(0)}) > 0$, then:

(a) If $q > 0$ and $q > \dfrac{m\exp(pb)}{g_0^2+1} + \alpha - \theta$, then $f(G) > 0$ on $[0;1]$.

(b) If $q < 0$ and $q > \dfrac{m\exp(pb)}{g_0^2+1} + \alpha - \theta$, then $\exists G_3^* \in [0;G^{(0)}]$ is the unique root of f.

(c) If $q > 0$ and $q < \dfrac{m\exp(pb)}{g_0^2+1} + \alpha - \theta$, then $G_4^* \in [G^{(0)};1]$ is the unique root of f on $[0;1]$.

(d) If $q < 0$ and $q < \dfrac{m\exp(pb)}{g_0^2+1} + \alpha - \theta$, then $\exists G_3^* \in [0;G^{(0)}]$ and $G_4^* \in [G^{(0)};1]$ such that $f(G_3^*) = f(G_4^*) = 0$.

$(I.2)$ If $q > m + \alpha g_0^2$ then $f''(G)$ has a unique positive root on $[0;+\infty[$.

$(I.2.1)$ If $q > 6\alpha - 3\theta + \alpha g_0^2 + \dfrac{1}{2}m\left[(pb)^2 + 4(pb) + 2\right]\exp(pb)$ then $f''(G) > 0$ on $[0;1]$, then f' strictly increases on $[0;1]$.

$(I.2.1.1)$ If $\theta > 0$ then $f'(G) > 0$ on $[0;1]$. So, f strictly increases on $[0;1]$.

$(I.2.1.1.1)$ If $q > 0$, then $f(G) > 0$ on $[0;1]$.

$(I.2.1.1.1)$ If $q < 0$, then:

(a) If $q < \dfrac{m\exp(pb)}{g_0^2+1} + \alpha - \theta$, then $f(G) < 0$ on $[0;1]$.

(b) If $q > \dfrac{m\exp(pb)}{g_0^2+1} + \alpha - \theta$, then $\exists G_5^* \in [0;1]$ such that $f(G_5^*) = 0$.

$(I.2.1.2)$ If $\theta < 0$, then because f' is strictly increasing on $[0;1]$ we have:

$(I.2.1.2.1)$ If $q < \dfrac{1}{2}\left[4\alpha - 3\theta + (2\alpha-\theta)g_0^2 + m\exp(pb)\,[pb+2]\right]$, then $f'(G) < 0$ on $[0;1]$. Then, f strictly decreases on $[0;1]$.

(a) If $q < 0$ then, $f(G) < 0$ on $[0;1]$.

(b) If $q > 0$ then,

$(b.1)$ If $q > \dfrac{m\exp(pb)}{g_0^2+1} + \alpha - \theta$, then $f(G) > 0$ on $[0;1]$.

$(b.2)$ If $q < \dfrac{m\exp(pb)}{g_0^2+1} + \alpha - \theta$, then $\exists G_6^* \in [0;1]$ such that $f(G_6^*) = 0$.

$(I.2.1.2.2)$ If $q > \dfrac{1}{2}\left[4\alpha - 3\theta + (2\alpha-\theta)g_0^2 + m\exp(pb)\,[pb+2]\right]$, then $\exists G^{(00)} \in [0;1]$ such that $f'(G^{(00)}) = 0$ and then $f'(G) < 0$ on $[0;G^{(00)}]$ and $f'(G) > 0$ on $[G^{(00)};1]$.

(a) If $f(G^{(00)}) > 0$ then $f(G) > 0$ on $[0;1]$.

(b) If $f(G^{(00)}) < 0$ then,

$(b.1)$ If $q < 0$ and $q < \dfrac{m\exp(pb)}{g_0^2+1} + \alpha - \theta$, then $f(G) < 0$ on $[0;1]$.

$(b.2)$ If $q > 0$ and $q < \dfrac{m\exp(pb)}{g_0^2+1} + \alpha - \theta$, then $\exists G_7^* \in [0; G^{(00)}]$ such that $f(G_7^*) = 0$.

$(b.3)$ If $q < 0$ and $q > \dfrac{m\exp(pb)}{g_0^2+1} + \alpha - \theta$, then $\exists G_8^* \in [G^{(00)}; 1]$ such that $f(G_8^*) = 0$.

$(b.4)$ If $q > 0$ and $q > \dfrac{m\exp(pb)}{g_0^2+1} + \alpha - \theta$, then $G_7^* \in [0; G^{(00)}]$ and $G_8^* \in [G^{(00)}; 1]$ are the two roots of f.

$(I.2.2)$ If $q < 6\alpha - 3\theta + \alpha g_0^2 + \dfrac{1}{2}m\left[(pb)^2 + 4(pb) + 2\right]\exp(pb)$, then $\exists\ G^{(000)} \in [0;1]$ such that $f''(G^{(000)}) = 0$. Then, $f''(G) > 0$ on $[0; G^{(000)}]$ and $f''(G) < 0$ on $[G^{(000)}; 1]$.

$(I.2.2.1)$ If $f'(G^{(000)}) < 0$, then $f'(G) < 0$ on $[0;1]$ and f strictly decreases on that interval.

(a) If $q < 0$ then $f(G) < 0$ on $[0;1]$.

(b) If $q > 0$, then:

$(b.1)$ If $q > \dfrac{m\exp(pb)}{g_0^2+1} + \alpha - \theta$, then $f(G) > 0$ on $[0;1]$.

$(b.2)$ If $q < \dfrac{m\exp(pb)}{g_0^2+1} + \alpha - \theta$, then, $\exists G_9^* \in [0;1]$ such that $f(G_9^*) = 0$.

$(I.2.2.2)$ If $f'(G^{(000)}) > 0$, then:

$(I.2.2.2.1)$ If $\theta > 0$ and $q > \dfrac{1}{2}\left[4\alpha - 3\theta + (2\alpha - \theta)g_0^2 + m\exp(pb)\left[pb + 2\right]\right]$, then $f'(G) > 0$ on $[0;1]$ and f is increasing on $[0;1]$.

(a) If $q > 0$ then $f(G) > 0$ on $[0;1]$.

(b) If $q < 0$, then :

$(b.1)$ If $q < \dfrac{m\exp(pb)}{g_0^2+1} + \alpha - \theta$, then $f(G) < 0$ on $[0;1]$.

$(b.2)$ If $q > \dfrac{m\exp(pb)}{g_0^2+1} + \alpha - \theta$, then $\exists G_{10}^* \in [0;1]$ such that $f(G_{10}^*) = 0$.

$(I.2.2.2.2)$ If $\theta < 0$ and $q > \dfrac{1}{2}\left[4\alpha - 3\theta + (2\alpha - \theta)g_0^2 + m\exp(pb)\left[pb + 2\right]\right]$, then $\exists G^{(0000)} \in [0; G^{(000)}]$ such that $f'(G^{(0000)}) = 0$. Therefore $f'(G) < 0$ on $[0; G^{(0000)}]$ and $f'(G) > 0$ on $[G^{(0000)}; 1]$.

(a) If $f(G^{(0000)}) > 0$, then $f(G) > 0$ on $[0;1]$.

(b) If $f(G^{(0000)}) < 0$, then:

$(b.1)$ If $q < 0$ and $q < \dfrac{m\exp(pb)}{g_0^2+1} + \alpha - \theta$, then $f(G) < 0$ on $[0;1]$.

$(b.2)$ If $q > 0$ and $q < \dfrac{m\exp(pb)}{g_0^2+1} + \alpha - \theta$, then $\exists G_{11}^* \in [0; G^{(0000)}]$ such that $f(G_{11}^*) = 0$.

$(b.3)$ If $q < 0$ and $q > \dfrac{m\exp(pb)}{g_0^2+1} + \alpha - \theta$ then $\exists G_{12}^* \in [G^{(0000)}; 1]$ such that $f(G_{12}^*) = 0$.

$(b.4)$ If $q > 0$ and $q > \dfrac{m\exp(pb)}{g_0^2+1} + \alpha - \theta$ then $G_{11}^* \in [0; G^{(0000)}]$ and $G_{12}^* \in [G^{(0000)}; 1]$ are the two roots of f.

(I.2.2.2.3) If $\theta > 0$ and $q < \frac{1}{2}\left[4\alpha - 3\theta + (2\alpha - \theta)g_0^2 + m\exp(pb)\left[pb + 2\right]\right]$, then $\exists G^{(00000)} \in [G^{(000)}; 1]$ such that $f'(G^{(00000)}) = 0$. Therefore, $f'(G) > 0$ on $[0; G^{(00000)}]$ and $f'(G) < 0$ on $[G^{(00000)}; 1]$.

(a) If $f(G^{(00000)} < 0$, then $f(G) < 0$ on $[0; 1]$.

(b) If $f(G^{(00000)} > 0$, then:

(b.1) If $q > 0$ and $q > \frac{m\exp(pb)}{g_0^2 + 1} + \alpha - \theta$ then $f(G) > 0$ on $[0; 1]$.

(b.2) If $q < 0$ and $q > \frac{m\exp(pb)}{g_0^2 + 1} + \alpha - \theta$, then $\exists G_{13}^* \in [0; G^{(00000)}]$ such that $f(G_{13}^*) = 0$.

(b.3) If $q > 0$ and $q < \frac{m\exp(pb)}{g_0^2 + 1} + \alpha - \theta$, then $\exists G_{14}^* \in [G^{(00000)}; 1]$ such that $f(G_{14}^*) = 0$.

(b.4) If $q < 0$ and $q < \frac{m\exp(pb)}{g_0^2 + 1} + \alpha - \theta$, then $G_{13}^* \in [0; G^{(00000)}]$ and $G_{14}^* \in [G^{(00000)}; 1]$ are the two roots of f.

(I.2.2.2.4) If $\theta < 0$ and $q < \frac{1}{2}\left[4\alpha - 3\theta + (2\alpha - \theta)g_0^2 + m\exp(pb)\left[pb + 2\right]\right]$, then $\exists G^{(0000)} \in [0; G^{(000)}]$ and $G^{(00000)} \in [G^{(000)}; 1]$ such that $f'(G^{(0000)}) = f'(G^{(00000)}) = 0$. Therefore $f'(G) < 0$ on $[0; G^{(0000)}] \cup [G^{(00000)}; 1]$ and $f'(G) > 0$ on $[G^{(0000)}; G^{(00000)}]$.

(a) If $f(G^{(0000)}) > 0$, then

(a.1) If $q > \frac{m\exp(pb)}{g_0^2 + 1} + \alpha - \theta$, then $f(G) > 0$ on $[0; 1]$.

(a.2) If $q < \frac{m\exp(pb)}{g_0^2 + 1} + \alpha - \theta$, $G_{14}^* \in [G^{(00000)}; 1]$ is the unique root of f.

(b) If $f(G^{(0000)}) < 0$ and $f(G^{(00000)}) < 0$ then

(b.1) $q < 0$ on then $f(G) < 0$ on $[0; 1]$.

(b.2) $q > 0$ then $\exists G_{11}^* \in [0; G^{(0000)}]$ is the unique root of f.

(c) If $f(G^{(0000)}) < 0$ and $f(G^{(00000)}) > 0$ then $\exists G_{15}^* \in [G^{(0000)}; G^{(00000)}]$ such that $f(G_{13}^*) = 0$.

(c.1) If $q < 0$ and $q > \frac{m\exp(pb)}{g_0^2 + 1} + \alpha - \theta$ then G_{15}^* is the unique root of f in the interval $[0; 1]$.

(c.2) If $q < 0$ and $q < \frac{m\exp(pb)}{g_0^2 + 1} + \alpha - \theta$, then with G_{15}^* we have also $G_{14}^* \in [G^{(00000)}; 1]$ roots of f. Therefore,$f(G_{15}^*) = f(G_{14}^*) = 0$.

(c.3) If $q > 0$ and $q > \frac{m\exp(pb)}{g_0^2 + 1} + \alpha - \theta$,then with G_{15}^* we have also $G_{11}^* \in [0; G^{(0000)}]$ roots of f. Therefore,$f(G_{15}^*) = f(G_{11}^*) = 0$.

(c.4) If $q > 0$ and $q < \frac{m\exp(pb)}{g_0^2 + 1} + \alpha - \theta$,then with G_{15}^* we have also $G_{11}^* \in [0; G^{(0000)}]$ and $G_{14}^* \in [G^{(00000)}; 1]$ roots of f. Therefore,$f(G_{15}^*) = f(G_{11}^*) = f(G_{14}^*) = 0$.

(II) we suppose that $\theta > mpb$, because f''' is decreasing on $[0; 1]$, by the intermediate value theorem f''' has a unique positive root on $[0; +\infty[$.

(II.1) If $\theta > \frac{1}{6}\left[24\alpha + mpb\left((pb)^2 + 6(pb) + 6\right)\exp(pb)\right]$, then $f'''(G) > 0$ on $[0; 1]$ and therefore, f'' is increasing on $[0; 1]$.

(II.1.1) If $q > m + \alpha g_0^2$, then $f''(G) > 0$ on $[0; 1]$ therefore, f' strictly increases on $[0; 1]$.

(II.1.1.1) If $\theta > 0$, then $f'(G) > 0$ on $[0;1]$ and therefore f strictly increases on $[0;1]$.

(a) If $q > 0$, then $f(G) > 0$ on $[0;1]$.

(b) If $q < 0$, then:

(b.1) If $q < \dfrac{m\exp(pb)}{g_0^2+1} + \alpha - \theta$, then $f(G) < 0$, on $[0;1]$.

(b.2) If $q > \dfrac{m\exp(pb)}{g_0^2+1} + \alpha - \theta$, then $\exists G_{17}^* \in [0;1]$ such that $f(G_{17}^*) = 0$.

(II.1.1.2) If $\theta < 0$, then :

(II.1.1.2.1) If $q < \dfrac{1}{2}\left[4\alpha - 3\theta + (2\alpha-\theta)g_0^2 + m\exp(pb)\left[pb+2\right]\right]$, then $f'(G) < 0$ on $[0;1]$ and then f decrease strictly on $[0;1]$.

(a) If $q < 0$ then $f(G) < 0$ on $[0;1]$.

(b) If $q > 0$ then:

(b.1) If $q > \dfrac{m\exp(pb)}{g_0^2+1} + \alpha - \theta$, then $f(G) > 0$ on $[0;1]$.

(b.2) If $q < \dfrac{m\exp(pb)}{g_0^2+1} + \alpha - \theta$, then $\exists G_{18}^* \in [0;1]$ such that $f(G_{18}^*) = 0$.

(II.1.1.2.2) If $q > \dfrac{1}{2}\left[4\alpha - 3\theta + (2\alpha-\theta)g_0^2 + m\exp(pb)\left[pb+2\right]\right]$, then $\exists G_{(0)} \in [0;1]$ such that $f'(G_{(0)}) = 0$. Therefore, $f'(G) < 0$ on $[0;G_{(0)}]$ and $f'(G) > 0$ on $[G_{(0)};1]$.

(a) If $f(G_{(0)}) > 0$ then $f(G) > 0$ on $[0;1]$.

(b) If $f(G_{(0)}) < 0$, then:

(b.1) If $q < 0$ and $q < \dfrac{m\exp(pb)}{g_0^2+1} + \alpha - \theta$ then $f(G) < 0$ on $[0;1]$.

(b.2) If $q > 0$ and $q < \dfrac{m\exp(pb)}{g_0^2+1} + \alpha - \theta$, then $G_{19}^* \in [0;G_{(0)}]$ such that $f(G_{19}^*) = 0$.

(b.3) If $q < 0$ and $q > \dfrac{m\exp(pb)}{g_0^2+1} + \alpha - \theta$, then $\exists G_{20}^* \in [G_{(0)};1]$ such that $f(G_{20}^*) = 0$.

(b.4) If $q > 0$ and $q > \dfrac{m\exp(pb)}{g_0^2+1} + \alpha - \theta$, then $G_{19}^* \in [0;G_{(0)}]$ and $G_{20}^* \in [G_{(0)};1]$ are the two roots of f.

(II.1.2) If $q < m + \alpha g_0^2$, then we have the following situations:

(II.1.2.1) If $q < 6\alpha - 3\theta + \alpha g_0^2 + \dfrac{1}{2}m\exp(pb)\left[(pb)^2 + pb + 2\right]$, then $f''(G) < 0$ on $[0;1]$. Then f' decrease strictly on $[0;1]$.

(II.1.2.1.1) If $\theta < 0$, then $f'(G) < 0$ on $[0;1]$ and f is therefore decreasing on $[0;1]$.

(a) If $q < 0$, then $f(G) < 0$ on $[0;1]$.

(b) If $q > 0$, then:

(b.1) If $q > \dfrac{m\exp(pb)}{g_0^2+1} + \alpha - \theta$,then $f(G) < 0$ on $[0;1]$.

(b.2) If $q < \dfrac{m\exp(pb)}{g_0^2+1} + \alpha - \theta$, then $\exists G_{21}^* \in [0;1]$ such that $f(G_{21}^*) = 0$.

(II.1.2.1.2) If $\theta > 0$, then, we have the following situations:

(a) If $q > \dfrac{1}{2}\left[4\alpha - 3\theta + (2\alpha-\theta)g_0^2 + m\exp(pb)\left[pb+2\right]\right]$,then $f'(G) > 0$ on $[0;1]$ and f increase strictly on $[0;1]$.

(a.1) If $q > 0$, then $f(G) > 0$ on $[0;1]$.

(a.2) If $q < 0$, then:

(a.2.1) If $q < \dfrac{m\exp(pb)}{g_0^2+1} + \alpha - \theta$,then $f(G) < 0$ on $[0;1]$.

(a.2.2) If $q > \dfrac{m\exp(pb)}{g_0^2+1} + \alpha - \theta$, then $\exists G_{22}^* \in [0;1]$ such that $f(G_{22}^*) = 0$.

(b) If $q < \dfrac{1}{2}\left[4\alpha - 3\theta + (2\alpha-\theta)g_0^2 + m\exp(pb)\,[pb+2]\right]$. We use the fact that f' is decreasing (strictly) on $[0;1]$. By the intermediate values theorem: $\exists G_{(00)} \in [0;1]$ such that $f'(G_{(00)}) = 0$. Therefore, $f'(G) > 0$ on $[0;G_{(00)}]$ and $f'(G) < 0$ on $[G_{(00)};1]$.

(b.1) If $f(G_{(00)}) < 0$, then $f(G) < 0$ on $[0;1]$.

(b.2) If $f(G_{(00)}) > 0$, then:

(b.2.1) If $q > 0$ and $q > \dfrac{m\exp(pb)}{g_0^2+1} + \alpha - \theta$ then $f(G) > 0$ on $[0;1]$.

(b.2.2) If $q < 0$ and $q > \dfrac{m\exp(pb)}{g_0^2+1} + \alpha - \theta$, then $\exists G_{23}^* \in [0;G_{(00)}]$ such that $f(G_{23}^*) = 0$.

(b.2.3) If $q > 0$ and $q < \dfrac{m\exp(pb)}{g_0^2+1} + \alpha - \theta$, then $G_{24}^* \in [G_{(00)};1]$ such that $f(G_{24}^*) = 0$.

(b.2.4) If $q < 0$ and $q < \dfrac{m\exp(pb)}{g_0^2+1} + \alpha - \theta$, then $G_{23}^* \in [0;G_{(00)}]$ and $G_{24}^* \in [G_{(00)};1]$ are the two roots of f.

(II.1.2.2) If $q > 6\alpha - 3\theta + \alpha g_0^2 + \dfrac{1}{2}m\exp(pb)\left[(pb)^2 + pb + 2\right]$, because f'' increase strictly on $[0;1]$, by the intermediate values theorem $\exists G_{(000)} \in [0;1]$ such that $f''(G_{(000)}) = 0$. So, $f''(G) < 0$ on $[0;G_{(000)}]$ and there $f''(G) > 0$ on $[G_{(000)};1]$.

(II.1.2.2.1) If $f'(G_{(000)}) > 0$, then $f'(G) > 0$ on $[0;1]$, therefore f is increasing on that interval.

(a) If $q > 0$, then $f(G) > 0$ on $[0;1]$.

(b) If $q < 0$, then

(b.1) If $q < \dfrac{m\exp(pb)}{g_0^2+1} + \alpha - \theta$, then $f(G) < 0$ on $[0;1]$.

(b.2) If $q > \dfrac{m\exp(pb)}{g_0^2+1} + \alpha - \theta$, then $\exists G_{25}^* \in [0;1]$ such that $f(G_{25}^*) = 0$.

(II.1.2.2.2) If $f'(G_{(000)}) < 0$, then:

(a) If $\theta < 0$ and $q < \dfrac{1}{2}\left[4\alpha - 3\theta + (2\alpha-\theta)g_0^2 + m\exp(pb)\,[pb+2]\right]$, then $f'(G) < 0$ on $[0;1]$. Therefore f strictly decreases on $[0;1]$.

(a.1) If $q < 0$, then $f(G) < 0$ on $[0;1]$.

(a.2) If $q > 0$, then:

(a.2.1) If $q > \dfrac{m\exp(pb)}{g_0^2+1} + \alpha - \theta$, then $f(G) > 0$ on $[0;1]$.

(a.2.2) If $q < \dfrac{m\exp(pb)}{g_0^2+1} + \alpha - \theta$, then $\exists G_{26}^* \in [0;1]$ such that $f(G_{26}^*) = 0$.

(b) If $\theta > 0$ and $q < \dfrac{1}{2}\left[4\alpha - 3\theta + (2\alpha-\theta)g_0^2 + m\exp(pb)\,[pb+2]\right]$, then $\exists G_{(0000)} \in [0;G_{(000)}]$ such that $f'(G_{(0000)}) = 0$. Therefore $f'(G) > 0$ on $[0;G_{(0000)}]$ and $f'(G) < 0$ on $[G_{(0000)};1]$.

(b.1) If $f(G_{(0000)}) < 0$, then $f(G) < 0$ on $[0;1]$.

(b.2) If $f(G_{(0000)}) > 0$, then:

(b.2.1) If $q > 0$, and $q > \dfrac{m\exp(pb)}{g_0^2+1} + \alpha - \theta$, then $f(G) > 0$ on $[0;1]$.

(b.2.2) If $q < 0$, and $q > \dfrac{m\exp(pb)}{g_0^2+1} + \alpha - \theta$, then $\exists G^*_{27} \in [0; G_{(0000)}]$ such that $f(G^*_{27}) = 0$.

(b.2.3) If $q > 0$, and $q < \dfrac{m\exp(pb)}{g_0^2+1} + \alpha - \theta$, then $\exists G^*_{28} \in [G_{(0000)}; 1]$ such that $f(G^*_{28}) = 0$.

(b.2.4) If $q < 0$, and $q < \dfrac{m\exp(pb)}{g_0^2+1} + \alpha - \theta$, then $^*_{27} \in [0; G_{(0000)}]$ and $G^*_{28} \in [G_{(0000)}; 1]$ are the two roots of f.

(c) If $\theta < 0$ and $q > \dfrac{1}{2}\left[4\alpha - 3\theta + (2\alpha - \theta)g_0^2 + m\exp(pb)\left[pb + 2\right]\right]$, then $\exists G_{(00000)} \in [G_{(000)}; 1]$ such that $f'(G_{(00000)}) = 0$. Therefore $f'(G) < 0$ on $[0; G_{(00000)}]$ and $f'(G) > 0$ on $[G_{(00000)}; 1]$.

(c.1) If $f(G_{(00000)}) > 0$, then $f(G) > 0$ on $[0;1]$.

(c.2) If $f(G_{(00000)}) < 0$:

(c.2.1) If $q < 0$, and $q < \dfrac{m\exp(pb)}{g_0^2+1} + \alpha - \theta$, then $f(G) < 0$ on $[0;1]$.

(c.2.2) If $q > 0$, and $q < \dfrac{m\exp(pb)}{g_0^2+1} + \alpha - \theta$, then $\exists G^*_{29} \in [0; G_{(00000)}]$ such that $f(G^*_{29}) = 0$.

(c.2.3) If $q < 0$, and $q > \dfrac{m\exp(pb)}{g_0^2+1} + \alpha - \theta$, then $\exists G^*_{30} \in [0; G_{(00000)}]$ such that $f(G^*_{30}) = 0$.

(c.2.4) If $q > 0$, and $q > \dfrac{m\exp(pb)}{g_0^2+1} + \alpha - \theta$, then $G^*_{29} \in [0; G_{(00000)}]$ and $G^*_{30} \in [0; G_{(00000)}]$ are the two roots of f.

(d) If $\theta > 0$ and $q > \dfrac{1}{2}\left[4\alpha - 3\theta + (2\alpha - \theta)g_0^2 + m\exp(pb)\left[pb + 2\right]\right]$, then: $\exists G_{(0000)} \in [0; G_{(000)}]$ and $G_{(00000)} \in [G_{(000)}; 1]$ such that $f'(G_{(0000)}) = f'(G_{(00000)}) = 0$. Therefore $f'(G) > 0$ on $[0; G_{(0000)}] \cup [G_{(00000)}; 1]$ and $f'(G) > 0$ on $[G_{(0000)}; G_{(0000)}]$.

(d.1) If $f(G_{(0000)}) < 0$,then

(d.1.1) if $q < \dfrac{m\exp(pb)}{g_0^2+1} + \alpha - \theta$ then $f(G) < 0$ on $[0;1]$.

(d.1.2) if $q > \dfrac{m\exp(pb)}{g_0^2+1} + \alpha - \theta$, then G^*_{30} is the unique root of f.

(d.2) If $f(G_{(0000)}) > 0$ and $f(G_{(00000)}) > 0$, then:

(d.2.1) If $q > 0$, then $f(G) > 0$ on $[0;1]$.

(d.2.2) If $q < 0$, then $G^*_{27} \in [0; G_{(0000)}]$ is the unique root of f.

(d.3) If $f(G_{(0000)}) > 0$ and $f(G_{(00000)}) < 0$, then: $\exists G^*_{31} \in [G_{(0000)}; G_{(00000)}]$ such that $f(G^*_{31}) = 0$.

(d.3.1) If $q > 0$ and $q > \dfrac{m\exp(pb)}{g_0^2+1} + \alpha - \theta$, then with G^*_{31}, we have also $G^*_{30} \in [G_{(00000)}; 1]$ such that $f(G^*_{31}) = f(G^*_{30}) = 0$.

(d.3.2) If $q > 0$ and $q < \dfrac{m\exp(pb)}{g_0^2+1} + \alpha - \theta$, then G^*_{31} is the unique root of f. Therefore $f(G^*_{31}) = 0$.

(d.3.3) If $q<0$ and $q<\dfrac{m\exp(pb)}{g_0^2+1}+\alpha-\theta$, then with G_{31}^*, we have also $G_{27}^*\in[0;G_{(0000)}]$ such that $f(G_{31}^*)=f(G_{27}^*)=0$.

(d.3.4) If $q<0$ and $q>\dfrac{m\exp(pb)}{g_0^2+1}+\alpha-\theta$, then with G_{31}^* and $G_{30}^*\in[G_{(00000)};1]$, we have also $G_{27}^*\in[0;G_{(0000)}]$ such that $f(G_{29}^*)=f(G_{30}^*)=f(G_{32}^*)=0$

(II.2) If $\theta<\dfrac{1}{6}\left[24\alpha+mpb\left((pb)^2+6(pb)+6\right)\exp(pb)\right]$, then because of the decreasing of f''' on $[0;1]$ and by using the intermediate values theorem, $\exists\tilde{G}^{(0)}\in[0;1]$ such that $f'''(\tilde{G}^{(0)})=0$. Then $f'''(G)>0$ on $[0;\tilde{G}^{(0)}]$ and $f'''(G)<0$ on $[\tilde{G}^{(0)};1]$.

(II.2.1) If $f''(\tilde{G}^{(0)})<0$, then $f''(G)<0$ on $[0;1]$. Therefore f is decreasing on that interval.

(II.2.1.1) If $\theta<0$, then $f'(G)<0$ on $[0;1]$ and f is decreasing on $[0;1]$.

(II.2.1.1.1) If $q<0$, then $f(G)<0$ on $[0;1]$.

(II.2.1.1.2) If $q>0$, then:

(a) If $q>\dfrac{m\exp(pb)}{g_0^2+1}+\alpha-\theta$, then $f(G)>0$ on $[0;1]$.

(b) If $q<\dfrac{m\exp(pb)}{g_0^2+1}+\alpha-\theta$, then $\exists G_{33}^*\in[0;1]$ such that $f(G_{33}^*)=0$.

(II.2.1.2) If $\theta>0$, then we have the following cases:

(II.2.1.2.1) If $q>\dfrac{1}{2}\left[4\alpha-3\theta+(2\alpha-\theta)g_0^2+m\exp(pb)\left[pb+2\right]\right]$, then $f'(G)>0$ on $[0;1]$. Therefore f is increasing on $[0;1]$.

(a) If $q>0$, then $f(G)>0$ on $[0;1]$.

(b) If $q<0$, then:

(b.1) If $q<\dfrac{m\exp(pb)}{g_0^2+1}+\alpha-\theta$, then $f(G)<0$ on $[0;1]$.

(b.2) If $q>\dfrac{m\exp(pb)}{g_0^2+1}+\alpha-\theta$, then $\exists G_{34}^*\in[0;1]$ such that $f(G_{34}^*)=0$.

(II.2.1.2.2) If $q<\dfrac{1}{2}\left[4\alpha-3\theta+(2\alpha-\theta)g_0^2+m\exp(pb)\left[pb+2\right]\right]$, then $\exists\tilde{G}^{(1)}\in[0;1]$ such that $f'(\tilde{G}^{(1)})=0$.Therefore $f'(G)>0$ on $[0;\tilde{G}^{(1)}]$ and $f'(G)>0$ on $[\tilde{G}^{(1)};1]$.

(a) If $f(\tilde{G}^{(1)})<0$, then $f(G)<0$ on $[0;1]$.

(b) If $f(\tilde{G}^{(1)})>0$, then:

(b.1) If $q>0$ and $q>\dfrac{m\exp(pb)}{g_0^2+1}+\alpha-\theta$, then $f(G)>0$ on $[0;1]$.

(b.2) If $q<0$ and $q>\dfrac{m\exp(pb)}{g_0^2+1}+\alpha-\theta$, then $\exists G_{35}^*\in[0;\tilde{G}^{(1)}]$ such that $f(G_{35}^*)=0$.

(b.3) If $q>0$ and $q<\dfrac{m\exp(pb)}{g_0^2+1}+\alpha-\theta$, then $\exists G_{36}^*\in[\tilde{G}^{(1)};1]$ such that $f(G_{36}^*)=0$.

(b.3) If $q<0$ and $q<\dfrac{m\exp(pb)}{g_0^2+1}+\alpha-\theta$, then G_{35}^* and G_{36}^* are the two roots on $[0;1]$ of f.

(II.2.2) If $f''(\tilde{G}^{(0)})>0$, then:

(II.2.2.1) If $q>m+\alpha g_0^2$ and $q>6\alpha-3\theta+\alpha g_0^2+\dfrac{1}{2}m\exp(pb)\left[(pb)^2+pb+2\right]$, then $f''(G)>0$ on $[0;1]$.Therefore f' is increasing on $[0;1]$.

(II.2.2.1.1) If $\theta > 0$, then $f'(G) > 0$ on $[0;1]$. Therefore f is increasing on $[0;1]$.

(a) If $q > 0$, then $f(G) > 0$ on $[0;1]$.

(b) If $q < 0$, then:

(b.1) If $q < \dfrac{m\exp(pb)}{g_0^2+1} + \alpha - \theta$, then $f(G) < 0$ on $[0;1]$.

(b.2) If $q > \dfrac{m\exp(pb)}{g_0^2+1} + \alpha - \theta$, then $\exists G_{37}^* \in [0;1]$ such that $f(G_{37}^*) = 0$.

(II.2.2.1.2) If $\theta < 0$, then:

(a) If $q < \dfrac{1}{2}\left[4\alpha - 3\theta + (2\alpha-\theta)g_0^2 + m\exp(pb)\left[pb+2\right]\right]$, then $f'(G) < 0$ on $[0;1]$. Therefore f is decreasing on $[0;1]$.

(a.1) If $q < 0$, then $f(G) < 0$ on $[0;1]$.

(a.2) If $q > 0$, then:

(a.2.1) If $q > \dfrac{m\exp(pb)}{g_0^2+1} + \alpha - \theta$, then $f(G) > 0$ on $[0;1]$.

(a.2.2) If $q < \dfrac{m\exp(pb)}{g_0^2+1} + \alpha - \theta$, then $\exists G_{38}^* \in [0;1]$ such that $f(G_{38}^*) = 0$.

(b) If $q > \dfrac{1}{2}\left[4\alpha - 3\theta + (2\alpha-\theta)g_0^2 + m\exp(pb)\left[pb+2\right]\right]$, then $\exists \tilde{G}^{(2)} \in [0;1]$ such that $f'(\tilde{G}^{(2)}) = 0$. Therefore $f'(G) < 0$ on $[0;\tilde{G}^{(2)}]$ and $f'(G) > 0$ on $[\tilde{G}^{(2)};1]$.

(b.1) If $f(\tilde{G}^{(2)}) > 0$, then $f(G) > 0$ on $[0;1]$.

(b.2) If $f(\tilde{G}^{(2)}) < 0$, then we have the following cases:

(b.2.1) If $q < 0$ and $q < \dfrac{m\exp(pb)}{g_0^2+1} + \alpha - \theta$, then $f(G) < 0$ on $[0;1]$.

(b.2.2) If $q > 0$ and $q < \dfrac{m\exp(pb)}{g_0^2+1} + \alpha - \theta$, then $\exists G_{39}^* \in [0;\tilde{G}^{(2)}]$ such that $f(G_{39}^*) = 0$.

(b.2.3) If $q < 0$ and $q > \dfrac{m\exp(pb)}{g_0^2+1} + \alpha - \theta$, then $\exists G_{40}^* \in [\tilde{G}^{(2)};1]$ such that $f(G_{40}^*) = 0$.

(b.2.4) If $q > 0$ and $q > \dfrac{m\exp(pb)}{g_0^2+1} + \alpha - \theta$, then G_{39}^* and G_{40}^* are the two roots on $[0;1]$ of f.

(II.2.2.2) If $q < m + \alpha g_0^2$ and $q > 6\alpha - 3\theta + \alpha g_0^2 + \dfrac{1}{2}m\exp(pb)\left[(pb)^2 + pb + 2\right]$, then: $\exists \tilde{G}^{(3)} \in [0;\tilde{G}^{(0)}]$ such that $f''(\tilde{G}^{(3)}) = 0$. Therefore $f''(G) < 0$ on $[0;\tilde{G}^{(3)}]$ and $f''(G) > 0$ on $[\tilde{G}^{(3)};1]$.

(II.2.2.2.1) If $f'(\tilde{G}^{(3)}) > 0$, then $f'(G) > 0$ on $[0;1]$. Therefore f is increasing on $[0;1]$.

(a) If $q > 0$, then $f(G) > 0$ on $[0;1]$.

(b) If $q < 0$, then:

(b.1) If $q < \dfrac{m\exp(pb)}{g_0^2+1} + \alpha - \theta$, then $f(G) < 0$ on $[0;1]$.

(b.2) If $q > \dfrac{m\exp(pb)}{g_0^2+1} + \alpha - \theta$, then $\exists G_{41}^* \in [0;1]$ such that $f(G_{41}^*) = 0$.

(II.2.2.2.2) If $f'(\tilde{G}^{(3)}) < 0$, then we have the following cases:

(*a*) If $\theta < 0$ and $q < \frac{1}{2}\left[4\alpha - 3\theta + (2\alpha - \theta)g_0^2 + m\exp(pb)\left[pb + 2\right]\right]$, then $f'(G) < 0$ on $[0;1]$. Therefore f is decreasing on $[0;1]$.
(a.1) If $q < 0$, then $f(G) < 0$ on $[0;1]$.
(a.2) If $q > 0$, then:
(a.2.1) If $q > \frac{m\exp(pb)}{g_0^2+1} + \alpha - \theta$, then $f(G) > 0$ on $[0;1]$.
(a.2.2) If $q < \frac{m\exp(pb)}{g_0^2+1} + \alpha - \theta$, then $\exists G_{42}^* \in [0;1]$ such that $f(G_{42}^*) = 0$.

(*b*) If $\theta > 0$ and $q < \frac{1}{2}\left[4\alpha - 3\theta + (2\alpha - \theta)g_0^2 + m\exp(pb)\left[pb + 2\right]\right]$, then $\exists \tilde{G}^{(4)} \in [0;\tilde{G}^3]$ such that $f'(\tilde{G}^{(4)}) = 0$. Therefore $f'(G) > 0$ on $[0;\tilde{G}^{(4)}]$ and $f'(G) < 0$ on $[\tilde{G}^{(4)};1]$.
(b.1) If $f(\tilde{G}^{(4)}) < 0$, then $f(G) < 0$ on $[0;1]$.
(b.2) If $f(\tilde{G}^{(4)}) > 0$, then:
(b.2.1) If $q > 0$ and $q > \frac{m\exp(pb)}{g_0^2+1} + \alpha - \theta$, then $f(G) > 0$ on $[0;1]$.
(b.2.2) If $q < 0$ and $q > \frac{m\exp(pb)}{g_0^2+1} + \alpha - \theta$, then $\exists G_{43}^* \in [0;\tilde{G}^{(4)}]$ such that $f(G_{43}^*) = 0$.
(b.2.3) If $q > 0$ and $q < \frac{m\exp(pb)}{g_0^2+1} + \alpha - \theta$, then $\exists G_{44}^* \in [\tilde{G}^{(4)};1]$ such that $f(G_{44}^*) = 0$.
(b.2.4) If $q < 0$ and $q < \frac{m\exp(pb)}{g_0^2+1} + \alpha - \theta$, then G_{44}^* and G_{43}^* are the two roots on $[0;1]$ of f.

(*c*) If $\theta < 0$ and $q > \frac{1}{2}\left[4\alpha - 3\theta + (2\alpha - \theta)g_0^2 + m\exp(pb)\left[pb + 2\right]\right]$, then $\exists \tilde{G}^{(5)} \in [\tilde{G}^3;1]$ such that $f'(\tilde{G}^{(5)}) = 0$. Therefore $f'(G) < 0$ on $[0;\tilde{G}^{(5)}]$ and $f'(G) > 0$ on $[\tilde{G}^{(5)};1]$.
(c.1) If $f(\tilde{G}^{(5)}) > 0$, then $f(G) > 0$ on $[0;1]$.
(c.2) If $f(\tilde{G}^{(5)}) < 0$, then:
(c.2.1) If $q < 0$ and $q < \frac{m\exp(pb)}{g_0^2+1} + \alpha - \theta$, then $f(G) < 0$ on $[0;1]$.
(c.2.2) If $q > 0$ and $q < \frac{m\exp(pb)}{g_0^2+1} + \alpha - \theta$, then $\exists G_{45}^* \in [0;\tilde{G}^{(5)}]$ such that $f(G_{45}^*) = 0$.
(c.2.3) If $q < 0$ and $q > \frac{m\exp(pb)}{g_0^2+1} + \alpha - \theta$, then $\exists G_{46}^* \in [\tilde{G}^{(5)};1]$ such that $f(G_{46}^*) = 0$.
(c.2.4) If $q > 0$ and $q > \frac{m\exp(pb)}{g_0^2+1} + \alpha - \theta$, then G_{45}^* and G_{46}^* are the two roots of f on $[0;1]$.

(*d*) If $\theta > 0$ and $q > \frac{1}{2}\left[4\alpha - 3\theta + (2\alpha - \theta)g_0^2 + m\exp(pb)\left[pb + 2\right]\right]$, then $\tilde{G}^{(4)}$ and $\tilde{G}^{(5)}$ are the two roots of f'. Therefore $f'(G) > 0$ on $[0;\tilde{G}^{(4)}] \cup [\tilde{G}^{(5)};1]$ and $f'(G) < 0$ on $[\tilde{G}^{(4)};\tilde{G}^{(5)}]$.
(d.1) If $f(\tilde{G}^{(4)}) < 0$, then we have the following cases:
(d.1.1) If $q < \frac{m\exp(pb)}{g_0^2+1} + \alpha - \theta$, then $f(G) < 0$ on $[0;1]$.

(d.1.2) If $q > \dfrac{m\exp(pb)}{g_0^2+1} + \alpha - \theta$, then G_{46}^* is the unique roots of f.

(d.2) If $f(\tilde{G}^{(4)}) > 0$ and $f(\tilde{G}^{(5)}) > 0$, then:

(d.2.1) If $q > 0$, then $f(G) > 0$ on $[0;1]$.

(d.2.2) If $q < 0$, then G_{43}^* is the unique roots of f.

(d.3) If $f(\tilde{G}^{(4)}) > 0$ and $f(\tilde{G}^{(5)}) < 0$, then: $\exists G_{47}^* \in [\tilde{G}^{(4)}; \tilde{G}^{(5)}]$ such that $f(G_{47}^*) = 0$.

(d.3.1) If $q > 0$ and $q > \dfrac{m\exp(pb)}{g_0^2+1} + \alpha - \theta$, then G_{47}^* and G_{46}^* are the two roots of f.

(d.3.2) If $q > 0$ and $q < \dfrac{m\exp(pb)}{g_0^2+1} + \alpha - \theta$, then G_{47}^* is the unique root of f.

(d.3.3) If $q < 0$ and $q < \dfrac{m\exp(pb)}{g_0^2+1} + \alpha - \theta$, then G_{47}^* and G_{43}^* are the two roots of f.

(d.3.4) If $q < 0$ and $q > \dfrac{m\exp(pb)}{g_0^2+1} + \alpha - \theta$, then G_{47}^* ,G_{46}^* and G_{43}^* are the three roots of f.

(II.2.2.3) If $q > m + \alpha g_0^2$ and $q < 6\alpha - 3\theta + \alpha g_0^2 + \dfrac{1}{2} m\exp(pb)\left[(pb)^2 + pb + 2\right]$, then: $\exists \tilde{G}^{(6)} \in [\tilde{G}^{(0)}; 1]$ such that $f''(\tilde{G}^{(6)}) = 0$. Therefore, $f''(G) > 0$ on $[0; \tilde{G}^{(6)}]$ and $f''(G) < 0$ on $[\tilde{G}^{(6)}; 1]$.

(II.2.2.3.1) If $f'(\tilde{G}^{(6)}) < 0$, then $f'(G) < 0$ on $[0;1]$. Therefore f is decreasing on $[0;1]$.

(a) If $q < 0$, then $f(G) < 0$ on $[0;1]$.

(b) If $q > 0$, then:

(b.1) If $q > \dfrac{m\exp(pb)}{g_0^2+1} + \alpha - \theta$, then $f(G) > 0$ on $[0;1]$.

(b.2) If $q < \dfrac{m\exp(pb)}{g_0^2+1} + \alpha - \theta$, then $\exists G_{48}^* \in [0;1]$ such that $f(G_{48}^*) = 0$.

(II.2.2.3.2) If $f'(\tilde{G}^{(6)}) > 0$, then

(a) If $\theta > 0$ and $q > \dfrac{1}{2}\left[4\alpha - 3\theta + (2\alpha - \theta)g_0^2 + m\exp(pb)\left[pb + 2\right]\right]$, then $f'(G) > 0$ on $[0;1]$ and therefore f is increasing on $[0;1]$.

(a.1) If $q > 0$, then $f(G) > 0$ on $[0;1]$.

(a.2) If $q < 0$, then:

(a.2.1) If $q < \dfrac{m\exp(pb)}{g_0^2+1} + \alpha - \theta$, then $f(G) < 0$ on $[0;1]$.

(a.2.2) If $q > \dfrac{m\exp(pb)}{g_0^2+1} + \alpha - \theta$, then $\exists G_{49}^* \in [0;1]$ such that $f(G_{49}^*) = 0$.

(b) If $\theta < 0$ and $q > \dfrac{1}{2}\left[4\alpha - 3\theta + (2\alpha - \theta)g_0^2 + m\exp(pb)\left[pb + 2\right]\right]$, then $\exists \tilde{G}^{(7)} \in [0; \tilde{G}^{(6)}]$ such that $f'(\tilde{G}^{(7)}) = 0$. Therefore $f'(G) < 0$ on $[0; \tilde{G}^{(7)}]$ and $f'(G) > 0$ on $[\tilde{G}^{(7)}; 1]$

(b.1) If $f(\tilde{G}^{(7)}) > 0$, then $f(G) > 0$ on $[0;1]$.

(b.2) If $f(\tilde{G}^{(7)}) < 0$, then:

(b.2.1) If $q < 0$ and $q < \dfrac{m\exp(pb)}{g_0^2+1} + \alpha - \theta$, then $f(G) < 0$ on $[0;1]$.

(b.2.2) If $q > 0$ and $q < \dfrac{m\exp(pb)}{g_0^2+1} + \alpha - \theta$, then $\exists G_{50}^* \in [0; \tilde{G}^{(7)}]$ such that $f(G_{50}^*) = 0$.

(b.2.3) If $q < 0$ and $q > \dfrac{m\exp(pb)}{g_0^2+1} + \alpha - \theta$, then $\exists G_{51}^* \in [\tilde{G}^{(7)}; 1]$ such that $f(G_{51}^*) = 0$.

(b.2.4) If $q > 0$ and $q > \dfrac{m\exp(pb)}{g_0^2+1} + \alpha - \theta$, then G_{50}^* and G_{51}^* are the two roots on $[0; 1]$ of f.

(c) If $\theta > 0$ and $q < \dfrac{1}{2}\left[4\alpha - 3\theta + (2\alpha - \theta)g_0^2 + m\exp(pb)\,[pb+2]\right]$, then $\exists \tilde{G}^{(8)} \in [\tilde{G}^{(6)}; 1]$ such that $f'(\tilde{G}^{(8)}) = 0$. Therefore $f'(G) > 0$ on $[0; \tilde{G}^{(8)}]$ and $f'(G) < 0$ on $[\tilde{G}^{(8)}; 1]$

(c.1) If $f(\tilde{G}^{(8)}) < 0$, then $f(G) < 0$ on $[0; 1]$.

(c.2) If $f(\tilde{G}^{(8)}) > 0$, then:

(c.2.1) If $q > 0$ and $q > \dfrac{m\exp(pb)}{g_0^2+1} + \alpha - \theta$, then $f(G) > 0$ on $[0; 1]$.

(c.2.2) If $q < 0$ and $q > \dfrac{m\exp(pb)}{g_0^2+1} + \alpha - \theta$, then $\exists G_{52}^* \in [0; \tilde{G}^{(8)}]$ such that $f(G_{52}^*) = 0$.

(c.2.3) If $q > 0$ and $q < \dfrac{m\exp(pb)}{g_0^2+1} + \alpha - \theta$, then $\exists G_{53}^* \in [\tilde{G}^{(8)}; 1]$ such that $f(G_{53}^*) = 0$.

(c.2.4) If $q < 0$ and $q < \dfrac{m\exp(pb)}{g_0^2+1} + \alpha - \theta$, then G_{52}^* and G_{53}^* are the two roots on $[0; 1]$ of f.

(d) If $\theta < 0$ and $q < \dfrac{1}{2}\left[4\alpha - 3\theta + (2\alpha - \theta)g_0^2 + m\exp(pb)\,[pb+2]\right]$, then $\tilde{G}^{(8)}$ and $\tilde{G}^{(7)}$ are the two positive roots of f'. Therefore $f'(G) > 0$ on $[\tilde{G}^{(7)}; \tilde{G}^{(8)}]$ and $f'(G) < 0$ on $[0; \tilde{G}^{(7)}] \cup [\tilde{G}^{(8)}; 1]$.

(d.1) If $f(\tilde{G}^{(7)}) > 0$, then:

(d.1.1) If $q > \dfrac{m\exp(pb)}{g_0^2+1} + \alpha - \theta$, then $f(G) > 0$ on $[0; 1]$.

(d.1.2) If $q < \dfrac{m\exp(pb)}{g_0^2+1} + \alpha - \theta$, then G_{53}^* is the unique root of f.

(d.2) If $f(\tilde{G}^{(7)}) < 0$ and $f(\tilde{G}^{(8)}) < 0$, then :

(d.2.1) If $q < 0$, then $f(G) < 0$ on $[0; 1]$.

(d.2.2) If $q > 0$, then G_{50}^* is the unique root of f.

(d.3) If $f(\tilde{G}^{(7)}) < 0$ and $f(\tilde{G}^{(8)}) > 0$, then :$\exists G_{54}^* \in [\tilde{G}^{(7)}; \tilde{G}^{(8)}]$ such that $f(G_{54}^*) = 0$.

(d.3.1) If $q < 0$ and $q < \dfrac{m\exp(pb)}{g_0^2+1} + \alpha - \theta$, then with G_{54}^* we have also G_{53}^* as a root of f.

(d.3.2) If $q < 0$ and $q > \dfrac{m\exp(pb)}{g_0^2+1} + \alpha - \theta$, then G_{54}^* is the unique root of f. .

(d.3.3) If $q > 0$ and $q > \dfrac{m\exp(pb)}{g_0^2+1} + \alpha - \theta$, then with G_{54}^* we have also G_{50}^* as a root of f.

(d.3.4) If $q > 0$ and $q < \dfrac{m\exp(pb)}{g_0^2+1} + \alpha - \theta$, then G_{50}^*, G_{54}^* and G_{53}^* are the three roots on $[0; 1]$ of f.

(II.2.2.4) If $q < m+\alpha g_0^2$ and $q < 6\alpha-3\theta+\alpha g_0^2+\frac{1}{2}m\exp(pb)\left[(pb)^2+pb+2\right]$, then:$\tilde{G}^{(3)}$ and $\tilde{G}^{(6)}$ are the two roots of f''. Therefore, $f''(G) > 0$ on $[\tilde{G}^{(3)};\tilde{G}^{(6)}]$ and $f''(G) < 0$ on $[0;\tilde{G}^{(3)}] \cup [\tilde{G}^{(6)};1]$.

(II.2.2.4.1) If $f'(\tilde{G}^{(3)}) > 0$, then:

(a) If $q > \frac{1}{2}\left[4\alpha-3\theta+(2\alpha-\theta)g_0^2+m\exp(pb)\left[pb+2\right]\right]$, then $f'(G) > 0$ on $[0;1]$, therefore f is increasing on that interval.

(a.1) If $q > 0$, then $f(G) > 0$ on $[0;1]$.

(a.2) If $q < 0$, then:

(a.2.1) If $q < \frac{m\exp(pb)}{g_0^2+1}+\alpha-\theta$, then $f(G) < 0$ on $[0;1]$.

(a.2.2) If $q > \frac{m\exp(pb)}{g_0^2+1}+\alpha-\theta$, then $\exists G_{41}^* \in [\tilde{G}^{(6)};1]$ such that $f(G_{41}^*) = 0$.

(b) If $q < \frac{1}{2}\left[4\alpha-3\theta+(2\alpha-\theta)g_0^2+m\exp(pb)\left[pb+2\right]\right]$, then $\tilde{G}^{(8)}$ is the unique root of f'. Therefore

(b.1) If $f(\tilde{G}^{(8)}) < 0$, then $f(G) < 0$ on $[0;1]$.

(b.2) If $f(\tilde{G}^{(8)}) > 0$, then:

(b.2.1) If $q > 0$ and $q > \frac{m\exp(pb)}{g_0^2+1}+\alpha-\theta$, then $f(G) > 0$ on $[0;1]$.

(b.2.2) If $q < 0$ and $q > \frac{m\exp(pb)}{g_0^2+1}+\alpha-\theta$, then $\exists G_{52}^* \in [0;\tilde{G}^{(8)}]$ such that $f(G_{52}^*) = 0$.

(b.2.3) If $q > 0$ and $q < \frac{m\exp(pb)}{g_0^2+1}+\alpha-\theta$, then $\exists G_{53}^* \in [\tilde{G}^{(8)};1]$ such that $f(G_{53}^*) = 0$.

(b.2.4) If $q < 0$ and $q < \frac{m\exp(pb)}{g_0^2+1}+\alpha-\theta$, then G_{52}^* and G_{53}^* are the two roots on $[0;1]$ of f.

(II.2.2.4.2) If $f'(\tilde{G}^{(3)}) < 0$ and $f'(\tilde{G}^{(6)}) < 0$, then we have the following cases:

(a) If $\theta < 0$, then $f'(G) < 0$ on $[0;1]$. Therefore f is decreasing on $[0;1]$.

(a.1) If $q < 0$, then $f(G) < 0$ on $[0;1]$.

(a.2) If $q > 0$, then :

(a.2.1) If $q > \frac{m\exp(pb)}{g_0^2+1}+\alpha-\theta$, then $f(G) > 0$ on $[0;1]$.

(a.2.2) If $q < \frac{m\exp(pb)}{g_0^2+1}+\alpha-\theta$, then G_{42}^* is the unique root of f.

(b) If $\theta > 0$, then $\tilde{G}^{(4)}$ is the unique root of f'. Therefore:

(b.1) If $f(\tilde{G}^{(4)}) < 0$, then $f(G) < 0$ on $[0;1]$.

(b.2) If $f(\tilde{G}^{(4)}) > 0$, then:

(b.2.1) If $q > 0$ and $q > \frac{m\exp(pb)}{g_0^2+1}+\alpha-\theta$, then $f(G) > 0$ on $[0;1]$.

(b.2.2) If $q < 0$ and $q > \frac{m\exp(pb)}{g_0^2+1}+\alpha-\theta$, then $\exists G_{43}^* \in [0;\tilde{G}^{(4)}]$ such that $f(G_{43}^*) = 0$.

(b.2.3) If $q > 0$ and $q < \frac{m\exp(pb)}{g_0^2+1}+\alpha-\theta$, then $\exists G_{44}^* \in [\tilde{G}^{(4)};1]$ such that $f(G_{44}^*) = 0$.

(b.2.4) If $q<0$ and $q<\dfrac{m\exp(pb)}{g_0^2+1}+\alpha-\theta$, then G_{44}^* and G_{43}^* are the two roots on $[0;1]$ of f.

(II.2.2.4.3) If $f'(\tilde{G}^{(3)})<0$ and $f'(\tilde{G}^{(6)})>0$, then $\exists\tilde{G}^9\in[\tilde{G}^3;\tilde{G}^6]$ such that $f'(\tilde{G}^{(9)})=0$.

(a) If $\theta<0$ and $q>\dfrac{1}{2}\left[4\alpha-3\theta+(2\alpha-\theta)g_0^2+m\exp(pb)\left[pb+2\right]\right]$, then $\tilde{G}^9$ is the unique roots of f'.

(a.1) If $f(\tilde{G}^9)>0$, then $f(G)>0$ on $[0;1]$.

(a.2) If $f(\tilde{G}^9)<0$, then:

(a.2.1) If $q<0$ and $q<\dfrac{m\exp(pb)}{g_0^2+1}+\alpha-\theta$, then $f(G)<0$ on $[0;1]$.

(a.2.2) If $q>0$ and $q<\dfrac{m\exp(pb)}{g_0^2+1}+\alpha-\theta$, then $\exists G_{55}^*\in[0;\tilde{G}^{(9)}]$ such that $f(G_{55}^*)=0$.

(a.2.3) If $q<0$ and $q>\dfrac{m\exp(pb)}{g_0^2+1}+\alpha-\theta$, then $\exists G_{56}^*\in[\tilde{G}^{(9)};1]$ such that $f(G_{56}^*)=0$.

(a.2.4) If $q>0$ and $q>\dfrac{m\exp(pb)}{g_0^2+1}+\alpha-\theta$, then G_{55}^* and G_{56}^* are the roots of f.

(b) If $\theta>0$ and $q>\dfrac{1}{2}\left[4\alpha-3\theta+(2\alpha-\theta)g_0^2+m\exp(pb)\left[pb+2\right]\right]$, then with $\tilde{G}^9$ we have also $\tilde{G}^4$ root of f'. Therefore $f'(G)<0$ on $[\tilde{G}^4;\tilde{G}^9]$ and $f'(G)>0$ on $[0;\tilde{G}^4]\cup[\tilde{G}^9;1]$.

(b.1) If $f(\tilde{G}^4)<0$, then:

(b.1.1) If $q<\dfrac{m\exp(pb)}{g_0^2+1}+\alpha-\theta$, then $f(G)<0$ on $[0;1]$.

(b.1.2) If $q>\dfrac{m\exp(pb)}{g_0^2+1}+\alpha-\theta$, then $G_{56}^*\in[\tilde{G}^{(9)};1]$ is the unique root of f.

(b.2) If $f(\tilde{G}^4)>0$ and $f(\tilde{G}^9)>0$, then:

(b.2.1) If $q>0$, then $f(G)>0$ on $[0;1]$.

(b.2.1) If $q<0$, then G_{43}^* is the unique root of f.

(b.3) If $f(\tilde{G}^4)>0$ and $f(\tilde{G}^9)<0$, then $\exists G_{57}^*\in[\tilde{G}^4;\tilde{G}^9]$ such that $f(G_{57}^*)=0$.

(b.3.1) If $q>0$ and $q<\dfrac{m\exp(pb)}{g_0^2+1}+\alpha-\theta$,then G_{57}^* is the unique root of f.

(b.3.2) If $q<0$ and $q<\dfrac{m\exp(pb)}{g_0^2+1}+\alpha-\theta$, then with G_{57}^* we have also G_{43}^* roots of f.

(b.3.3) If $q>0$ and $q>\dfrac{m\exp(pb)}{g_0^2+1}+\alpha-\theta$, then with G_{57}^* we have also G_{56}^* roots of f.

(b.3.4) If $q<0$ and $q>\dfrac{m\exp(pb)}{g_0^2+1}+\alpha-\theta$, then with G_{57}^* we have also G_{56}^* and G_{43}^* roots of f.

(c) If $\theta<0$ and $q<\dfrac{1}{2}\left[4\alpha-3\theta+(2\alpha-\theta)g_0^2+m\exp(pb)\left[pb+2\right]\right]$, then with $\tilde{G}^9$ we have also $\tilde{G}^8$ roots of f'. Therefore $f'(G)>0$ on $[\tilde{G}^9;\tilde{G}^8]$ and $f'(G)<0$ on $[0;\tilde{G}^9]\cup[\tilde{G}^8;1]$.

(c.1) If $f(\tilde{G}^9) > 0$, then:

(c.1.1) If $q > \dfrac{m\exp(pb)}{g_0^2+1} + \alpha - \theta$, then $f(G) > 0$ on $[0;1]$.

(c.1.2) If $q < \dfrac{m\exp(pb)}{g_0^2+1} + \alpha - \theta$, then G^*_{53} is the unique root of f.

(c.2) If $f(\tilde{G}^9) < 0$ and $f(\tilde{G}^8) < 0$ then

(c.2.1) If $q < 0$, then $f(G) < 0$ on $[0;1]$.

(c.2.2) If $q > 0$, then G^*_{55} is the unique root of f.

(c.3) If $f(\tilde{G}^9) < 0$ and $f(\tilde{G}^8) > 0$, then $\exists G^*_{58} \in [\tilde{G}^9; \tilde{G}^8]$ such that $f(G^*_{58}) = 0$.

(c.3.1) If $q < 0$ and $q > \dfrac{m\exp(pb)}{g_0^2+1} + \alpha - \theta$, then G^*_{58} is the unique root of f.

(c.3.2) If $q > 0$ and $q > \dfrac{m\exp(pb)}{g_0^2+1} + \alpha - \theta$,then with G^*_{58} we have also G^*_{55} root of f.

(c.3.3) If $q < 0$ and $q < \dfrac{m\exp(pb)}{g_0^2+1} + \alpha - \theta$, then with G^*_{58} we have also G^*_{53} root of f.

(c.3.3) If $q > 0$ and $q < \dfrac{m\exp(pb)}{g_0^2+1} + \alpha - \theta$, then with G^*_{58} we have also G^*_{53} and G^*_{55} root of f.

(d) If $\theta > 0$ and $q < \dfrac{1}{2}\left[4\alpha - 3\theta + (2\alpha - \theta)g_0^2 + m\exp(pb)\left[pb+2\right]\right]$, then with $\tilde{G}^9$ we have also $\tilde{G}^4$ and $\tilde{G}^8$ roots of f'. Therefore $f'(G) > 0$ on $[0;\tilde{G}^4] \cup [\tilde{G}^9;\tilde{G}^8]$ and $f'(G) < 0$ on $[\tilde{G}^4;\tilde{G}^9] \cup [\tilde{G}^8;1]$.

(d.1) If $f(\tilde{G}^4) < 0$ and $f(\tilde{G}^8) < 0$, then $f(G) < 0$ on $[0;1]$.

(d.2) If $f(\tilde{G}^4) > 0$ and $f(\tilde{G}^8) < 0$, then $f(\tilde{G}^9) < 0$ and therefore $\exists G^*_{59} \in [\tilde{G}^4;\tilde{G}^9]$ such that $f(G^*_{59}) = 0$. Then:

(d.2.1) If $q > 0$, then G^*_{59} is the unique root of f.

(d.2.2) If $q < 0$, then with G^*_{59}, we have also G^*_{43} roots of f.

(d.3) If $f(\tilde{G}^4) < 0$ and $f(\tilde{G}^8) > 0$, then $f(\tilde{G}^9) < 0$ and therefore $\exists G^*_{60} \in [\tilde{G}^9;\tilde{G}^8]$ such that $f(G^*_{60}) = 0$. Then:

(d.3.1) If $q > \dfrac{m\exp(pb)}{g_0^2+1} + \alpha - \theta$, then G^*_{60} is the unique root of f.

(d.3.2) If $q < \dfrac{m\exp(pb)}{g_0^2+1} + \alpha - \theta$, with G^*_{60} we have also G^*_{53} roots of f.

(d.4) If $f(\tilde{G}^4) > 0$ and $f(\tilde{G}^8) > 0$, then:

(d.4.1) If $f(\tilde{G}^9) > 0$, then:

(d.4.1.1) If $q > 0$ and $q > \dfrac{m\exp(pb)}{g_0^2+1} + \alpha - \theta$, then $f(G) > 0$ on $[0;1]$.

(d.4.1.2) If $q > 0$ and $q < \dfrac{m\exp(pb)}{g_0^2+1} + \alpha - \theta$, then f has an unique root G^*_{53}.

(d.4.1.3) If $q < 0$ and $q > \dfrac{m\exp(pb)}{g_0^2+1} + \alpha - \theta$, then f has an unique root G^*_{43}.

(d.4.1.4) If $q < 0$ and $q < \dfrac{m\exp(pb)}{g_0^2+1} + \alpha - \theta$, G^*_{43} and G^*_{53} are the two roots of f.

(d.4.2) If $f(\tilde{G}^9) < 0$, then with G^*_{59} and G^*_{58}, we have also:

(d.4.2.1) If $q > 0$ and $q > \dfrac{m\exp(pb)}{g_0^2+1} + \alpha - \theta$, G^*_{59} and G^*_{58} roots of f.

(d.4.2.2) If $q < 0$ and $q > \dfrac{m\exp(pb)}{g_0^2+1} + \alpha - \theta$,$G^*_{43}$. Therefore G^*_{59},G^*_{58},G^*_{43} are the three roots of f.

(d.4.2.3) If $q > 0$ and $q < \dfrac{m\exp(pb)}{g_0^2+1} + \alpha - \theta$, G^*_{53}. Therefore G^*_{59},G^*_{58},G^*_{53} are the three roots of f.

(d.4.2.4) If $q < 0$ and $q < \dfrac{m\exp(pb)}{g_0^2+1} + \alpha - \theta$, G^*_{43} and G^*_{53}. Therefore G^*_{59},G^*_{58}, G^*_{53} and G^*_{43} are the fourth roots of f

Appendix C. Proof of Proposition 4

Set:

$$\begin{aligned} a_{11} &= -\gamma_G G^*, \\ a_{12} &= -\gamma_{TG} G^*, \\ a_{21} &= -\lambda_{fT} f\omega'(G^*)\exp(-pT^*)T^*, \\ a_{22} &= -\gamma_T\left[(1-\Omega)T^* + 2\Omega(T^*)^2\right] + p\lambda_{fT} f\omega(G^*)\exp(-pT^*)T^*. \end{aligned}$$

For the savanna steady state, we have the Jacobian Matrix:

$$M(G^*;T^*) = \begin{pmatrix} a_{11} & a_{12} \\ a_{21} & a_{22} \end{pmatrix}. \tag{C.1}$$

If $f = 0$, then:

$$\begin{aligned} a_{11} &= -\gamma_G G^*, \\ a_{12} &= -\gamma_{TG} G^*, \\ a_{21} &= 0, \\ a_{22} &= -\gamma_T\left[(1-\Omega)T^* + 2\Omega(T^*)^2\right] = -\gamma_T T^*\left[(1-\Omega) + 2\Omega T^*\right]. \end{aligned}$$

Therefore:

(a) If $\Omega = 0$, then $a_{22} < 0$. Consequently $a_{11} < 0$ and $a_{22} < 0$. So because $a_{21} = 0$, $(G^*;T^*)$ is LAS.

(b) If $\Omega > 0$, then

$$a_{22} = -\gamma_T T^* \sqrt{(1-\Omega)^2 + 4\Omega\left(1 - \frac{\delta_T}{\gamma_T}\right)} < 0,$$

then $a_{11} < 0$ and $a_{22} < 0$. So, $(G^*;T^*)$ is LAS.

If $f \neq 0$,

$$\begin{aligned} Tr(M(G^*;T^*)) &= a_{11} + a_{22}, \\ Det((G^*;T^*)) &= a_{11}a_{22} - a_{12}a_{21}. \end{aligned} \tag{C.2}$$

$Det(M) > 0 \Leftrightarrow a_{11}a_{22} - a_{12}a_{21} > 0$

$$\begin{aligned} a_{11}a_{22} - a_{21}a_{12} > 0 \quad \Leftrightarrow \quad & \gamma_G\gamma_T G^*T^*\left[(1-\Omega) + 2\Omega T^*\right] - p\gamma_G\lambda_{fT} f\omega(G^*)\exp(-pT^*)G^*T^* \\ & -\gamma_{TG}\lambda_{fT} f\omega'(G^*)\exp(-pT^*)G^*T^* > 0, \end{aligned}$$

$$\Leftrightarrow \quad \frac{\gamma_T\left[(1-\Omega) + 2\Omega T^*\right]}{p\lambda_{fT} f\omega(G^*)\exp(-pT^*)} - \frac{\gamma_{TG}\omega'(G^*)}{p\gamma_G\omega(G^*)} > 1.$$

Second $Tr(M(G^*,T^*)) < 0 \Leftrightarrow \dfrac{\gamma_G G^*}{p\lambda_{fT} f\omega(G^*\exp(-pT^*)T^*} + \dfrac{\gamma_T\left[(1-\Omega)+2\Omega T^*\right]}{p\lambda_{fT} f\omega(G^*\exp(-pT^*)} > 1.$

But,

$$\frac{\gamma_T\left[(1-\Omega)+2\Omega T^*\right]}{p\lambda_{fT} f\omega(G^*)\exp(-pT^*)} - \frac{\gamma_{TG}\omega'(G^*)}{p\gamma_G\omega(G^*)} > 1 \Rightarrow \frac{\gamma_G G^*}{p\lambda_{fT} f\omega(G^*\exp(-pT^*)T^*} + \frac{\gamma_T\left[(1-\Omega)+2\Omega T^*\right]}{p\lambda_{fT} f\omega(G^*\exp(-pT^*)} > 1.$$

Consequently, if $\dfrac{\gamma_T\left[(1-\Omega)+2\Omega T^*\right]}{p\lambda_{fT} f\omega(G^*)\exp(-pT^*)} - \dfrac{\gamma_{TG}\omega'(G^*)}{p\gamma_G\omega(G^*)} > 1$, then $(G^*;T^*)$ is stable.

Appendix D. Proof of Proposition 5

We have $h = T - T_s$ and $g = G - G_s$, then $\dfrac{\partial h}{\partial t} = \dfrac{\partial T}{\partial t}$ and $\dfrac{\partial^2 h}{\partial x^2} = \dfrac{\partial T^2}{\partial x^2}$

In the same way $\dfrac{\partial g}{\partial t} = \dfrac{\partial G}{\partial t}$ and $\dfrac{\partial^2 g}{\partial x^2} = \dfrac{\partial G^2}{\partial x^2}$, So:

$$\begin{aligned}\frac{\partial h}{\partial t} &= D_T\frac{\partial^2 h}{\partial x^2} + \gamma_T\left(h+T_s\right)\left(1+\Omega\left(h+T_s\right)\right)\left(1-\int_{-\infty}^{+\infty}\phi_{M_2}(x-y)(h(t,y)+T_s)dy\right)\\ &\quad -\delta_T(h+T_s) - \lambda_{fT} f\omega(g+G_s)\exp\left(-p\int_{-\infty}^{+\infty}\phi_{M_2}(x-y)(h(t,y)+T_s)dy\right)(h+T_s)\end{aligned} \tag{D.1}$$

Developing the right-hand side of equation (D.1) and neglecting the nonlinear expressions in h we get:

$$\begin{aligned}\frac{\partial h}{\partial t} &= D_T\frac{\partial^2 h}{\partial x^2} + \left(\gamma_T(1+\Omega T_s) + \gamma_T\Omega T_s\right)(1-T_s)\,h - \delta_T h - \lambda_{fT} f\omega(G_s)\exp(-pT_s)h\\ &\quad -\lambda_{fT} f\omega'(G_s)\exp(-pT_s)T_s g - \gamma_T T_s(1+\Omega T_s)\int_{-\infty}^{+\infty}\phi_{M_2}(x-y)h(y,t)dy\\ &\quad +\lambda_{fT} fp\omega(G_s)\exp(-pT_s)T_s\int_{-\infty}^{+\infty}\phi_{M_2}(x-y)h(y,t)dy.\\ &= D_T\frac{\partial^2 h}{\partial x^2} + \left[(\gamma_T(1+\Omega T_s)(1-T_s) - \delta_T - \lambda_{fT} f\omega(G_s)\exp(-pT_s)) + \gamma_T\Omega T_s(1-T_s)\right]h\\ &\quad + \left(p\lambda_{fT} f\omega(G_s)\exp(-pT_s)T_s - \gamma_T T_s(1+\Omega T_s)\right)\int_{-\infty}^{+\infty}\phi_{M_2}(x-y)h(y,t)dy\\ &\quad -\lambda_{fT} f\omega'(G_s)\exp(-pT_s)T_s g.\end{aligned}$$

In the same way we have :

$$\begin{aligned}\frac{\partial g}{\partial t} &= D_G\frac{\partial^2 g}{\partial x^2} + \gamma_G(g+G^*)\left(1-\int_{-\infty}^{+\infty}\phi_{M_1}(x-y)(g(y,t)+G^*)dy\right) - \delta_G(g+G^*) - \lambda_{fG} f(g+G^*)\\ &\quad -\gamma_{TG}\left(\int_{-\infty}^{+\infty}\phi_{M_2}(x-y)(h(y,t)+T^*)dy\right)(g+G^*).\end{aligned} \tag{D.2}$$

Developing the right-hand side of equation (D.2) and neglecting the nonlinear expressions in g we get:

$$\begin{aligned}\frac{\partial g}{\partial t} &= D_G\frac{\partial^2 g}{\partial x^2} + \left[\gamma_G(1-G_s) - \delta_G - \gamma_{TG}T_s - \lambda_{fG} f\right]g - \gamma_G G_s\int_{-\infty}^{+\infty}\phi_{M_1}(x-y)g(y,t)dy\\ &\quad -\gamma_{TG}G_s\int_{-\infty}^{+\infty}\phi_{M_2}(x-y)h(y,t)dy.\end{aligned}$$

Appendix E. Proof of Theorem 3

Assume that $\mathcal{R}_T < 1$ (then $b_{22} < 0$) and we have a range of positive values of z such that: $\overline{\phi_1}(z) < 0$. Writing $Det(M)$ as a binomial expression of $\frac{z^2}{M_1^2}$ implies:

$$\begin{aligned}
Det(M) &= D_G D_T \frac{z^4}{M_1^4} + \left[b_{11} D_T \overline{\phi_1}(z) - b_{22} D_G\right] \frac{z^2}{M_1^2} - b_{11} b_{22} \overline{\phi_1}(z), \\
&= D_G D_T \left[\left(\frac{z^2}{M_1^2} + \frac{b_{11} D_T \overline{\phi_1}(z) - b_{22} D_G}{2 D_G D_T} \right)^2 - \frac{\left(b_{11} D_T \overline{\phi_1}(z) - b_{22} D_G\right)^2}{4 (D_G D_T)^2} - \frac{b_{11} b_{22} \overline{\phi_1}(z)}{D_G D_T} \right] \\
&= \frac{1}{D_G D_T} \left[D_G D_T \frac{z^2}{M_1^2} + \frac{b_{11} D_T \overline{\phi_1}(z) - b_{22} D_G}{2} \right]^2 - \frac{1}{4 D_G D_T} \Big[\left(b_{11} D_T \overline{\phi_1}(z) - b_{22} D_G\right)^2 \\
&\quad + 4 D_G D_T b_{11} b_{22} \overline{\phi_1}(z) \Big] \\
&= \frac{1}{D_G D_T} \left[D_G D_T \frac{z^2}{M_1^2} + \frac{b_{11} D_T \overline{\phi_1}(z) - b_{22} D_G}{2} \right]^2 - \frac{1}{4 D_G D_T} \left[b_{11} D_T \overline{\phi_1}(z) + b_{22} D_G \right]^2 \\
&= \frac{1}{D_G D_T} \left[D_G D_T \frac{z^2}{M_1^2} - b_{22} D_G \right] \times \left[D_G D_T \frac{z^2}{M_1^2} + b_{11} D_T \overline{\phi_1}(z) \right].
\end{aligned} \tag{E.1}$$

$D_G D_T \frac{z^2}{M_1^2} - b_{22} D_G > 0$ because $b_{22} < 0$ and therefore $Det(M) \leq 0$ gives:

$$\frac{1}{(M_1)^2} \leq \frac{-\overline{\phi}_1(z)}{z^2} \left(\frac{b_{11}}{D_G} \right).$$

Therefore, $(G_e, 0)$ is unstable. To show that system (5) undergoes spatial Turing bifurcation at M_1^T, we need to verify that spatial Turing bifurcation occurs prior to the temporal Hopf bifurcation (case where $Tr(M) = 0$ and $Det(M) > 0$) as M_1 increases to M_1^T. From the above argument, we only need to show that if (35) fails then (36) must have already failed as M_1 increases. When (35) fails, we have:

$$\overline{\phi}_1(z) = \frac{-(D_G + D_T)\frac{z^2}{M_1^2} + b_{22}}{b_{11}}. \tag{E.2}$$

Plugging (E.2) into E.1), we see that

$$Det(M) = -\left(D_T \frac{z^2}{(M_1)^2} + b_{22} \right)^2 \leq 0. \tag{E.3}$$

Thus, (36) does not hold and this ends the proof.

Appendix F. Proof of Theorem 6

Suppose that $\mathcal{R}_1^* - \mathcal{R}_2^* > 1$ and $\frac{a_{11}(c - a_{22})\mu_1\mu_2}{c a_{11}\mu_1 - a_{12}a_{21}\mu_2} < 1$, we have:

$$\begin{aligned}
Det(k, M_1, M_2) &= D_G D_T k^4 - \left[a_{22} D_G \overline{\phi_{M_2}}(k) + a_{11} D_T \overline{\phi_{M_1}}(k) + c D_G (1 - \overline{\phi_{M_2}}(k)) \right] k^2 + \\
&\quad a_{11}(a_{22} - c) \overline{\phi_{M_1}}(k) \overline{\phi_{M_2}}(k) + c a_{11} \overline{\phi_{M_1}}(k) - a_{12} a_{21} \overline{\phi_{M_2}}(k)
\end{aligned}$$

and

$$\overline{\phi_{M_i}}(k) = \frac{\sin(kM_i)}{kM_i}, \quad i = 1, 2.$$

We are interested by the determination of thresholds k^T, M_1^T and M_2^T so that:

$$Det(k^T, M_1^T, M_2^T) = 0.$$

These thresholds are solutions of the equations:

$$Det(k, M_1, M_2) = 0, \quad \frac{\partial Det(k, M_1, M_2)}{\partial M_1} = 0, \quad \frac{\partial Det(k, M_1, M_2)}{\partial M_2} = 0 \quad \frac{\partial Det(k, M_1, M_2)}{\partial k} = 0. \quad \text{(F.1)}$$

Differentiating $Det(k, M_1, M_2)$ with respect to M_1 and M_2 and using the fact that:
$\frac{\partial Det(k, M_1, M_2)}{\partial M_1} = 0$ and $\frac{\partial Det(k, M_1, M_2)}{\partial M_2} = 0$ we obtain:

$$(a_{11}a_{22} - ca_{11}) \left(\phi_{M_2}(k) + \frac{ca_{11} - a_{11}D_T k^2}{a_{11}a_{22} - ca_{11}} \right) \frac{\partial \overline{\phi_{M_1}}}{\partial M_1} = 0,$$

and

$$(a_{11}a_{22} - ca_{11}) \left(\phi_{M_1}(k) - \frac{D_G(a_{22} - c)k^2 + a_{12}a_{21}}{a_{11}a_{22} - ca_{11}} \right) \frac{\partial \overline{\phi_{M_2}}}{\partial M_2} = 0.$$

Then we have:

$$\begin{cases} \overline{\phi_{M_2}}(k) = \dfrac{a_{11}D_T k^2 - ca_{11}}{a_{11}a_{22} - ca_{11}} = \dfrac{D_T k^2 - c}{a_{22} - c} \quad \text{or} \quad \dfrac{\partial \overline{\phi_{M_1}}}{\partial M_1} = 0, \\ \\ \overline{\phi_{M_1}}(k) = \dfrac{D_G(a_{22} - c)k^2 + a_{12}a_{21}}{a_{11}a_{22} - ca_{11}} \quad \text{or} \quad \dfrac{\partial \overline{\phi_{M_2}}}{\partial M_2} = 0. \end{cases} \quad \text{(F.2)}$$

First, if:

$$\overline{\phi_{M_2}}(k) = \frac{D_T k^2 - c}{a_{22} - c} \quad \text{and} \quad \overline{\phi_{M_1}}(k) = \frac{D_G(a_{22} - c)k^2 + a_{12}a_{21}}{a_{11}a_{22} - ca_{11}}$$

then, $Det(k, M_1, M_2) = \frac{a_{12}a_{21}}{c - a_{22}} D_T k^2 + c\frac{a_{12}a_{21}}{a_{22} - c}$. Using the fact that $\frac{\partial Det(k, M_1, M_2)}{\partial k} = 0$, we obtain $k = 0$ and then we return to the temporal case.
Second, if:

$$\overline{\phi_{M_2}}(k) = \frac{D_T k^2 - c}{a_{22} - c} \quad \text{and} \quad \frac{\partial \overline{\phi_{M_2}}}{\partial M_2} = 0$$

then as previously: $Det(k, M_1, M_2) = \frac{a_{12}a_{21}}{c - a_{22}} D_T k^2 + c\frac{a_{12}a_{21}}{a_{22} - c}$ and we can not have Turing bifurcation there.
Third, if:

$$\overline{\phi_{M_1}}(k) = \frac{D_G(a_{22} - c)k^2 + a_{12}a_{21}}{a_{11}a_{22} - ca_{11}} \quad \text{and} \quad \frac{\partial \overline{\phi_{M_2}}}{\partial M_2} = 0$$

then we have the same results as before. Finally, if:

$$\frac{\partial \overline{\phi_{M_1}}}{\partial M_1} = 0 \quad \text{and} \quad \frac{\partial \overline{\phi_{M_2}}}{\partial M_2} = 0,$$

we obtain

$$\tan(kM_1) = kM_1 \quad \text{and} \quad \tan(kM_2) = kM_2.$$

Set $z_1 = kM_1$ and $z_2 = kM_2$, then z_1 and z_2 are solutions of :

$$\tan(z) = z. \tag{F.3}$$

Set:

$$\mu_1 = \frac{\sin(z_1)}{z_1} \quad \text{and} \quad \mu_2 = \frac{\sin(z_2)}{z_2}.$$

$Det(k, M_1, M_2) = 0$ gives that:

$$(k^T)^2 = \frac{D_G a_{22}\mu_2 + a_{11}D_T\mu_1 + cD_G(1-\mu_2) + \sqrt{\Sigma}}{2D_G D_T} \tag{F.4}$$

with

$$\Sigma = \left(D_G a_{22}\mu_2 + a_{11}D_T\mu_1 + cD_G(1-\mu_2)\right)^2 - 4D_G D_T\left((a_{11}a_{22} - ca_{11})\mu_1\mu_2 - a_{12}a_{21}\mu_2 + ca_{11}\mu_1\right)$$

and using the fact that $\dfrac{\partial Det(k, M_1, M_2)}{\partial k} = 0$, we obtain:

$$\left(D_G a_{22}\mu_2 + a_{11}D_T\mu_1 + cD_G(1-\mu_2)\right)^2 = 4D_G D_T\left((a_{11}a_{22} - ca_{11})\mu_1\mu_2 - a_{12}a_{21}\mu_2 + ca_{11}\mu_1\right). \tag{F.5}$$

Note that $(a_{11}a_{22} - ca_{11})\mu_1\mu_2 - a_{12}a_{21}\mu_2 + ca_{11}\mu_1 > 0$ thanks to the second assumption in (52). Thus, the relation in (F.5) is well defined and therefore:

$$(k^T)^2 = \sqrt{\frac{(a_{11}a_{22} - ca_{11})\mu_1\mu_2 - a_{12}a_{21}\mu_2 + ca_{11}\mu_1}{D_G D_T}}. \tag{F.6}$$

The associated values of M_1 and M_2 are

$$M_1^T = z_1\left(\frac{D_G D_T}{(a_{11}a_{22} - ca_{11})\,\mu_1\mu_2 + ca_{11}\mu_1 - a_{12}a_{21}\mu_2}\right)^{1/4}, \tag{F.7}$$

and

$$M_2^T = z_2\left(\frac{D_G D_T}{(a_{11}a_{22} - ca_{11})\,\mu_1\mu_2 + ca_{11}\mu_1 - a_{12}a_{21}\mu_2}\right)^{1/4}. \tag{F.8}$$

Appendix G. Numerical scheme

The numerical scheme for the problem given by system (5) is obtained by using non standard finite method for the discretization of the temporal part of the system and difference finite method for the spatial part. We subdivided the space domain $(0, l)$ in $n+1$ intervals such that:

$$x_0 = 0 < x_1 < x_2 < ... < x_n < x_{n+1} = l,$$

where

$$\forall \;\; j = 1, ..., n \quad \Delta x = x_{j+1} - x_j = \frac{l}{n+1} \quad \text{and} \quad x_j = j\Delta x.$$

In the same way, we subdivided the time interval such that:

$$t_0 < t_1 < t_2 < ... < t_i < t_{j+1} < ... \quad \text{and} \quad t_i = i\Delta t.$$

We denote by G_j^i and T_j^i respectively the value of G and T at the time t_i and at the space point x_j. Remark first that in non standard method, non linear terms are substituted by a non local approximation. Second, the standard denominator Δt in each discrete derivative is replaced by a

time-step function $0 < \varphi(\Delta t) < 1$ such that $\varphi(\Delta t) = \Delta t + \mathcal{O}(\Delta t)$. The non-standard approximation for the system (5) are given by:

$$\left\{\begin{array}{rcl} \dfrac{G_j^{i+1} - G_j^i}{\varphi_1(\Delta t)} & = & D_G \dfrac{G_{j+1}^i + G_{j-1}^i - 2G_j^i}{\Delta x^2} + (\gamma_G - \delta_G - \lambda_{fG} f)\, G_j^i - \left(\gamma_G \phi_{M_1} * G_j^i + \gamma_{TG} \phi_{M_2} * T_j^i\right) G_j^{i+1}, \\ \dfrac{T_j^{i+1} - T_j^i}{\varphi_2(\Delta t)} & = & D_T \dfrac{T_{j+1}^i + T_{j-1}^i - 2T_j^i}{\Delta x^2} + \left(\gamma_T - \delta_T + \Omega \gamma_T T_j^i\right) T_j^i - \left(\gamma_T \phi_{M_2} * T_j^i + \Omega \gamma_T T_j^i \phi_{M_2} * T_j^i\right) T_j^{i+1} \\ & & -\lambda_{fT} f \omega(G_j^i) \exp\left(-p \phi_{M_2} * T_j^i\right) T_j^{i+1}, \end{array}\right. \tag{G.1}$$

with

$$\left\{\begin{array}{rcl} \varphi_1(\Delta t) & = & \dfrac{e^{(\gamma_G - \delta_G - \lambda_{fG} f)\Delta t} - 1}{\gamma_G - \delta_G - \lambda_{fG} f}, \\ \varphi_2(\Delta t) & = & \dfrac{e^{(\gamma_T - \delta_T)\Delta t} - 1}{\gamma_T - \delta_T}, \end{array}\right. \tag{G.2}$$

and

$$\left\{\begin{array}{rcl} \Delta x & \leq & \min\left(\sqrt{\dfrac{2D_G}{\gamma_G - \delta_G - \lambda_{fG} f}}; \sqrt{\dfrac{2D_T}{\gamma_T - \delta_T}}\right) \\ \Delta t & \leq & \min\left(\dfrac{\ln\left[1 + \dfrac{\gamma_G - \delta_G - \lambda_{fG} f}{\frac{2D_G}{\Delta x^2} - (\gamma_G - \delta_G - \lambda_{fG} f)}\right]}{\gamma_G - \delta_G - \lambda_{fG} f}; \dfrac{\ln\left[1 + \dfrac{\gamma_T - \delta_T}{\frac{2D_T}{\Delta x^2} - \gamma_T - \delta_T}\right]}{\gamma_T - \delta_T}\right). \end{array}\right. \tag{G.3}$$

Recall that $\mathcal{R}_G > 1$ implies that $\gamma_G - \delta_G - \lambda_{fG} f > 0$ and $\mathcal{R}_{T,0} > 1$ implies that $\gamma_T - \delta_T > 0$.

Second, in system (G.1) $\phi_{M_2} * T_j^i$ is an approximation of the convolution term $\displaystyle\int_{-\infty}^{+\infty} \phi_{M_2}(x - y) T(y,t) dy$, done by the Matlab function "trapz". It is the same for $\phi_{M_1} * G_j^i$.